

IDENTIFICATION AND CHARACTERIZATION OF REGULATORS OF THE
LONGEVITY FACTOR DAF-16 IN *C. ELEGANS*

A Dissertation

Presented to the Faculty of the Graduate School
of Cornell University

In Partial Fulfillment of the Requirements for the Degree of
Doctor of Philosophy

by

Ji Li

January 2009

© 2009 Ji Li
ALL RIGHTS RESERVED

IDENTIFICATION AND CHARACTERIZATION OF REGULATORS OF THE LONGEVITY FACTOR DAF-16 IN *C. ELEGANS*

Ji Li, Ph. D.

Cornell University 2009

The transcription factor DAF-16/FOXO is a critical longevity determinant in diverse organisms. It is the major effector of the insulin/IGF-1 signaling (IIS) cascade which is critical for regulating development, longevity, metabolism and stress resistance. However the molecular basis of how its transcriptional activity is regulated remains largely unknown. The aim of my research is to better understand the regulation of DAF-16 using *C. elegans* as a model system.

My work reveals that the 14-3-3 protein FTT-2 is a new regulatory factor of DAF-16 in response to IIS. I found that RNAi knock down of *ftt-2* specifically enhanced the IIS-mediated dauer formation. Furthermore, *ftt-2* knock down caused the nuclear accumulation of DAF-16 and enhanced its transcriptional activities. In contrast to *ftt-2*, RNAi knock down of *par-5/ftt-1*, the only other 14-3-3 gene in *C. elegans*, did not show any notable effect on DAF-16 regulation, underscoring the functional specification of FTT-2 and PAR-5 despite their high sequence similarity. Using co-immunoprecipitation, I showed that FTT-2 formed a complex with DAF-16. My work indicates that FTT-2 binds DAF-16 in *C. elegans* and regulates DAF-16 by sequestering it in the cytoplasm. A similar mechanism of regulation of FOXO by 14-3-3 has been reported in

mammalian cells, highlighting the high degree of conservation of DAF-16/FOXO regulation.

My work also shows that the *C. elegans* homolog of host cell factor 1 (HCF-1) represents a new longevity modulator and functions as a negative regulator of DAF-16. In *C. elegans*, *hcf-1* inactivation caused a *daf-16*-dependent lifespan extension up to 40% and heightened resistance to specific stress stimuli. HCF-1 showed ubiquitous nuclear localization and physically associated with DAF-16 in worms. Furthermore, loss of *hcf-1* resulted in elevated DAF-16 recruitment to the promoters of its target genes and altered expression of a subset of DAF-16-regulated genes. We propose that HCF-1 modulates *C. elegans* longevity and stress response by forming a complex with DAF-16. This complex limits a fraction of DAF-16 from accessing its target gene promoters, and thereby regulating DAF-16-mediated transcription of selective target genes. As HCF-1 is highly conserved, my results have important implication for aging and FOXO regulation in mammals.

BIOGRAPHICAL SKETCH

Ji Li was born in Ling Jia, a very small town of Sichuan Province in China in 1978. His birth brought great joy to the family as well as surprises, for he was brought to the world with an unusual XXL-sized head. He learned to walk later than the other kids and his parents started to worry about the size issue. After consulting a doctor, they were relieved that he was not genetically retarded. Although not rich, he had very happy childhood in the peaceful small town. Then he moved to Neijiang, a small city nearby, with his family when he was 6 years old. There he spent 12 years with his mom and dad and his little sister, and received education from the elementary school and high school. He was a good student in most teachers' eyes, except that he didn't put enough time on books as the other good students did. However, there was one teacher in the world, his mom, who always supported and trusted him and gave him a lot of space to develop his interests outside of the class. He was attracted by art design and learned to play guitar. He was even indulged in video games and computers and spent a lot of time in traveling. Study hard and play hard, that's what he was taught when he was a kid. In 1996 he entered Tsinghua University in Beijing as No.1 in the National College Entrance Examination in his city. Although he had a very strong background of physics and mathematics, he was attracted by the mystery of biology and chose it as his major in college. In 2000, he received his bachelor degree in Biosciences and Biotechnology and in 2003 he earned his master degree in Molecular Biology and Biochemistry from Tsinghua University. Right after that, he came to U.S. and entered the PhD program of Genetics and Development in Cornell University where he spent 5 years in studying the molecular mechanism of aging in Professor Sylvia Lee's lab. In May 2008 right before his

graduation, his hometown Sichuan was struck by a devastating earthquake. The tragic disaster destroyed everything and took away ~70,000 innocent lives. He decided to go back to his homeland soon after he finishes his training to help his people and serve his mother country.

献给我亲爱的父母和妻子

To my beloved parents and wife

ACKNOWLEDGMENTS

I would like to express my sincere gratitude to a great many people who made my graduate study possible. I would like to thank, first and foremost, my advisor Dr. Sylvia Lee for her guidance and for providing such sound training in scientific insight and criticism. I learned a lot from her, not only the hand-to-hand experience, but most importantly, the critical thinking to be an independent researcher. I also thank the other members of my special committee, Dr. Kenneth Kemphues and Dr. Andrew Clark, for their valuable comments, suggestions and criticisms in my research. I especially thank Dr. Kenneth Kemphues, Dr. Diane Morton, Dr. David Pruyne and Dr. Kelly Liu for their insightful inputs for my work in the joint lab meetings.

I am grateful to the other principal investigators who kindly provided help and guidance during my graduate study: Drs. John Lis, Michael Goldberg, Eric Alani, Bik Tye, Tom Fox, Lee Kraus and Olena Vatamaniuk. Special thanks go to Eric Alani. As the former Director of Graduate Study, he is a considerate and very nice person who always cares about the life of graduate students and is ready to provide advice both scientifically and non-scientifically. I also want to thank Diane Colf for her assistance in many aspects of my graduate studies. She has done a great job to make my life and the lives of the other graduate students much easier.

I am also very grateful for the support from the past and present lab members: Benjamin Hamilton, Dr. Yuqing Dong, Penny Hurd, Mami Shindo, Atsushi Ebata, Dr. Zoey Ni, Dr. Ludivine Walter, Nicole Liachko, Gizem Rizki, Terri Iwata and Rada Omanovic. Thanks to Benjamin Hamilton, Penny Hurd, Atsushi Ebata and Rada Omanovic for their hard work to keep everything organized and help the lab run smoothly. Thanks to Dr. Yuqing Dong for

initiating the HCF-1 project and building a good foundation for me to reply. Thanks to all the girls in the lab, Dr. Zoey Ni, Dr. Ludivine Walter, Mami Shindo, Nicole Liachko, Gizem Rizki and Terri Iwata not only for their kind help in the lab, but also for bringing in all the happiness and making the lab a nice environment to work in. Special thanks go to Atsushi Ebata. As a good friend and a colleague, I always enjoy the stimulating conversations with him inside and outside of science. In addition, I also want to thank many other people for their suggestions and technical help in my research, especially Behfar Ardehali, Dr. Man-Hee Suh, Dr. Yuang Jiang, Nirav Amin, Wendy Hoose and Bingsi Li.

Thanks to all my friends who have offered great help and kept my spirit up in living in Ithaca over the years. The list is too long to include everyone: Frank Shotkoski, Jiangtao Yu, Xiaoqing Zhao, Xue Xia, Yong Zhao, Jun Cui, Xin Li, Chenxi Tian, Zheng Wang, Jian Li, Li Xu, Jian Zhou, Li Li and Miao Wang.

Last but never least, I appreciate everything my parents and my wife Lijie has done for me. They respect every important decision I make for my life and always stand with me in the ups and downs. Without their love and support, I could not have finished my PhD.

TABLE OF CONTENTS

BIOGRAPHICAL SKETCH.....	iii
ACKNOWLEDGMENTS.....	vi
TABLE OF CONTENTS.....	viii
LIST OF FIGURES.....	xii
LIST OF TABLES.....	xiv
LIST OF ABBREVIATIONS.....	xv
CHAPTER 1 INTRODUCTION	1
1.1 THE FORKHEAD TRANSCRIPTION FACTOR DAF-16/FOXO AND ITS FUNCTIONS	1
1.2 SIGNALING PATHWAYS THAT REGULATE DAF-16/FOXO	8
1.2.1 <i>IIS</i>	8
1.2.2 <i>Germline signaling</i>	12
1.2.3 <i>JNK signaling</i>	15
1.2.4 <i>SIR2 signaling</i>	16
1.3 OTHER DAF-16/FOXO REGULATORS	18
1.4 DISSERTATION OUTLINE.....	22
CHAPTER 2 THE 14-3-3 PROTEIN FTT-2 BINDS DAF-16 AND RETAINS IT IN THE CYTOPLASM	23
2.1 INTRODUCTION.....	23
2.2 MATERIALS AND METHODS.....	25
2.2.1 <i>Strains and maintenance</i>	25
2.2.2 <i>Construction of ftt-2 and par-5 specific RNAi constructs</i>	25
2.2.3 <i>RNAi</i>	26

2.2.4	<i>Dauer assay</i>	26
2.2.5	<i>DAF-16::GFP localization assay</i>	27
2.2.6	<i>Lifespan assay</i>	27
2.2.7	<i>IP and Western Blot</i>	28
2.2.8	<i>qRT-PCR</i>	29
2.2.9	<i>Brood size assay</i>	31
2.2.10	<i>Developmental rate assay</i>	31
2.3	RESULTS AND DISCUSSION	31
2.3.1	<i>RNAi inactivation of ftt-2, but not par-5, enhances dauer formation.</i>	31
2.3.2	<i>RNAi inactivation of ftt-2 promotes DAF-16::GFP nuclear localization</i>	37
2.3.3	<i>Enhanced DAF-16 transcriptional activities upon ftt-2 RNAi.</i>	39
2.3.4	<i>RNAi inactivation of ftt-2 leads to shortened lifespan.</i>	43
2.3.5	<i>FTT-2 forms a complex with DAF-16 in vivo.</i>	45
2.4	ACKNOWLEDGEMENTS	50
CHAPTER 3	THE HOST CELL FACTOR HCF-1 NEGATIVELY REGULATES DAF-16 IN THE NUCLEUS BY LIMITING ITS ACCESS TO ITS TARGET GENES	52
3.1	INTRODUCTION	52
3.2	MATERIALS AND METHODS	54
3.2.1	<i>C. elegans strains</i>	54
3.2.2	<i>Lifespan assays</i>	55
3.2.3	<i>Transgenic animals</i>	56
3.2.4	<i>Embryonic and brood size assays</i>	56

3.2.5	<i>Nile Red staining.....</i>	57
3.2.6	<i>Stress and dauer assays</i>	57
3.2.7	<i>DAF-16::GFP localization assay</i>	58
3.2.8	<i>Immunostaining.....</i>	59
3.2.9	<i>IP and immunoblotting</i>	59
3.2.10	<i>Antibodies</i>	60
3.2.11	<i>RNA isolation and qRT-PCR.....</i>	60
3.2.12	<i>ChIP.....</i>	61
3.3	RESULTS	65
3.3.1	<i>hcf-1 is a novel longevity gene.....</i>	65
3.3.2	<i>HCF-1 is ubiquitously expressed and localizes to the nucleus..</i>	71
3.3.3	<i>hcf-1 modulates lifespan in a daf-16-dependent manner.</i>	78
3.3.4	<i>hcf-1 likely acts in parallel to the IIS and germline pathway to modulate lifespan.</i>	78
3.3.5	<i>Loss of hcf-1 promotes resistance to specific environmental stress.....</i>	82
3.3.6	<i>HCF-1 regulates the expression of a subset of DAF-16 regulated genes.....</i>	87
3.3.7	<i>HCF-1 forms a protein complex with DAF-16.....</i>	99
3.3.8	<i>Loss of hcf-1 leads to enhanced enrichment of DAF-16 on its target gene promoters.</i>	104
3.4	DISCUSSION.....	108
3.5	ACKNOWLEDGEMENTS.....	115
CHAPTER 4	CONCLUSIONS AND FUTURE PERSPECTIVES.....	116

APPENDIX I	GENETIC INTERACTIONS BETWEEN <i>HCF-1</i> AND OTHER KNOWN LONGEVITY FACTORS IN <i>C. ELEGANS</i>	121
APPENDIX II	HCF-1 INTERACTS WITH THE PROTEIN DEACETYLASE SIR-2.1	126
APPENDIX III	ATTEMPTS TO DISSECT THE HCF-1/DAF-16 COMPLEX BY GEL FILTRATION.....	132
REFERENCES	135

LIST OF FIGURES

Figure 1.1 The diverse functions of DAF-16.	7
Figure 1.2 The conserved IIS pathway.	10
Figure 1.3 Germline signaling in lifespan regulation.	14
Figure 1.4 Regulations of DAF-16 in <i>C. elegans</i>	21
Figure 2.1 The <i>ftt-2</i> and <i>par-5</i> RNAi constructs are gene-specific.	33
Figure 2.2 The brood size of <i>ftt-2</i> RNAi worms upon one generation (A) or two generations (B) of RNAi treatment.	36
Figure 2.3 <i>ftt-2</i> RNAi, but not <i>par-5</i> RNAi, causes DAF-16::GFP accumulation in the nucleus.	40
Figure 2.4 RNAi inactivation of <i>ftt-2</i> results in the up-regulation of <i>daf-16</i> - dependent mRNA expression of <i>sod-3</i> (A), C24B9.9 (B) and F53C3.12 (C).	42
Figure 2.5 FTT-2 forms a complex with DAF-16::GFP in <i>C. elegans</i>	47
Figure 3.1 <i>hcf-1</i> modulates lifespan by acting upstream of <i>daf-16</i> , but in parallel to the IIS and germline signaling pathway.	66
Figure 3.2 The <i>hcf-1(ok559)</i> mutant shows reduced brood size and increased embryonic lethality.	70
Figure 3.3 The <i>hcf-1(ok559)</i> mutant shows weak expression of a truncated HCF-1 protein and the <i>hcf-1(pk924)</i> mutant shows no detectable expression of any HCF-1 peptide.	72
Figure 3.4 HCF-1 is a ubiquitously expressed nuclear protein.	74
Figure 3.5 GFP-fused HCF-1 is expressed in the nucleus of somatic and germline cells.	76

Figure 3.6 Loss of <i>hcf-1</i> results in heightened resistance to specific environmental stresses.	84
Figure 3.7 Loss of <i>hcf-1</i> does not affect fat storage.	89
Figure 3.8 Loss of <i>hcf-1</i> does not result in altered DAF-16 subcellular localization or a change in DAF-16 expression level.	90
Figure 3.9 Loss of <i>hcf-1</i> promotes the DAF-16 transcriptional regulation of several target genes.	93
Figure 3.10 <i>Psod-3::gfp</i> expression level is elevated in <i>hcf-1(pk924)</i> mutants.	95
Figure 3.11 HCF-1 co-localizes with DAF-16::GFP in the nucleus.	101
Figure 3.12 HCF-1 forms a protein complex with DAF-16 in <i>C. elegans</i>	102
Figure 3.13 Loss of <i>hcf-1</i> enhances the enrichment of DAF-16 on the promoters of its target genes.	105
Figure 3.14 The model.	110
Figure I.1 A possible epistasis relationship between <i>hcf-1</i> and <i>sir-2.1</i> and <i>smk-1</i> in regulating <i>daf-16</i>	123
Figure II.1 HCF-1 forms protein complexes with SIR-2.1 in <i>C. elegans</i>	128
Figure II.2 Loss of <i>hcf-1</i> promotes the SIR-2.1-mediated transcriptional regulation of several target genes.	130
Figure III.1 DAF-16, HCF-1 and SIR-2.1 are likely in the same protein complex.	135

LIST OF TABLES

Table 2.1 Primers for qRT-PCR.	30
Table 2.2 RNAi inactivation of <i>ftt-2</i> promotes dauer formation in <i>daf-2(e1370)</i> at 22°C.	38
Table 2.3 RNAi inactivation of <i>ftt-2</i> shortens the lifespan of N2 worms but has no effect on the lifespan of <i>daf-2(e1370)</i> worms.	44
Table 3.1 Primers for qRT-PCR.	62
Table 3.2 qPCR Primers for ChIP.	64
Table 3.3 Inactivation of <i>hcf-1</i> results in lifespan increase that is completely dependent on <i>daf-16</i> , but likely independent of the IIS and germline pathway.	68
Table 3.4 Expression of a <i>hcf-1::gfp</i> transgene partially rescues the lifespan phenotype of <i>hcf-1(pk924)</i>	73
Table 3.5 Inactivation of <i>hcf-1</i> results in lifespan increase that is completely dependent on <i>daf-16</i> , but likely independent of the IIS pathway.	79
Table 3.6 Inactivation of <i>hcf-1</i> results in a weak dauer exit phenotype.	88
Table 3.7 Inactivation of <i>hcf-1</i> results in significant expression changes of a subset of DAF-16 regulated genes.	97
Table I.1 <i>hcf-1</i> acts upstream of <i>smk-1</i> and <i>sir-2.1</i> in lifespan regulation.	124

LIST OF ABBREVIATIONS

bp	Base pair
ChIP	Chromatin immunoprecipitation
CREB	Cyclic-AMP responsive element binding
CBP	CREB-binding protein
DAF-2	Abnormal dauer formation 2
DAF-16	Abnormal dauer formation 16
DR	Dietary restriction
Fn3	Fibronectin type 3
FoxO	Forkhead box O transcription factor
FTT	Fourteen three three (protein)
GFP	Green fluorescent protein
HCF-1	Host cell factor 1
HSF-1	Heat-shock factor 1
hr	Hour
IGF	Insulin-like growth factor
IP	Immunoprecipitation
JNK	c-Jun N-terminal kinase
MAPK	Mitogen-activated protein kinase
MS	Mass spectrometry
NGM	Nematode growth medium
PI(3)K	Phosphatidylinositol 3-kinase
PIP ₃	Phosphatidylinositol-3,4,5-trisphosphate
PKB	Protein kinase B
qRT-PCR	Quantitative reverse transcription PCR

RNAi	RNA interference
SIR2	Silent information regulator 2
USP7	Ubiquitin-specific protease 7
UTR	Untranslated region
wt	Wild type

CHAPTER 1

INTRODUCTION

Aging is an unsolved fundamental mystery in biology. The complexity of the process has made the study of aging a purely descriptive scientific endeavor for a long time until the discovery of genetic longevity determinants in different organisms during the last two decades. Among the many model organisms, the nematode *Caenorhabditis elegans* (*C. elegans*) is emerging as one of the most powerful model systems for aging studies due to its simple biology. It has a short lifespan (2~3 weeks) and can be easily maintained in the laboratory. Most importantly, the ease of RNA interference (RNAi) in *C. elegans* has made it a powerful tool for genetic analyses. Recent studies using *C. elegans* as well as the other model organisms have revealed a handful of evolutionarily conserved genes and genetic pathways important for lifespan regulation, for example, the insulin/IGF-1 signaling (IIS) (see the next chapter), genes involved in mitochondrial respiration, the protein deacetylase SIR2 (see the next chapter) and the dietary restriction pathway (Antebi, 2007; Bishop and Guarente, 2007; Giannakou and Partridge, 2007; Kaeberlein et al., 2007; Kenyon, 2005; Lambert and Brand, 2007). Among the many conserved longevity factors discovered in *C. elegans* to date, the forkhead transcription factor DAF-16 is the best characterized and it is emerging as a master regulator of the aging process in worms.

1.1 The forkhead transcription factor DAF-16/FOXO and its functions

Despite its important role in the aging process, *daf-16* was initially discovered as one of the genes that caused a dauer defective phenotype when mutated in worms (Albert et al., 1981; Riddle et al., 1981). Dauer is an

alternative larval stage in *C. elegans*. When worms at early larval stage (L1) are exposed to unfavorable environmental conditions (food deprivation, overcrowding, high temperature), they can exit the regular larval cycle and form dauer larvae (Riddle and Albert, 1997). The dauer larvae are highly stress resistant, hypometabolic and extremely long-lived which help the worms survive unfavorable conditions. In addition to the dauer defective phenotype, the *daf-16(0)* mutant was subsequently found to be short-lived and sensitive to various stresses (Kenyon et al., 1993; Larsen et al., 1995; Murakami and Johnson, 1996).

daf-16 was cloned by two independent groups (Lin et al., 1997; Ogg et al., 1997) and was found to encode a forkhead transcription factor (FOXO). The FOXO family proteins are conserved across species. Whereas invertebrates such as worms and flies have only one FoxO gene, in mammalian systems, there are four DAF-16 orthologs: FOXO1, FOXO3a, FOXO4 and FOXO6 (Calnan and Brunet, 2008). Accumulated evidence suggests that DAF-16/FOXO proteins have a wide range of cellular functions. They are involved in development (e.g., dauer formation), metabolism (e.g., fat storage), stress resistance, lifespan regulation, and apoptosis (Antebi, 2007; Calnan and Brunet, 2008; van der Horst and Burgering, 2007).

Although *daf-16* is the only FoxO gene in *C. elegans*, further molecular analyses suggested that there are at least seven alternatively spliced isoforms of *daf-16* (<http://www.wormbase.org>). *daf-16a* and *daf-16b* are the two major isoforms and they are found to be functionally distinct (Lee et al., 2001; Lin et al., 2001). *daf-16a* is expressed in almost all somatic cells, including intestine, muscles and neurons except the somatic gonad and pharynx. The intestinal expression of DAF-16 was found to be responsible for lifespan regulation by

DAF-16 and the neuronal expression was thought to be sufficient for dauer regulation by DAF-16 (Libina et al., 2003). Thus, *daf-16a* contributes to the lifespan regulation and dauer formation role of the *daf-16* locus. *daf-16b* is expressed in the pharynx and many neurons as well as the somatic gonad. Although it is also responsible for dauer formation, it is particularly important for the pharynx to enter the full dauer state. In contrast to *daf-16a*, *daf-16b* has little contribution to lifespan regulation (Lee et al., 2001; Lin et al., 2001). Interestingly, the functional differences between *daf-16a* and *daf-16b* are due to the differences between the promoter regions, but not the coding sequences, because the coding sequences of *daf-16a* and *daf-16b* could be swapped and were interchangeable for their functions (Lee et al., 2001).

DAF-16 is normally distributed both in the cytoplasm and the nucleus based on studies from DAF-16::GFP transgenic animals (Lee et al., 2001; Lin et al., 2001). Under certain conditions such as stress stimuli (high temperature, overcrowding, food deprivation) or reduced IIS (see chapter 1.2.1), DAF-16 is predominantly found in the nucleus where it can regulate the transcription of its target genes.

Early studies of individual genes have revealed a number of DAF-16 target genes. Those include the superoxide dismutase *sod-3* (Honda and Honda, 1999), metallothionein *mtl-1* (Barsyte et al., 2001) and heat shock protein genes *hsp* (Hsu et al., 2003). The expression of those genes was found to be *daf-16*-dependent. However, a comprehensive understanding of the functions of DAF-16 requires more systematic studies. Recently, several genome-wide studies using different approaches have largely expanded the list of putative DAF-16 downstream targets.

One of the first systematic studies was done using bioinformatics. When binding DNA, the FOXO family proteins can recognize a very conserved consensus binding motif TTG/ATTTAC (Furuyama et al., 2000). By taking advantage of this, Lee et al. (2003) scanned the genome of *C. elegans* and *Drosophila* and identified 947 *C. elegans* genes and 1760 *Drosophila* genes which contain the consensus DAF-16/FOXO binding motif within 1 kb upstream of ATG in the promoter regions (Lee et al., 2003a). Those genes were then compared and 17 orthologs between the two species were identified. Assuming that DAF-16/FOXO has evolutionarily conserved functions and targets across species, the 17 orthologous genes were picked as putative DAF-16/FOXO downstream targets, which included genes involved in stress response and metabolism (Lee et al., 2003a). To validate the bioinformatics-based predictions, functional studies of those genes were further performed and many of them were found to be expressed in a *daf-16*-dependent manner and function in processes regulated by DAF-16, e.g., lifespan regulation, dauer formation and fat storage (Lee et al., 2003a).

In addition to the bioinformatics-based study, a number of DAF-16 downstream genes were identified by microarray studies (McElwee et al., 2003; Murphy et al., 2003). They were classified as DAF-16 activated genes whose expression was up-regulated when DAF-16 was activated and DAF-16 repressed genes whose expression was down-regulated when DAF-16 was activated (Murphy et al., 2003). Previously identified DAF-16 target genes were also identified by the microarray studies such as *sod-3*, *mtl-1* and heat shock protein genes. The microarray analyses also revealed that certain functional groups of genes were over-represented in the DAF-16 downstream gene list. They include groups of stress response genes, antimicrobial genes

and metabolic genes (McElwee et al., 2003; Murphy et al., 2003). This finding is in agreement with the idea that DAF-16 has pleiotropic functions in lifespan regulation, stress resistance, and metabolism. Murphy et al. (2003) also found that many of the potential DAF-16 target genes have the canonical consensus DAF-16 binding motif in the promoter regions (Murphy et al., 2003).

Interestingly, another novel short motif CTTATCA was also over-represented in the promoter regions of many DAF-16 targets and thus it was proposed to be a new potential DAF-16 binding site (Murphy et al., 2003).

The bioinformatics-based method and microarray studies were very successful in identifying a number of potential DAF-16 downstream targets. However, it remained unclear whether those candidate genes are the direct targets of DAF-16. A close investigation of direct interactions between DAF-16 and its binding DNA would be very helpful to answer this question. Oh et al. (2006) accomplished the first systematical chromatin immunoprecipitation (ChIP) experiment in *C. elegans* (Oh et al., 2006). In their unbiased ChIP analyses, more than 100 putative DAF-16 direct target genes, including *sod-3*, were identified and further validated by quantitative reverse transcription PCR (qRT-PCR). Functional studies showed that many of them (more than 50%) are involved in the biological processes regulated by DAF-16, e.g., lifespan regulation, dauer formation or fat storage (Oh et al., 2006). The canonical consensus DAF-16 binding site or the potential novel DAF-16 binding site discovered by Murphy et al. (2003) were found in promoter regions or coding regions of many (68% and 11%, respectively) of those putative DAF-16 direct target genes. For the rest of the targets (21%), neither the canonical binding site nor the potential novel binding site was present. It is still not clear whether that reflected non-specific clones from the ChIP experiments or indicated that

there are other unidentified DAF-16 binding sites (Oh et al., 2006). However, it is worth mentioning that the DAF-16 target candidates identified by both the microarray and the ChIP experiments were not likely saturated, as the candidate genes recovered by the two methods had very little overlap (Oh et al., 2006).

In addition to the microarray and ChIP studies on the transcriptional outputs of DAF-16, the translational profile associated with DAF-16 was also determined by quantitative mass spectrometry (MS) (Dong et al., 2007). In the quantitative proteomic study, Dong et al. (2007) identified 86 proteins that were more or less abundant when DAF-16 was activated. Among them, 35 proteins were previously uncovered by the microarray and ChIP studies, whereas the remaining 51 proteins were not reported. Despite the obvious differences between individual genes revealed by the proteomic study and microarray studies, the functional groups of the targets revealed by the two studies are consistent in general. Many of those potential DAF-16 targets revealed by MS are annotated to have functions in metabolism and stress response. Indeed, functional studies showed that some of them are involved in dauer formation and lifespan regulation (Dong et al., 2007).

All the genome-wide studies consistently point out that the DAF-16 downstream target genes are involved in various biological processes including stress response, development and metabolism (Figure 1.1). However, as discussed above, none of the approaches was likely to have identified all the DAF-16 direct targets. A complete understanding of DAF-16-based gene regulation will require both additional direct experimental tests as well as bioinformatic analysis.

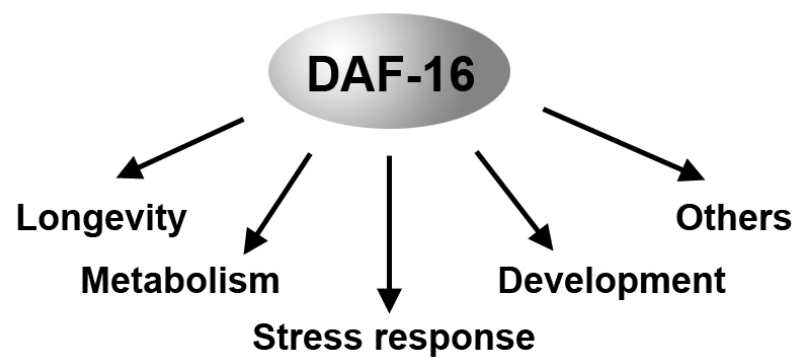


Figure 1.1 The diverse functions of DAF-16.

DAF-16 regulates the expression of its target genes that are involved in longevity, stress resistance, development and metabolism.

1.2 Signaling pathways that regulate DAF-16/FOXO

1.2.1 IIS

Since the first longevity gene *age-1* was identified from a series of long-lived *C. elegans* mutants (Friedman and Johnson, 1988), a handful of longevity genes were identified in the last decade. By genetic and biochemical studies, many of them were found to act in the insulin/IGF-1 signaling (IIS) pathway. So far the IIS pathway is the best characterized aging pathway in *C. elegans* and it was later found to be evolutionarily conserved in other organisms such as flies and mammals (Russell and Kahn, 2007) (Figure 1.2). The IIS pathway negatively regulates the activity of DAF-16/FOXO and has important functions in the regulation of lifespan, metabolism, stress resistance and development.

In the *C. elegans* IIS pathway, the insulin/IGF-like receptor DAF-2 (Kimura et al., 1997) is proposed to be activated by one or more insulin/IGF-like peptides (Figure 1.2). There are in total 40 insulin-like genes in *C. elegans* genome identified so far (Kawano et al., 2000; Li et al., 2003; Murphy et al., 2003; Pierce et al., 2001), which makes the studies complicated due to the potential functional redundancy. One of the insulin-like peptides INS-6 was found to bind directly and activate the human insulin receptor (Hua et al., 2003). However, the assumption that some of the insulin-like peptides serve as DAF-2 ligand(s) *in vivo* remains unvalidated.

The binding of insulin-like peptide(s) to DAF-2 is presumed to initiate an intracellular signaling cascade (Figure 1.4). The DAF-2 receptor activates a phosphatidylinositol 3-kinase (PI(3)K) consisting of a p55-like regulatory subunit (AAP-1) (Wolkow et al., 2002) and a p110 catalytic subunit (AGE-1)

(Morris et al., 1996) which generates phosphatidylinositol-3,4,5-trisphosphate (PIP₃). The activity of AGE-1 can be antagonized by the PIP₃ phosphatase DAF-18, a homolog of the human tumor suppressor PTEN (Ogg and Ruvkun, 1998). PIP₃ is presumed to activate the PDK kinase (Paradis et al., 1999) which phosphorylates the protein kinase B (PKB) AKT-1, AKT-2 (Paradis and Ruvkun, 1998) and a serum and glucocorticoid inducible kinase homolog SGK-1 (Hertweck et al., 2004). Those three kinases in turn phosphorylate the downstream effector DAF-16 and regulate dauer formation, stress response and lifespan (Hertweck et al., 2004; Ogg et al., 1997; Paradis and Ruvkun, 1998; Tullet et al., 2008). When DAF-16 is phosphorylated, it is retained in the cytosol (Lin et al., 1997; Ogg et al., 1997). In mammalian cells, the AKT phosphorylated FOXO3a is sequestered in the cytosol by binding to the 14-3-3 ζ protein (Brunet et al., 1999). My work and studies from other labs demonstrated that such a regulation is also conserved in *C. elegans*: phosphorylated DAF-16 can bind the *C. elegans* 14-3-3 protein FTT-2, which retains it in the cytosol (see Chapter 2). Consistent with the biochemical relationship, genetic studies showed that *daf-16* is epistatic to genes in the IIS pathway; mutations in *daf-16* can completely suppress phenotypes associated with reduced IIS such as lifespan extension, stress resistance, enhanced dauer formation and increased fat storage (Gottlieb and Ruvkun, 1994; Kenyon et al., 1993; Larsen et al., 1995). Thus, DAF-16 is negatively regulated by the IIS pathway. When IIS is reduced, DAF-16 translocates into the nucleus and regulates the transcription of its target genes which presumably confers altered metabolism, increased stress resistance and lifespan extension (Lee et al., 2003a; McElwee et al., 2003; Murphy et al., 2003; Oh et al., 2006).

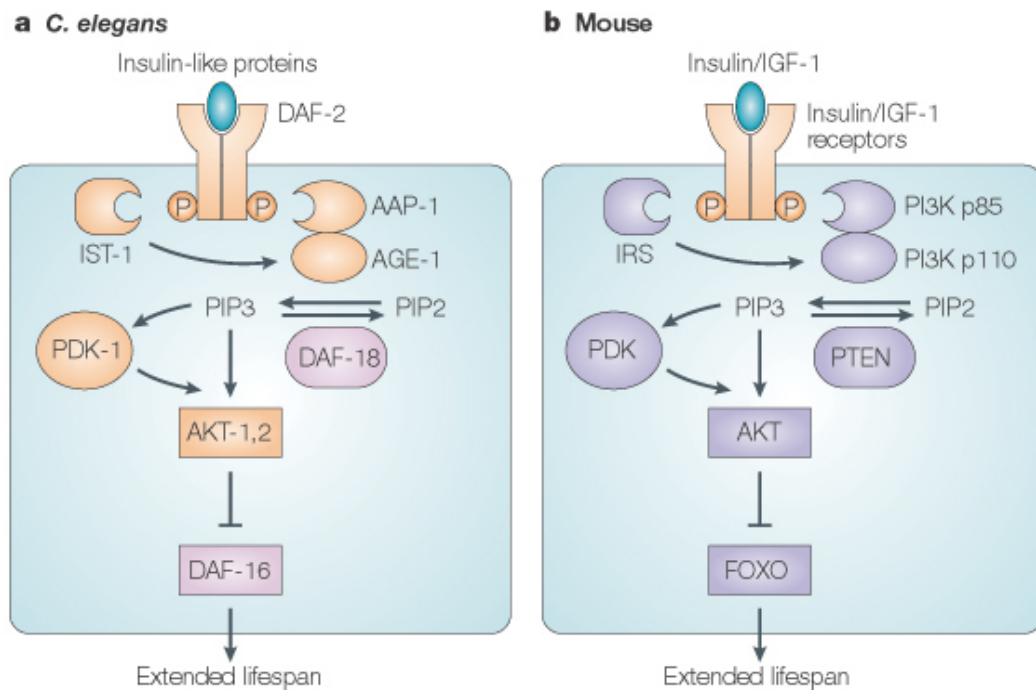


Figure 1.2 The conserved IIS pathway.

Stimulation of DAF-2 and insulin/IGF-1 receptors by their cognate ligands triggers a serine kinase cascade that culminates in phosphorylation and inactivation of the transcription factors DAF-16 and FOXO (in *C. elegans* and mouse, respectively). Reduced activity through this pathway activates DAF-16/FOXO, increasing the transcription of lifespan-promoting and disease-resistance genes. Positive regulators of lifespan in *C. elegans* are colored in pink, whereas negative regulators are colored in orange. Adapted and revised from (Curtis et al., 2005).

In humans, the insulin receptor acts in the target tissues such as muscle, fat and liver, as well as in the signaling cells that control the behavior of target tissues (Myers and White, 1996). It is interesting to know where IIS functions in *C. elegans*. Apfeld and Kenyon reported that IIS regulates dauer formation and lifespan in a cell non-autonomous manner (Apfeld and Kenyon, 1998). In the genetic mosaic studies, they found that a limited number of *daf-2(-)* cells in a wild type (wt) worm can result in increased lifespan and enhanced dauer formation. Consistent with the cell non-autonomy idea, tissue-specific rescue studies revealed that intestinal expression of DAF-16 is responsible for lifespan regulation, whereas the neuronal expression of DAF-16 is sufficient to regulate dauer formation (Libina et al., 2003).

Besides the spatial regulation of its functions, IIS also has temporal patterns in executing its functions. When worms become dauer larvae, the dauer decision needs to be made during L1 larval stage. Thus the IIS pathway is required in the early stages to execute its functions in dauer formation. However, when it comes to lifespan regulation, the temporal requirement of the IIS pathway is different. By reducing IIS at different developmental stages, Dillin et al. (2002) found that manipulating IIS in the larval stages has no impact on the adult lifespan. Instead, the IIS level in the adulthood is crucial for lifespan regulation (Dillin et al., 2002).

It is worth noting that DAF-16 is not the only downstream effector of the IIS pathway. The transcription factor SKN-1 has been recently found to be directly regulated by the IIS pathway in *C. elegans* (Tullet et al., 2008). Like DAF-16, SKN-1 can be phosphorylated by AKT-1, AKT-2 and SGK-1. Similarly, reduced IIS leads to constitutive SKN-1 nuclear accumulation in the intestine and SKN-1 target gene activation. SKN-1 also functions in lifespan

regulation and stress resistance. However, it acts independently of DAF-16. It is therefore proposed to act in parallel to DAF-16 and to be negatively regulated by IIS (Tullet et al., 2008). Another potential IIS downstream effector is the heat shock factor HSF-1. Like DAF-16, HSF-1 is also required for lifespan extension when IIS is reduced (Hsu et al., 2003) and it shares common target genes with DAF-16 such as the small heat shock genes (*shsp*). Hsu et al. (2003) proposed the possibility that IIS mutations could potentially increase the ability of HSF-1 to activate *shsp* expression. A recent genome-wide study implicated that there might be more factors acting downstream of the IIS pathway other than SKN-1 and HSF-1 (Samuelson et al., 2007). In their genome-wide RNAi screen for suppressors of *daf-2(-)* mutants, many genes were found by RNAi inactivation to function specifically in the IIS pathway to shorten lifespan, including *hsf-1*. Genes involved in vesicular trafficking to lysosomes were over-represented in their screen. Protein products encoded by those genes could be potential direct or indirect downstream targets of the IIS pathway and further examination of the relationship between the IIS pathway and those genes is required (Samuelson et al., 2007).

1.2.2 Germline signaling

The reproductive system was also found to influence the lifespan of *C. elegans* (Hsin and Kenyon, 1999). Worms with laser-ablated germline precursor cells can live 60% longer than the wt worms (Hsin and Kenyon, 1999). In contrast to the lifespan extension caused by germline ablation, when the entire gonad is removed, worms do not live longer, suggesting that the lifespan extension in the germline ablated worms is not due to sterility. Further

study demonstrated that neither sperm nor oocytes are required for the lifespan extension in the germline ablated worms, since mutants with sperm or oocyte defects have normal lifespan (Arantes-Oliveira et al., 2002). Interestingly, the lifespan extension of the germline ablated worms requires *daf-16* as well as the nuclear hormone receptor *daf-12* (Hsin and Kenyon, 1999). Consistent with the laser ablation results, genetic mutants with defects in germ cell proliferation such as *glp-1(-)* and *mes-1(-)* also showed *daf-16*-dependent lifespan extension (Arantes-Oliveira et al., 2002). Interestingly, a very recent study revealed that eliminating germ cells in *Drosophila* also increases lifespan, suggesting that the regulation of aging by the germline is evolutionarily conserved (Flatt et al., 2008).

Unlike wt worms, when the entire gonad is removed in some classes of *daf-2(-)* mutants, the lifespan of those mutants can be further increased (Hsin and Kenyon, 1999). It suggests that the germline signaling is independent of the IIS pathway in regulating lifespan. Hsin and Kenyon (1999) proposed that there are two types of gonad-dependent signals that influence lifespan. A signal from the germ cells decreases lifespan by down-regulating the activity of DAF-16. A counterbalancing signal from the somatic gonad increases life span by down-regulating the IIS activity (Figure 1.3).

In the germline ablated worms, DAF-16 was found to localize to the nucleus of intestinal cells (Lin et al., 2001). It remains unclear how the germ cells signal to the intestine. Recently, an intestinal ankyrin repeat protein KRI-1 was identified to be required for the lifespan extension caused by germline defects (Berman and Kenyon, 2006). In addition, it also mediates the intestinal nuclear localization of DAF-16 in those germline defected animals. Based on their study, Berman and Kenyon (2006) proposed that the reproductive system

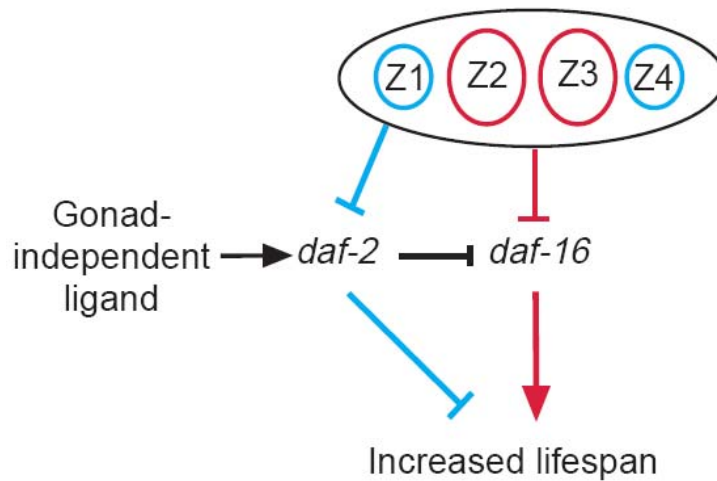


Figure 1.3 Germline signaling in lifespan regulation.

Two types of gonad-dependent signals influence lifespan. A signal from the germ cells decreases lifespan by down-regulating the activity of *daf-16* (red lines) and *daf-12* (not shown). A counterbalancing signal from the somatic gonad increases lifespan by down-regulating *daf-2* activity (blue lines). The somatic gonad signal may be, or may control, a second insulin-like ligand for *daf-2*. In addition to signals from the reproductive system, a gonad-independent signal shortens lifespan by activating *daf-2*, which in turn down-regulates *daf-16* activity. The site of integration of the three signals is not known. In principle, all these signals could act on the same cells, or different signals could act on different cells. Adapted and modified from (Hsin and Kenyon, 1999).

communicates with the intestine, at least in part, via the DAF-9/DAF-12 lipophilic hormone pathway which involves KRI-1 (Berman and Kenyon, 2006).

1.2.3 JNK signaling

The c-Jun N-terminal kinase (JNK) family, a subgroup of the mitogen-activated protein kinase (MAPK) superfamily, is part of a signal transduction cascade that is triggered by external stimuli, including UV radiation and oxidative stress (Davis, 2000). Studies from *Drosophila* first revealed that JNK signaling is an important genetic factor for lifespan regulation (Wang et al., 2003). Further genetic studies suggested that the fly FOXO ortholog dFOXO is required for the lifespan regulation by JNK (Wang et al., 2005). In addition, JNK promotes the nuclear translocation of dFOXO and induces the expression of small heat shock proteins to protect cells from oxidative stress (Wang et al., 2005). In *C. elegans*, over-expression of the JNK orthologs *jnk-1* confers tolerance to oxidative and heat stress, and increases lifespan up to 40% (Oh et al., 2005). The lifespan extension by *jnk-1* over-expression is completely dependent on *daf-16*. In addition, over-expression of *jnk-1* can further increase the lifespan of *daf-2(-)* mutant, suggesting that the JNK signaling acts in parallel with the IIS pathway to regulate lifespan, and both pathways converge on DAF-16 (Figure 1.4). In contrast to IIS, JNK signaling positively regulates DAF-16. Biochemical studies further revealed that JNK-1 physically interacts with and phosphorylates DAF-16 which promotes its nuclear translocation. Consistent with the idea that JNK signaling acts in parallel with the IIS pathway, the JNK-1 phosphorylation sites are different from AKT phosphorylation sites (Oh et al., 2005). Studies from mammalian systems further support the evolutionarily conserved role of JNK signaling in regulating

DAF-16/FOXO. In human, FOXO4 is phosphorylated by JNK at residues Thr447 and Thr451 and the phosphorylation triggers the nuclear translocation of FOXO4 (Essers et al., 2004). Interestingly, JNK also phosphorylates 14-3-3 protein directly, and thereby helps release FOXO proteins from the cytoplasm (Sunayama et al., 2005). It remains unclear whether that phosphorylation is the mechanism by which JNK signaling promotes DAF-16/FOXO nuclear localization in worms and flies. Further studies are required to elucidate the molecular mechanisms for JNK signaling to regulate DAF-16/FOXO.

1.2.4 *SIR2 signaling*

The evolutionary conserved longevity factor silent information regulator 2 (SIR2) belongs to a family of NAD⁺-dependent protein deacetylases. It responds to metabolic changes in the cellular environment, including nutrient/energy availability and cellular stress and has important roles in aging, oncogenesis, metabolism and neurodegeneration (Longo and Kennedy, 2006).

SIR2 was originally isolated from the yeast *Saccharomyces cerevisiae* as a gene important for gene silencing (Rine and Herskowitz, 1987). Later on, it was found that increased dosage of SIR2 in yeast, flies and worms can increase lifespan up to 50% (Kaeberlein et al., 1999; Rogina and Helfand, 2004; Tissenbaum and Guarente, 2001). In yeast, SIR2 promotes the replicative lifespan by inhibiting recombination in the rDNA repeats and therefore inhibiting the formation of extrachromosomal rDNA circles. In worms, lifespan extension resulting from over-expressing *sir-2.1* is completely dependent on *daf-16* (Tissenbaum and Guarente, 2001). Further work suggested that SIR-2.1 physically interacts with DAF-16 *in vivo* and the interaction is promoted by stress stimuli (Berdichevsky et al., 2006). In

addition, over-expression *sir-2.1* promotes *daf-16*-dependent transcription and promotes stress resistance. It is therefore proposed that SIR-2.1 is an activator of DAF-16 following stress in *C. elegans* (Berdichevsky et al., 2006).

Studies from mammalian systems also suggest that SIR2 has a conserved role in regulating DAF-16/FOXO. The human SIR2 ortholog SIRT1 binds and deacetylates FOXOs *in vivo* and *in vitro* at lysine residues that are acetylated by the cyclic-AMP responsive element binding (CREB)-binding protein (CBP/p300) (Brunet et al., 2004; Daitoku et al., 2004; Kobayashi et al., 2005; Motta et al., 2004; van der Horst et al., 2004). Like *C. elegans*, the interactions between SIRT1 and FOXOs in mammalian cells are also in response to stress stimuli (Brunet et al., 2004; Daitoku et al., 2004; Kobayashi et al., 2005; Motta et al., 2004; van der Heide and Smidt, 2005). The interaction and deacetylation regulates the activity of FOXOs. Brunet et al. (2004) proposed a ‘tipping the balance towards survival’ model that SIRT1 inhibits the expression of FoxO-induced pro-apoptotic genes and stimulates the expression of FoxO-induced genes that are involved in cell-cycle regulation and stress resistance (Brunet et al., 2004).

Besides its role in regulating DAF-16/FOXO, SIR2 is also implicated in dietary restriction (DR) mediated lifespan extension in the yeast *Saccharomyces cerevisiae* and the fruit fly *Drosophila melanogaster*. It remains ambiguous whether the worm ortholog SIR-2.1 is also involved in DR (Antebi, 2007; Longo and Kennedy, 2006) and it will not be the focus of this review.

1.3 Other DAF-16/FoxO regulators

Recent studies revealed that DAF-16/FOXO can also be modified by ubiquitination which in turn regulates protein stability (polyubiquitination) or localization (monoubiquitination). Though relatively stable, in response to insulin and serum growth factors, the mammalian FOXOs can be polyubiquitinated and degraded (Aoki et al., 2004; Hu et al., 2004; Huang et al., 2005; Matsuzaki et al., 2003; Plas and Thompson, 2003). The ubiquitin-dependent degradation of DAF-16/FOXO requires its interaction with the F-box protein Skp2, the substrate-binding component of the Skp1/culin 1/F-box protein (SCFSkp2) E3 ligase complex (Huang et al., 2005). Akt-dependent phosphorylation is required for the Skp2-dependent polyubiquitination of FoxO1 (Huang et al., 2005). I κ B kinase (IKK β) mediated phosphorylation of FoxO3a also leads to its polyubiquitination and degradation (Hu et al., 2004). However, the E3 ligase responsible for this event is unknown.

Besides polyubiquitination, FOXOs can also be monoubiquitinated. van der Horst et al. (2006) found that under oxidative stress, monoubiquitination of FOXO4 occurs rapidly and induces its nuclear localization and transcriptional activation (van der Horst et al., 2006). Monoubiquitinated FOXO4 is subsequently deubiquitinated by the deubiquitinating enzyme ubiquitin-specific protease USP7. USP7-mediated deubiquitylation of FoxO4 results in the relocalization of FoxO4 from the nucleus to the cytoplasm. In contrast to the phospho-dependent polyubiquitination, this reversible monoubiquitination does not influence FOXO protein stability. Two conserved lysine residues, K199 and K211 are targeted for monoubiquitination (van der Horst et al., 2006). Interestingly, the lysine residues are also the targets for CBP/p300-mediated

acetylation, suggesting that the competition between monoubiquitination and acetylation may play an important role in the regulation of FOXO.

In worms, DAF-16 can also be regulated by polyubiquitination. Li et al. (2006) reported that RLE-1 is the putative E3 ubiquitin ligase for the polyubiquitination of DAF-16 (Li et al., 2007b). Eliminating RLE-1 resulted in elevated DAF-16 protein without affecting *daf-16* mRNA level. Biochemical studies supported that RLE-1 catalyzes DAF-16 polyubiquitination which leads to degradation by the proteasome (Li et al., 2007b).

Recently, two other DAF-16 regulators have been identified. SMK-1, ortholog of mammalian SMEK1, was identified as an essential regulator for DAF-16-mediated longevity (Wolff et al., 2006). However, it does not regulate dauer formation or the reproductive functions of DAF-16. SMK-1 colocalizes with DAF-16 and serves as a transcriptional regulator specific for the regulation of oxidative stress, UV, and innate immunity, but is not required for the thermal response functions of DAF-16. Thus, SMK-1 appears specific to the regulation of DAF-16-mediated longevity and specific stress response in *C. elegans* (Wolff et al., 2006). It is not yet known whether orthologs of SMK-1 proteins in the other organisms affect longevity and the stress response although this protein is evolutionarily conserved.

Another DAF-16 regulator that was recently identified is BAR-1. BAR-1 is the *C. elegans* ortholog of β -Catenin factor. Esser et al. (2005) found that loss of BAR-1 reduces the activity of DAF-16 in dauer formation and life span (Essers et al., 2005). BAR-1 physically interacts with DAF-16 and the interaction can be enhanced by oxidative stress. Furthermore, BAR-1 is required for the oxidative stress-induced expression of DAF-16 target gene *sod-3* and for resistance to oxidative damage. The regulation of DAF-

16/FOXO by β -Catenin seems to be evolutionarily conserved. In mammalian cells, β -Catenin can also directly bind FOXO and enhances FOXO transcriptional activity (Essers et al., 2005).

As reviewed above, DAF-16/FOXO can be regulated at different levels, e.g., nuclear translocation (promoted by JNK signaling and monoubiquitination and inhibited by IIS), protein stability (polyubiquitination) and transcriptional activity (SIR-2.1 and SMK-1) once it is inside of the nucleus. It is subjected to several post-translational modifications including phosphorylation (IIS and JNK signaling), acetylation/deacetylation (SIR-2.1 signaling) and polyubiquitination / monoubiquitination / deubiquitination. Given the important roles of DAF-16/FOXO in diverse biological processes, it is not surprising that it needs fine-tuned regulation to elicit appropriate cellular responses. Although much effort has been taken to understand how it is regulated, we still have very limited knowledge about it and many open questions remain. For example, additional regulators of DAF-16 must be required to modulate DAF-16 activity once it is inside of the nucleus since constitutive nuclear localization of DAF-16 is not sufficient to increase lifespan when IIS is reduced (Lin et al., 2001). The hunting for DAF-16/FOXO regulators has just begun and in this dissertation, I will discuss my work on two DAF-16 regulators in *C. elegans*.

1.4 Dissertation outline

This dissertation describes the identification and characterization of factors that regulate the transcription factor DAF-16 in *C. elegans*.

Chapter 2 focuses on the 14-3-3 protein FTT-2 which regulates the cytoplasm/nuclear translocation of DAF-16. In this chapter, the DAF-16-regulating role of the other *C. elegans* 14-3-3 protein PAR-5 was also examined and compared to FTT-2. My work demonstrates the conserved role of 14-3-3 proteins in DAF-16/FOXO regulation in *C. elegans* and distinguishes the two *C. elegans* 14-3-3 proteins FTT-2 and PAR-5 in DAF-16/FOXO regulation.

Chapter 3 describes the distinct role of the host cell factor HCF-1 as a DAF-16 negative regulator. My work suggests that HCF-1 genetically and physically interacts with DAF-16. It functions in the nucleus and regulates DAF-16 activity by limiting DAF-16 from accessing its target gene promoters, and thereby regulating DAF-16-mediated transcription of selective target genes.

Chapter 4 summarizes my work as well as my thoughts on directions for future study.

Appendix I describes the tests of genetic interactions between *hcf-1* and the other known longevity genes in *C. elegans*.

Appendix II summarizes the interaction between HCF-1 and the protein deacetylase SIR-2.1 and the regulation of SIR-2.1 by HCF-1.

Appendix III describes my effort to use gel filtration to dissect the HCF-1/DAF-16 protein complex.

CHAPTER 2

THE 14-3-3 PROTEIN FTT-2 BINDS DAF-16 AND RETAINS IT IN THE CYTOPLASM¹

2.1 Introduction

C. elegans DAF-16 is the major downstream effector of the *daf-2*/insulin-like signaling pathway. When *daf-2*/insulin-like signaling is reduced or inactivated, DAF-16 becomes dephosphorylated and migrates into the nucleus to affect gene expression (Halaschek-Wiener et al., 2005; Lin et al., 2001; McElwee et al., 2003; Murphy et al., 2003). Nuclear translocation and eventual activation of DAF-16 likely induces gene expression changes that promote dauer formation and longevity extension (Halaschek-Wiener et al., 2005; Lee et al., 2003a; McElwee et al., 2003; Murphy et al., 2003). The *daf-2* pathway in *C. elegans* is entirely orthologous to the insulin/IGF-1 signaling pathways in fruit flies and mammals (Clancy et al., 2001; Holzenberger et al., 2003; Tatar et al., 2001). Four mammalian DAF-16 orthologs (FOXO1, FOXO3a, FOXO4 and FOXO6) have been characterized to regulate apoptosis, oxidative stress response, DNA repair, and metabolism (Birkenkamp and Coffey, 2003). In mammalian cultured cells, the subcellular localization of FOXO3a is regulated by binding to the 14-3-3 ζ protein. When FOXO3a is phosphorylated by protein kinase B/Akt, it is bound by 14-3-3 ζ and sequestered in the cytoplasm (Brunet et al., 1999). Since the insulin/IGF-1 signaling pathway is highly conserved, it is possible that *C. elegans* DAF-16 is also regulated by a similar mechanism.

¹ This chapter is modified slightly from Li, Tewari, Vidal and Lee (2007) *Developmental Biology* 301, 82-91. Dr. Tewari and Dr. Vidal constructed the RNAi library for signaling molecules in *C. elegans*.

14-3-3 proteins are a family of highly conserved, abundant cytoplasmic proteins identified in all eukaryotic organisms examined. They are small (~30 kD), acidic proteins that usually function as hetero or homo-dimers (Jones et al., 1995). In general, 14-3-3 proteins bind to the phosphorylated form of substrate proteins. A large number of proteins are found to contain a consensus 14-3-3 recognition motif: RSXpSXP or RXXXpSXP (Yaffe et al., 1997), in which the phosphorylated serine is essential for binding (Pozuelo Rubio et al., 2004). However, 14-3-3 proteins are also capable of binding to several unphosphorylated ligands (Masters et al., 1999). By binding to their substrates, 14-3-3 proteins can induce the conformational change of the substrate proteins (Obsil et al., 2001; Yaffe, 2002), or sequester the substrate proteins in the cytoplasm (Grozingier and Schreiber, 2000), or act as a scaffold that bridges two interacting partners (Agarwal-Mawal et al., 2003). By binding to a diverse group of signaling molecules, such as Raf -1 (Fu et al., 1994; Irie et al., 1994), Cdc25 phosphatase family members (Chen et al., 2003; Forrest and Gabrielli, 2001; Peng et al., 1997) and Bad (Datta et al., 2000), 14-3-3 proteins are thought to participate in a wide variety of cellular processes, including cell cycle checkpoints, DNA repair, cell differentiation and apoptosis (Fu et al., 2000). 14-3-3 proteins typically have several isoforms in one given organism. For example, there are seven known isoforms in mammals (Ichimura et al., 1988; Martin et al., 1993) and thirteen in *Arabidopsis* (DeLille et al., 2001). In *C. elegans*, two 14-3-3 encoding genes have been identified: *par-5/ftt-1* and *ftt-2* (Wang and Shakes, 1996). *par-5* is required for cellular asymmetry in the early *C. elegans* embryo. PAR-5 regulates the asymmetric cortical localization of PAR-1 and PAR-2 to the posterior and PAR-3, PAR-6 and PKC-3 to the anterior (Morton et al., 2002). Until recently, the function and

protein substrates of FTT-2 were not known (Berdichevsky et al., 2006; Wang et al., 2006a).

Using gene-specific RNAi knock down, we showed that the *C. elegans* 14-3-3 protein FTT-2 regulates DAF-16 activities by forming a protein complex with DAF-16 and preventing DAF-16 from entering the nucleus to regulate transcription. Our results indicate that the DAF-16 sub-cellular localization is regulated by a conserved mechanism similar to that of FOXO in mammalian cells. In contrast to *ftt-2*, *par-5*, the only other gene predicted to encode a 14-3-3-like protein in *C. elegans*, has no effect on dauer formation, DAF-16 localization or DAF-16 transcriptional activities, highlighting the functional specification of two highly homologous 14-3-3 members.

2.2 Materials and Methods

2.2.1 Strains and maintenance

The strains used in this paper were as follow: wild type N2 (from the *C. elegans* Genetic Center), *daf-16* (*mgDf47*), *rrf-3*(*pk1426*), *daf-2* (*e1370*), *daf-16*(*mgDf47*); *xrls87*[*daf-16a::gfp::DAF-16B*, *rol-6*(*su1006*)], *daf-2*(*e1370*); *daf-16*(*mgDf47*); *xrls87*[*daf-16a::gfp::DAF-16B*, *rol-6*(*su1006*)], *mul84*[*pAD76*(*sod-3::gfp*)]. All strains were maintained on NGM plates seeded with *Escherichia coli* OP50 as the food source.

2.2.2 Construction of *ftt-2* and *par-5* specific RNAi constructs

The sequences corresponding to the 3' end and 3'UTR of the predicted *ftt-2* and *par-5* transcripts were amplified from genomic DNA of N2 worms by PCR. The primers used for the *par-5* RNAi construct: Forward primer: 5'-*tggacatctgacgttgagactga* -3'; Reverse primer: 5'-*ggaatgacaatagtgacggagtg* -

3'. The primers used for the *ftt-2* RNAi construct: Forward primer: 5'-acgctgccaccgatgacactg -3'; Reverse primer: 5'-aaggggggaaaagccgtaacaaaa -3'. The *ftt-2* primers and the *par-5* forward primer are kind gifts from the Kemphues lab (K. Kemphues, Cornell University, Ithaca NY). The RNAi constructs were generated by inserting the *ftt-2* or *par-5* PCR products into the L4440 vector (a kind gift from Dr. A. Fire, Stanford). The RNAi plasmids were transformed into *Escherichia coli* HT115 (Timmons et al., 2001) for feeding RNAi experiments. All other feeding RNAi clones have been described previously (Lee et al., 2003b).

2.2.3 RNAi

Feeding RNAi was performed as described (Lee et al., 2003b). Briefly, RNAi bacteria were grown in Luria both with 50 $\mu\text{g ml}^{-1}$ ampicillin at 37°C for 10-16 hrs, seeded onto NGM plates containing 2mM IPTG, and induced at room temperature overnight.

2.2.4 Dauer assay

Dauer assay for *daf-2(e1370)* strain was performed as described (Lee et al., 2003b). *daf-2(e1370)* (Gems et al., 1998) worms at the L4 stage were put onto RNAi plates and allowed to lay egg over night. The resulting self-progeny were allowed to develop at 22°C. At ~96 hrs after egg lay, the number of dauers and adult worms on each plate were scored. Five plates were scored for each RNAi treatment. Dauer assay for N2 or *rrf-3(pk1426)* strain was performed at 25°C and the number of dauers in each population was scored at ~ 72 hrs after egg lay. The dauer assays were repeated three times.

2.2.5 DAF-16::GFP localization assay

The construction and characterization of the *daf-16(mgDf47); xrls87[daf-16a::gfp::DAF-16B, rol-6(su1006)]* transgenic strain have been described (Lee et al., 2001). DAF-16::GFP transgenic worms at the L4 stage were put onto the RNAi bacteria and allowed to lay egg at 16°C over night. Self-progeny were allowed to develop on the RNAi bacteria at 16°C till they were at the L3 stage. The worms were cultured at 16°C to allow for a longer time for RNAi to take effect before the worms reached the L3 stage for scoring. The GFP expression of the DAF-16::GFP worms feeding on the various RNAi bacteria was monitored using a fluorescent microscope (Leica MZFL III) and images were captured using a Hamamatsu ORCA-ER camera and OpenLab software.

2.2.6 Lifespan assay

Unless stated otherwise, lifespan assays were performed at 22°C. N2 or *daf-2(e1370)* L4 larvae worms were allowed to lay egg over night on RNAi plates and the progeny grew on RNAi plates at 16°C until the young adult stage. The young adult worms were transferred onto RNAi plates containing 0.1g/ml FUDR to prevent the growth of progeny and shifted to 22°C. The adult population was scored every day or every other day. Animals that failed to respond to a gentle prodding with a platinum wire were scored as dead. Day 0 of adult lifespan is the day that the adult worms were exposed to FUDR. Statistical analysis was performed with the Kaplan-Meier method to test the null hypothesis (SPSS v.11). The lifespan assays were repeated two times and similar results were observed in both experiments.

2.2.7 IP and Western Blot

N2, *daf-16::gfp*, *daf-2(e1370)*; *daf-16::gfp*, or *Psod-3::gfp* mixed staged worms were collected by washing with M9 buffer, packed by centrifugation at 3000g for 30 sec and frozen in liquid nitrogen in ~100 μ l aliquot. *Psod-3::gfp* worms were starved for 1 day to induce the GFP expression at a comparable level before collected. *daf-2(e1370)*; *daf-16::gfp* worms were shifted to 25°C for 6 hrs before collected to induce nuclear localization of DAF-16::GFP. Depending on the size of the frozen worm pellet, approximately 4X volume of lysis buffer (50 mM HEPES pH 7.5, 1 mM EDTA, 150 mM NaCl, 10% Glycerol, 0.1% Triton X-100, 1 mM sodium fluoride and protease inhibitor cocktail) was added. The worm pellets were allowed to thaw at room temperature completely and then frozen in liquid nitrogen again. The thaw-and-freeze procedures were repeated four times. The worm lysate was then sonicated using Markson Ultrasonic Processor for 10 x 15 sec bursts with 30 sec pauses at the output of 60. The debris was removed by centrifugation. The worm lysate was subsequently pre-cleared with 1/20 volume of protein A slurry (Pierce) over night at 4°C. The pre-cleared lysate was incubated with antibody (10 μ l antibody per 400 μ g total protein) for 1.5 hr at 4°C. 1/10 volume of BSA-blocked protein A slurry was then added and incubated for 1.5 hr at 4°C. The protein A beads were then washed with lysis buffer for six times and the bound proteins were eluted by boiling in 2X sample buffer for 5 min. The anti-FTT-2 and anti-PAR-5 antibodies used for IP are kind gifts from Dr. Andy Golden (NIDDK, National Institutes of Health, Bethesda, MD). The anti-FTT-2 antibody was generated against a small peptide at the extreme C-terminus of FTT-2 (CAATDDTDANETEGGN), and the anti-PAR-5 antibody has been previously reported (Morton et al., 2002). Protein samples eluted from the protein A

beads were separated on a 10% SDS gel and transferred onto nitrocellulose membrane (BA85 Protran® BioScience) followed by standard Western blot procedure. The primary antibodies used: anti-ACTIN (mouse, Chemicon International), anti-GFP (goat, Rockland), anti-FTT-2 (rabbit, a gift from Dr. Andy Golden) and anti-PAR-5 (rabbit, a gift from Dr. Andy Golden). The secondary antibodies are: anti-goat (Rockland), anti-mouse (Santa Cruz) and anti-rabbit (Rockland). The IP experiments were repeated three times.

2.2.8 qRT-PCR

Synchronized young adult worms of the indicated genotypes were grown at 16°C and collected by washing with M9 buffer and frozen in liquid nitrogen. Total RNA of ~100 µl worm pellet was isolated using the RNeasy® Mini Kit (Qiagen) and quality control was done by both gel electrophoresis and UV absorbance measurement. cDNAs were synthesized with random hexamers by using SuperScript™ III First-Strand Kit (Invitrogen) according to the manufacturer's protocol. Real-time PCR reactions were performed in a 20 µl volume using iQ™ SYBR® Green Supermix (BIO-RAD) in a 96-well plate. Duplicates for each sample were included for one single reaction. The real-time PCR primers are summarized in Table 2.1. *act-1* was used as the internal control and the RNA level of a gene of interest was normalized to the *act-1* level for comparison. PCR reaction was initiated at 95°C for 10 minutes for denaturation followed by a 40-cycles consisting of 15 sec at 95°C and 60 sec at 60°C. The real-time PCR experiments were repeated three to four times using independent RNAi worms and RNA preparations. Dauer worms grown at 22°C were not used for qRT-PCR experiments because the asynchrony among the different RNAi worms caused large variations in mRNA expression.

Table 2.1 Primers for qRT-PCR.

Gene	Sequence		Product
<i>act-1</i>	Forward	5'- CCAGGAATTGCTGATCGTATGCAGAA -3'	133 bp
	Reverse	5'- TGGAGAGGGAAGCGAGGATAGA -3'	
<i>sod-3</i>	Forward	5'- TCGCACTGCTTCAAAGCTTGTTCAA -3'	98 bp
	Reverse	5'- CCAAATCTGCATAGTCAGATGGGAGAT -3'	
<i>ftt-2</i>	Forward	5'- TCGACAAGTTCCTCATTCCA -3'	145 bp
	Reverse	5'- TAGCTTTGCTGCGACTTCTC -3'	
<i>par-5</i>	Forward	5'- AAGTCCCAGAAGGCTTACCA -3'	57 bp
	Reverse	5'- TGGCTGCATCTTGTCCTTAG -3'	
C24B9.9	Forward	5'- AAAAAGCCATGTTCCCGAAT -3'	137 bp
	Reverse	5'- GCTGCGAAAAGCAAGAAAAT -3'	
F53C3.12	Forward	5'- CGTGTACAGAGACCCCGAAT -3'	92 bp
	Reverse	5'- TGAAGTGCCACGTATTTGGA -3'	

2.2.9 Brood size assay

The brood size of RNAi treated worms was determined at 22°C. For each RNAi, ~10 N2 L4 larvae worms were singled onto each RNAi plate and allowed to lay egg over night and then transferred to fresh RNAi plate each subsequent days to lay egg until reproduction ended. The total number of eggs laid and hatched on each plate was counted every day. The brood size assays were repeated two times.

2.2.10 Developmental rate assay

The developmental rate of each RNAi worm population was determined at 22°C. For each RNAi, six gravid adults were allowed to lay egg for 1 hr. The times required for the progeny to reach adulthood were scored. The developmental rate assays were repeated two times.

2.3 Results and Discussion

2.3.1 RNAi inactivation of *ftt-2*, but not *par-5*, enhances dauer formation.

To identify new components of the *daf-2*/insulin-like signaling pathway, we used feeding RNAi to knock down a select group of molecules annotated as being involved in signal transduction (Rual et al., 2004) and specifically examined their potential role in *C. elegans* dauer formation. In general, feeding RNAi gene knock down is not an efficient way to reveal a possible dauer phenotype, probably because feeding RNAi does not work well in the nervous system (Tavernarakis et al., 2000; Timmons et al., 2001). Interestingly, at the semi-restrictive temperature 22°C, the *daf-2(e1370)* mutant worms form 100% dauer for ~72 hrs and then exit dauer to develop into gravid adults. This represents a sensitized genetic background for using feeding RNAi to identify

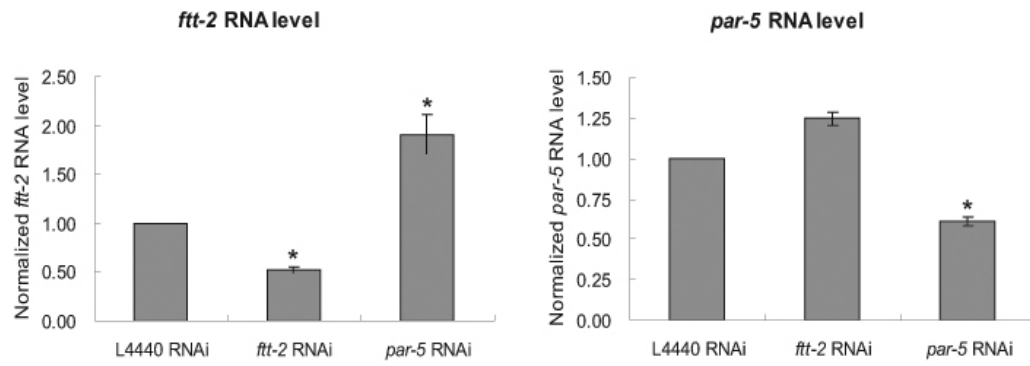
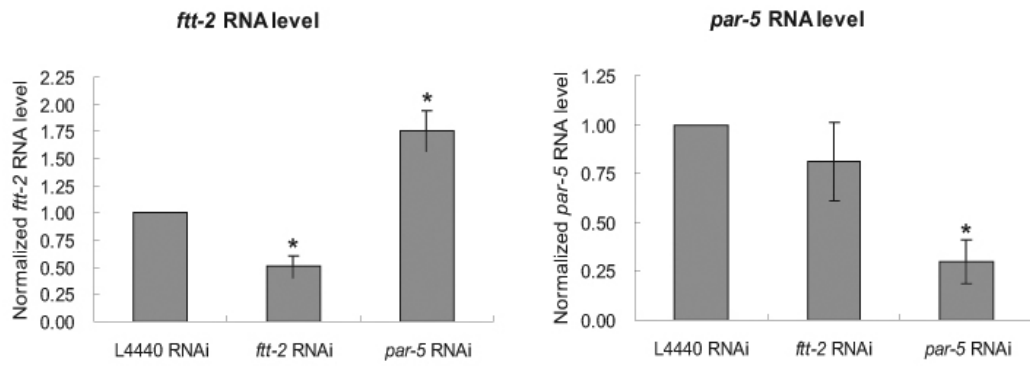
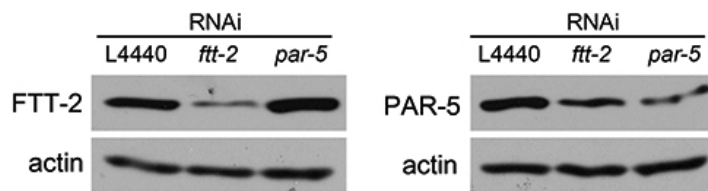
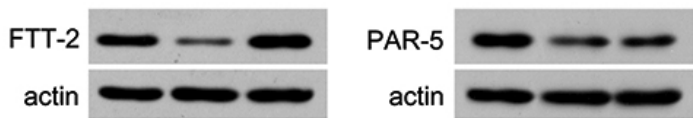
new players in *daf-2*-mediated dauer regulation. We found that RNAi knock down of the two 14-3-3 encoding genes, *ftt-2* and *par-5*, greatly enhanced the dauer arrest phenotype of *daf-2(e1370)*. At 22°C, 100% of the *daf-2(e1370)* worms fed with *ftt-2* RNAi and 45% of the *daf-2(e1370)* worms fed with *par-5* RNAi remained as dauer at the 96 hr time point, whereas only 4.5% of the *daf-2(e1370)* worms fed with the empty vector control L4440 RNAi remained as dauer at this time point.

ftt-2 and *par-5* are the two putative 14-3-3 encoding genes in *C. elegans*. The predicted transcripts of these two genes share ~78.2% sequence identity at the nucleotide level and ~85.9% sequence identity at the amino acid level (Wang and Shakes, 1997). The *ftt-2* and *par-5* RNAi constructs we initially used for the dauer screen include the full-length sequence of *ftt-2* and *par-5* respectively. Stretches of consecutive identical sequence as long as 19 bp are detected between the *ftt-2* and *par-5* RNAi constructs and we suspected that these two RNAi constructs might cross-react and caused the knock down of both *ftt-2* and *par-5*. In order to evaluate the specific roles of *ftt-2* and *par-5* in dauer formation, we generated gene-specific RNAi constructs that targeted unique fragments corresponding to the 3' coding and UTR regions of either *ftt-2* or *par-5* (Morton et al., 2002). Sequence alignment indicates that the longest stretch of sequence identity between the gene-specific *ftt-2* and *par-5* RNAi constructs is only 6 bp. To verify the specificity of the RNAi constructs, we used qRT-PCR to quantify the *ftt-2* and *par-5* mRNA levels in wild type (N2) and *daf-2(e1370)* animals that were undergoing RNAi against either the *ftt-2* or *par-5* gene (Figure 2.1A and 2.1B). We detected a specific 2-fold knock down of the *ftt-2* and *par-5* mRNA levels in worms exposed to the corresponding gene-specific RNAi. Furthermore, N2

Figure 2.1 The *ftt-2* and *par-5* RNAi constructs are gene-specific.

N2 (A) or *daf-2(e1370)* (B) worms were exposed to feeding RNAi bacteria starting as L1 at 16°C. Total RNA was extracted from young adult RNAi worms for real-time-PCR analysis. The y-axis indicates the relative RNA levels normalized to the RNA expression levels of the internal control *act-1*. The relative RNA levels for worms treated with the L4440 control RNAi is set as 1. The average of four independent experiments is shown and the error bars represent standard error of the mean (SEM). P-value of <0.01 (*) was determined by Student's t-test.

FTT-2 or PAR-5 immunoblotting was performed using young adult N2 worms exposed to the indicated RNAi bacteria at 16°C (C) or *daf-2(e1370)* dauer worms exposed to the indicated RNAi bacteria at 22°C (D).

A**B****C****D**

worms fed with the *par-5*-specific RNAi bacteria for two generations showed severe embryonic lethality (data not shown), similar to that reported previously (Morton et al., 2002). In contrast, N2 worms treated with the *ftt-2* specific RNAi for two generations exhibited reduced brood size but did not show noticeable embryonic lethality (Figure 2.2). The molecular and phenotypic evidence strongly supports that the *ftt-2* and *par-5* RNAi constructs we generated specifically targeted the corresponding genes.

We also used anti-FTT-2 and anti-PAR-5 immunoblotting to confirm that the FTT-2 and PAR-5 protein levels were reduced in the *daf-2(e1370)* dauer worms treated with the gene-specific RNAi at 22°C (Figure 2.1D). We found that the anti-FTT-2 signal was specifically reduced in *daf-2(e1370)* worms treated with the *ftt-2* RNAi, but not in worms treated with the *par-5* RNAi. In contrast, we noticed that the anti-PAR-5 signal was reduced in worms treated with either the *par-5* or *ftt-2* RNAi. Similar results were also observed in N2 worms (Figure 2.1C). Taken together, the immunoblotting, the qRT-PCR, and the phenotypic results let us to propose that the anti-FTT-2 antibody specifically recognizes FTT-2, whereas the anti-PAR-5 antibody may cross-react with both PAR-5 and FTT-2.

We retested whether specific knock downs of either *par-5* or *ftt-2* were able to enhance the dauer arrest phenotype of *daf-2(e1370)* at 22°C. *daf-2(e1370)* worms were exposed to *par-5* or *ftt-2* RNAi starting as embryos and allowed to develop at 22°C. The empty vector L4440 was used as a negative control, and the *daf-2* RNAi was included as a positive control. At 96 hr, when most of the worms treated with L4440 RNAi exited dauer and developed into sterile/gravid adults, the majority of the *ftt-2* RNAi worms remained in the dauer stage (Table 2.2). In fact, the *ftt-2* RNAi treated *daf-2(e1370)* worms

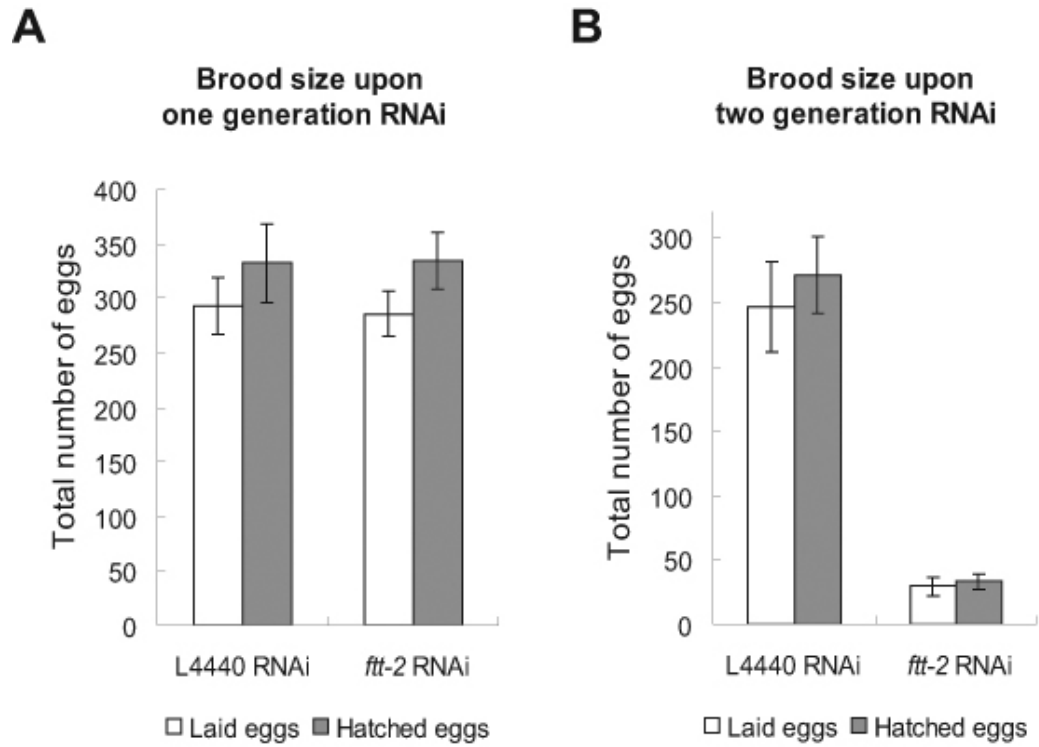


Figure 2.2 The brood size of *ftt-2* RNAi worms upon one generation (A) or two generations (B) of RNAi treatment.

The average brood size of ~10 worms for each RNAi treatment is shown. Error bars represent SEM.

remained arrested as dauer for the entire length of our experiments, which were usually carried out for ~240 hrs, similar to that of the positive control *daf-2* RNAi worms. In contrast, worms treated with *par-5* RNAi behaved similarly to worms treated with L4440 RNAi (Table 2.2). These results indicate that despite the high sequence homology between *par-5* and *ftt-2*, *ftt-2* has the unique function of interacting with the *daf-2* pathway and affecting dauer formation.

RNAi knock down of *ftt-2* in wild-type N2 or *rrf-3(pk1426)*, a strain that specifically enhances somatic RNAi effects (Simmer et al., 2002), background resulted in normal development and no observable dauer arrest phenotype at either 22°C or 25°C (Table 2.2 and data not shown). This is not surprising as RNAi inactivation of *daf-2* did not induce dauer formation in the N2 background (Table 2.2). Moreover, our qRT-PCR and immunoblotting experiments indicate that the gene-specific *ftt-2* RNAi only causes a ~2-fold decrease in FTT-2 levels (Fig. 2.1). It is possible that such a modest reduction in FTT-2, while sufficient to promote dauer arrest in a sensitized background, is not able to signal dauer arrest in a wild-type background. Although a *ftt-2* deletion mutant is available through the knockout consortium (<http://www.wormbase.org/>), we are not able to analyze its dauer formation phenotype because the homozygous *ftt-2* deletion mutant is not viable (JL & SSL, unpublished data; (Wang et al., 2006b).

2.3.2 RNAi inactivation of *ftt-2* promotes DAF-16::GFP nuclear localization.

Our results indicate that reduced *ftt-2* expression specifically enhances the dauer formation phenotype associated with reduced *daf-2*/insulin-like signaling. Because *daf-16* is the major downstream effector of *daf-2* signaling

Table 2.2 RNAi inactivation of *ftt-2* promotes dauer formation in *daf-2(e1370)* at 22°C.

	Gene inactivation by RNAi	L4440	<i>daf-2</i>	<i>daf-16</i>	<i>ftt-2</i>	<i>par-5</i>
<i>daf-2 (e1370)</i> at 22°C	% of worms in dauer stage	4.5%	100%	0%	99.5%	4.6%
	Total number of worms scored	334	214	423	184	328
N2 at 25°C	% of worms in dauer stage	0%	0.8%	0%	0%	0%
	Total number of worms scored	579	601	628	589	557

daf-2(e1370) mutant worms or N2 worms were exposed to the various RNAi bacteria starting as embryos and allowed to develop at the indicated temperature. Total number of worms scored and the percentage of worms remained in the dauer stage on day 4 (for *daf-2(e1370)*) or day 3 (for N2) are shown. *ftt-2* and *daf-2* RNAi dramatically enhances dauer formation in *daf-2(e1370)* at 22°C, whereas *par-5* RNAi behaves similarly to the L4440 control RNAi. However, neither *ftt-2* nor *daf-2* RNAi was able to significantly enhance dauer formation in N2 worms at 25°C.

and increased DAF-16 activity is critical for promoting dauer arrest, we investigated whether RNAi knock down of *ftt-2* might affect *daf-16* activity. A key step of DAF-16 regulation is the translocation of DAF-16 from the cytoplasm to the nucleus. We used feeding RNAi to inactivate *ftt-2* in worms carrying an integrated *gfp*-fused *daf-16* transgene (*daf-16::gfp*) (Lee et al., 2001). The *daf-16::gfp* worms fed with *ftt-2* RNAi tended to arrest at the L3 stage, but they developed to the L3 stage at a rate similar to that of control RNAi worms. We therefore monitored the DAF-16::GFP localization in L3 animals. When the *daf-16::gfp* worms were fed with the control L4440 RNAi, the DAF-16::GFP fusion protein was evenly distributed in the cytoplasm and nucleus of cells throughout the body of the worm (Figure 2.3A). Consistent with previous reports, when *daf-2* was inactivated by RNAi, the DAF-16::GFP fusion protein became intensely localized in the nucleus of cells, although some cytoplasmic staining remained detectable (Figure 2.3D) (Lin et al., 2001). Interestingly, when *ftt-2* was RNAi inactivated, the DAF-16::GFP fusion protein was also dramatically enriched in the nucleus of cells (Figure 2.3B), although a low level of cytoplasmic DAF-16::GFP remained detectable. In contrast, *par-5* RNAi knock down did not significantly affect the localization pattern of DAF-16::GFP (Figure 2.3C). These results indicate that reduced *ftt-2* expression specifically induces the nuclear enrichment of DAF-16.

2.3.3 Enhanced DAF-16 transcriptional activities upon *ftt-2* RNAi.

Because nuclear translocation of DAF-16 may allow DAF-16 to access its transcriptional targets, we next investigated whether *ftt-2* RNAi promoted the transcriptional activities of DAF-16. To accomplish this, we exposed N2 or *daf-16(mgDf47)* null mutant worms to *ftt-2* RNAi and monitored the mRNA

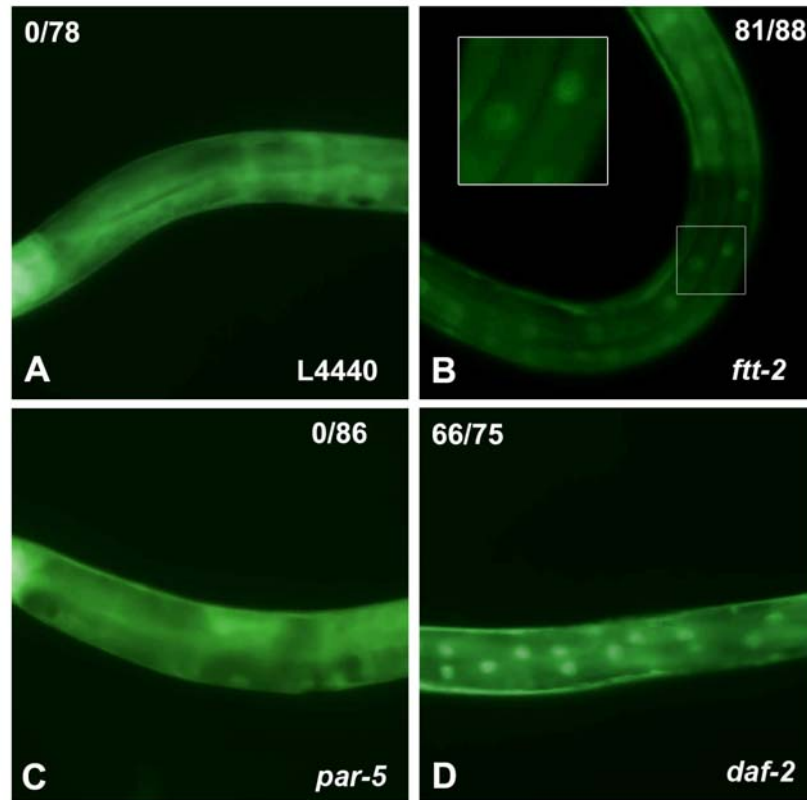


Figure 2.3 *ftt-2* RNAi, but not *par-5* RNAi, causes DAF-16::GFP accumulation in the nucleus.

DAF-16::GFP worms were exposed to the various RNAi bacteria starting as embryos at 16°C. DAF-16::GFP expression of the RNAi worms at the L3 stage are shown. None of the 78 worms exposed to the control L4440 RNAi (panel A) nor the 86 worms exposed to *par-5* RNAi (panel C) showed DAF-16::GFP nuclear localization. In contrast, 81 out of 88 worms exposed to *ftt-2* RNAi (panel B) and 66 out of 75 exposed to *daf-2* RNAi (panel D) exhibited prominent DAF-16::GFP nuclear localization. A small number of *daf-2* RNAi or *ftt-2* RNAi worms continued to exhibit cytoplasmic DAF-16::GFP, probably due to variable RNAi efficiency. The images (A-D) were captured using identical magnification and exposure time.

levels of *sod-3*, a well-characterized DAF-16 direct target gene (Honda and Honda, 1999; Wook Oh et al., 2006). Consistent with previous reports (Honda and Honda, 1999), we detected ~5-fold up-regulation of *sod-3* levels in N2 worms treated with *daf-2* RNAi (Figure 2.4A). Importantly, when N2 worms were fed *ftt-2* RNAi, the expression levels of *sod-3* were upregulated about 2-fold (Figure 2.4A), suggesting that the transcriptional activities of DAF-16 were elevated. The increased *sod-3* expression in *ftt-2* RNAi treated N2 worms was not due to a change in *daf-16* levels, as the *daf-16* mRNA levels were not significantly different in worms treated with the different RNAi (data not shown). Consistent with the distinction between *ftt-2* and *par-5* on dauer promotion and DAF-16::GFP translocation, reduction of *par-5* did not affect DAF-16 transcriptional activities. Similar RNAi experiments performed in the *daf-16(mgDf47)* null mutant indicate that the induction of *sod-3* expression observed in the *ftt-2* or *daf-2* RNAi worms was mediated by *daf-16*. In *daf-16(mgDf47)* null mutant worms treated with control L4440 RNAi, very low basal expression of *sod-3* was observed (Figure 2.4A). Furthermore, in *daf-16(mgDf47)* null mutant worms, neither *ftt-2* nor *daf-2* RNAi had any significant effect on the low basal level of *sod-3* expression (Figure 2.4A).

We examined the mRNA levels of additional DAF-16 downstream genes (Murphy et al., 2003). As expected, the DAF-16 activated genes C24B9.9 & F53C3.12 exhibited robust expression changes when worms were treated with *daf-2* RNAi vs. *daf-16* RNAi (Figure 2.4B & 2.4C). For these two genes, increased expression was also detected in *ftt-2* RNAi worms, consistent with an elevation of DAF-16 activities in *ftt-2* knock down worms. The results we described thus far suggest the model that RNAi inactivation of

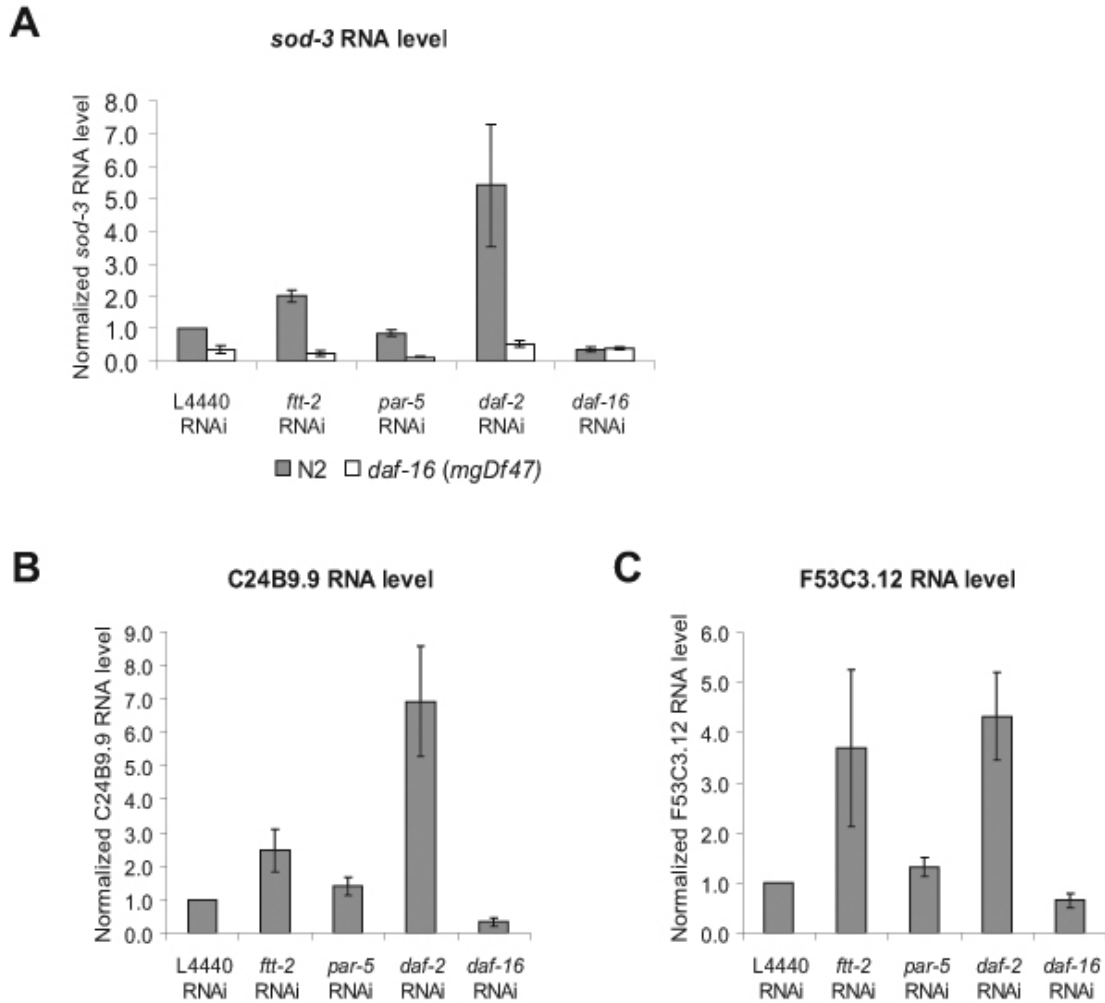


Figure 2.4 RNAi inactivation of *ftt-2* results in the up-regulation of *daf-16*-dependent mRNA expression of *sod-3* (A), C24B9.9 (B) and F53C3.12 (C).

N2 worms or *daf-16* (*mgDf47*) null mutant worms were exposed to the indicated RNAi starting as L1 at 16°C. Total RNA was extracted from young adult RNAi worms for real-time-PCR analysis. The y-axis indicates the RNA levels normalized to the RNA expression levels of the internal control *act-1*. The relative RNA levels for N2 worms treated with the L4440 control RNAi is set as 1. The average of four independent experiments is shown and the error bars represent SEM.

ftt-2 induces the nuclear translocation of DAF-16 and promotes the transcription of some DAF-16 downstream genes.

2.3.4 RNAi inactivation of *ftt-2* leads to shortened lifespan.

Because reduced *daf-2* signaling and increased *daf-16* activities are often associated with enhanced dauer formation and extended adult lifespan, we investigated whether RNAi inactivation of *ftt-2* in worms also affected adult lifespan. We found that the *ftt-2* RNAi knock down worms had a much shorter adult lifespan compared to the control RNAi worms (Table 2.3). In contrast, the *par-5* RNAi knock down worms exhibited normal lifespan (Table 2.3). Interestingly, *ftt-2* RNAi did not appear to affect the extended lifespan phenotype of *daf-2(e1370)* worms (Table 2.3). Moreover, we determined that the *ftt-2* RNAi treated worms developed into adults at a normal rate (*control RNAi*: 46.5 +/- 2.5 hr, N= 717; *ftt-2 RNAi*: 44.2 +/- 2.2 hr, N=186) and exhibited no obvious developmental defects. Taken together, the results indicate that *ftt-2* RNAi leads to a reduced lifespan in wild-type background, but *ftt-2* RNAi does not appear to shorten lifespan by causing non-specific sickness in worms (Berdichevsky et al., 2006; Wang et al., 2006b). The lifespan shortening effect of *ftt-2* RNAi knock down was somewhat unexpected based on our observation that *ftt-2* RNAi promoted dauer formation of *daf-2(e1370)* worms. On the other hand, the lifespan and dauer phenotypes associated with the *daf-2*/insulin-like signaling pathway have been shown to be mediated by distinct effector complexes. For instance, the *eak* mutations robustly enhance the dauer formation phenotype associated with the *akt-1* mutant (the serine/threonine kinase downstream of *daf-2*) but have little effect on the longevity of the *akt-1* mutant worms (Hu et al., 2006); the *smk-1* gene

Table 2.3 RNAi inactivation of *ftt-2* shortens the lifespan of N2 worms but has no effect on the lifespan of *daf-2(e1370)* worms.

		Mean (days)	Median (days)	# counted	P-value
N2	L4440 RNAi	15.200	15.000	36	N/A
	<i>ftt-2</i> RNAi	11.665	11.000	46	0.000 ^a
	<i>par-5</i> RNAi	16.440	19.000	39	0.380 ^a
	<i>daf-2</i> RNAi	39.925	40.000	40	0.000 ^a
	<i>daf-16</i> RNAi	10.216	10.000	38	0.000 ^a
<i>daf-2(e1370)</i>	L4440 RNAi	48.604	50.000	53	N/A
	<i>ftt-2</i> RNAi	46.846	52.000	52	0.737 ^b
	<i>par-5</i> RNAi	50.533	52.000	60	0.764 ^b
	<i>daf-2</i> RNAi	45.644	50.000	45	0.980 ^b
	<i>daf-16</i> RNAi	12.705	11.000	42	0.000 ^b

The lifespan of N2 or *daf-2(e1370)* worms treated with the indicated RNAi was determined at 22°C and the results of one representative experiment are shown.

^a: Compared to N2 worms fed with L4440 RNAi bacteria;

^b: Compared to *daf-2(e1370)* worms fed with L4440 RNAi bacteria.

specifically interferes with the ability of *daf-16* to affect lifespan but has little effect on *daf-16*-mediated dauer regulation (Wolff et al., 2006). Furthermore, because 14-3-3 proteins are known to bind to a large number of substrates, FTT-2 is most certainly involved in numerous diverse functions. RNAi inactivation of *ftt-2* will likely disrupt multiple biological pathways that together may result in lifespan shortening. Two recent papers implicated 14-3-3 proteins in mediating the longevity promoting effect of SIR-2.1 by bridging the interactions of SIR-2.1 and DAF-16 in the nucleus upon stress signals (Berdichevsky et al., 2006; Wang et al., 2006b). An interesting possibility is that, in the *ftt-2* knock down worms, although more cytoplasmic DAF-16 is released into the nucleus to turn on some DAF-16 downstream genes, such a beneficial effect may be countered by the dissociation of the nuclear 14-3-3/SIR-2.1/DAF-16 protein complexes and result in lifespan shortening.

2.3.5 *FTT-2 forms a complex with DAF-16 in vivo.*

14-3-3 proteins usually function by binding to phosphorylated ligands (Fu et al., 2000). Recent studies in cultured mammalian cells indicate that the 14-3-3 ζ isoform binds to phosphorylated FOXO3a, one of the DAF-16 mammalian homologs, and sequesters FOXO3a in the cytoplasm (Brunet et al., 1999). Furthermore, *in vitro* pull-down assays show that the mammalian 14-3-3 ζ isoform is able to bind to phosphorylated DAF-16 (Cahill et al., 2001). Therefore, it is possible that FTT-2 forms a complex with DAF-16 in *C. elegans*. We used co-immunoprecipitation (co-IP) experiments to test this possibility. Because we do not have an antibody that could detect endogenous DAF-16 robustly, we used worm extracts from the *daf-16::gfp* strains and an anti-FTT-2 antibody for immunoprecipitation. The co-IP experiments showed

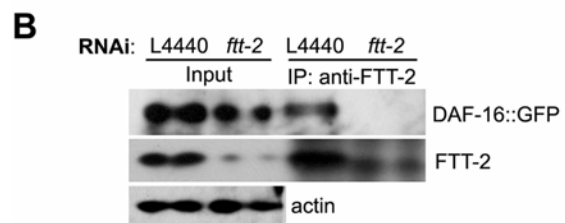
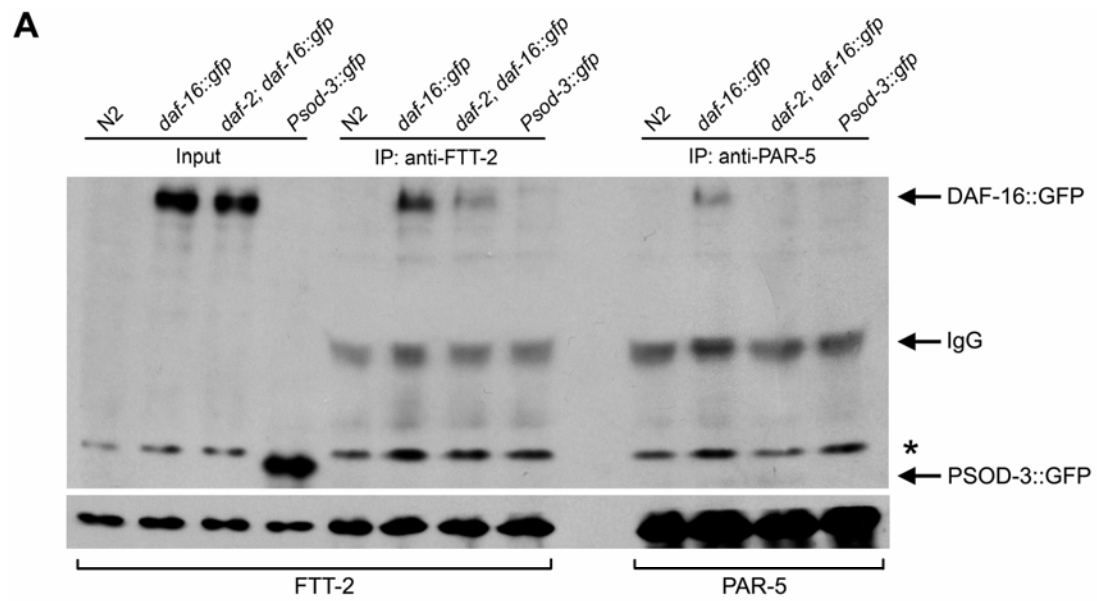
that when FTT-2 was specifically immunoprecipitated, DAF-16::GFP was also recovered (Figure 2.5A). In the same experiment, a GFP protein driven by the *sod-3* promoter (*Psod-3::gfp*) was not co-immunoprecipitated with FTT-2, indicating that FTT-2 and DAF-16::GFP forms a specific complex in worms. Furthermore, co-IP experiments carried out using worm extracts from animals treated with *ftt-2* RNAi showed that a much reduced level of FTT-2 was immunoprecipitated and consequently no detectable DAF-16::GFP was co-immunoprecipitated (Figure 2.5B). We also carried out co-IP experiments using *daf-2(e1370); daf-16::gfp* worms that were cultured at the non-permissive temperature for six hours. Under this condition, the majority of DAF-16::GFP was observed in the nuclei of cells, presumably due to the inactivation of DAF-2 at 25°C. We found that reduced levels of DAF-16::GFP was co-immunoprecipitated with FTT-2 in *daf-2(e1370); daf-16::gfp* worm extracts compared to that of *daf-16::gfp*, even though similar levels of FTT-2 was immunoprecipitated in both extracts (Figure 2.5A). These results are consistent with the model that when *daf-2*/insulin-like signaling is inactivated, DAF-16 becomes dephosphorylated and dissociates from 14-3-3 binding.

Our co-IP results together with the previously published *in vitro* pull-down evidence (Cahill et al., 2001) suggest that FTT-2 likely directly binds to phosphorylated DAF-16 in *C. elegans*. Because 14-3-3 proteins are abundantly distributed in the cytoplasm, the binding of FTT-2 with DAF-16 may sequester DAF-16 in the cytoplasm. We hypothesize that when *ftt-2* is depleted by RNAi, DAF-16 is free to move into the nucleus and execute its transcriptional role.

In our co-IP experiments, a low level of DAF-16::GFP also co-immunoprecipitated with PAR-5 when anti-PAR-5 was used for

Figure 2.5 FTT-2 forms a complex with DAF-16::GFP in *C. elegans*.

(A) Worm extracts from mixed staged *daf-16::gfp* worms (*daf-16(mgDf47)*; *xrls87[daf-16a::gfp::DAF-16B, rol-6(su1006)]*) or *daf-2(e1370); daf-16::gfp* worms that had been incubated at 25°C for 6 hrs were immunoprecipitated with an anti-FTT-2 or an anti-PAR-5 antibody and the precipitated proteins were immunoblotted with an anti-GFP antibody (upper panel) and an anti-FTT-2 or an anti-PAR-5 antibody (lower panel). Extracts from N2 and *Psod-3::gfp* worms were used as negative controls. (B) Worm extracts were prepared from *daf-16::gfp* L3 larvae treated with *ftt-2* RNAi or control L4440 RNAi and immunoprecipitated with an anti-FTT-2 antibody. Upper panel: immunoblotting with an anti-GFP antibody; middle panel: immunoblotting with an anti-FTT-2 antibody; lower panel: immunoblotting with an anti-actin antibody. Actin was included as a loading control for the input extracts.



immunoprecipitation. The FTT-2 and PAR-5 antibodies we used were generated against two distinct FTT-2 and PAR-5 peptides (kind gifts from Dr. Golden). However, as described earlier, in immunoblotting experiments, we found that whereas the anti-FTT-2 antibody appears to be highly specific, the anti-PAR-5 antibody may cross-react with the FTT-2 protein (Figure 2.1). Therefore, the weak binding we detected between PAR-5 and DAF-16::GFP may be due to cross-reactivity of the anti-PAR-5 antibody to FTT-2. Alternatively, PAR-5 may indeed form a complex with DAF-16::GFP in worms. Because our experiments indicate that PAR-5 does not affect *daf-2*-mediated dauer formation, DAF-16 subcellular localization or DAF-16 transcriptional activities, PAR-5 may be involved in other aspects of DAF-16 functions (Berdichevsky et al., 2006).

Our analyses demonstrate that specific knock down of *ftt-2*, but not *par-5*, affects dauer formation, DAF-16 localization, and DAF-16 transcriptional activities. Such specificity is consistent with the expression patterns of FTT-2 and PAR-5. Using northern blotting analyses, *par-5* is detected to express highly in the embryos and its mRNA level drops drastically by the L1 stage and remains low through larval development. *ftt-2* is also found to be the most highly expressed in embryos but its expression through larval stages only drops a little compared to that in embryos (Wang and Shakes, 1997). Also, whereas *par-5* expression is highly germline enriched, *ftt-2* is not (Wang and Shakes, 1997). Using GFP fusion strategies, PAR-5::GFP is shown to express strongly in the neurons and the intestine of transgenic larvae and FTT-2::GFP is shown to express most strongly in the pharynx and the nervous system, and weakly in the intestine of transgenic larvae (Wang et al., 2006b). Based on the expression patterns of FTT-2 and PAR-5, it is not surprising that FTT-2 has

important functions during *C. elegans* larval development. Furthermore, as FTT-2 and PAR-5 express in overlapping but distinct tissues, it is also expected that they will have different functions. Interestingly, in our qRT-PCR experiments (Figure 2.1), we noticed that specific knock down of *par-5* led to ~2-fold increase in *ftt-2* mRNA expression, probably due to a yet unknown compensation mechanism. Our results indicate that *C. elegans* has assigned different tasks for the closely related members of the 14-3-3 family, further supporting the notion that 14-3-3 proteins have isoform-specific functions (Roberts and de Bruxelles, 2002).

In summary, we report here that the 14-3-3 protein FTT-2 specifically regulates dauer formation, DAF-16 subcellular localization, and DAF-16 transcriptional activities in *C. elegans*. We provide evidence that FTT-2 forms a complex with DAF-16 in worm, similar to that in mammalian cultured cells. The complex formation between FTT-2 and DAF-16 likely results in cytoplasmic sequestration of DAF-16 and prevents it from regulating its transcriptional targets. Our results advance the understanding of the regulation of DAF-16, an important determinant of longevity, metabolism, and development, and further highlight the high degree of conservation between the *C. elegans daf-2* and the mammalian insulin/IGF-1 signal transduction pathways.

2.4 Acknowledgements

We thank members of the Lee, Liu, and Kemphues labs (Cornell University, Ithaca NY) for helpful discussion. We especially thank Dr. Diane Morton (Cornell University, Ithaca NY) for providing the PCR primers for *ftt-2* and *par-5*, and for insightful discussion. We thank the Lis lab (Cornell

University, Ithaca NY) for usage of the real-time PCR machine and we are grateful to Behfar Ardehali for technical assistance. We are especially grateful to Dr. Andy Golden (NIDDK, National Institutes of Health, Bethesda, MD) for providing the anti-FTT-2 and anti-PAR-5 antibodies. We thank Philippe Vaglio for assistance with the bioinformatics. We also thank CGC for providing strains. The RNAi resource used here was supported by a NCI grant to MV. This work was supported by a New Scholar Award in Aging from the Ellison Medical Foundation and a R01 grant AG024425-01 from the NIA awarded to SSL.

CHAPTER 3

THE HOST CELL FACTOR HCF-1 NEGATIVELY REGULATES DAF-16 IN THE NUCLEUS BY LIMITING ITS ACCESS TO ITS TARGET GENES²

3.1 Introduction

Recent studies in various model system have revealed multiple evolutionarily conserved genes and genetic pathways important for longevity (Antebi, 2007; Bishop and Guarente, 2007; Giannakou and Partridge, 2007; Kaeberlein et al., 2007; Kenyon, 2005; Lambert and Brand, 2007). One of the best characterized longevity determinants is the FOXO family of transcription factors, which function as major effectors of the insulin/IGF-1-like signaling (IIS) cascade. The IIS pathway is highly conserved and has been shown to modulate longevity in *C. elegans*, *Drosophila* and mice (Russell and Kahn, 2007).

From *C. elegans* to mammals, DAF-16/FOXO is emerging as a master regulator that is capable of responding to diverse environmental stimuli and coordinating development, metabolism, and stress response (Antebi, 2007; van der Horst and Burgering, 2007). In addition to the IIS pathway, DAF-

² This chapter is modified slightly from Li, Ebata, Dong, Rizki, Iwata and Lee, *Plos Biology* (In press). I, Atsushi Ebata, Dr. Yuqing Dong, Gizem Rizki, Terri Iwata and Dr. Sylvia Lee conceived and performed the experiments and analyzed the data. I and Atsushi Ebata performed the majority of the lifespan analyses with help from Dr. Yuqing Dong and Terri Iwata. I performed the immunostaining, DAF-16::GFP localization, qRT-PCR, co-IP and ChIP experiments; Atsushi Ebata generated *hcf-1::gfp* strains, performed the stress assays with help from Gizem Rizki and me, the dauer and Nile Red assays with help from me; Dr. Yuqing Dong generated the anti-HCF-1 antibody.

16/FOXO also responds to many other signaling cascades. Recent findings reveal that different signals induce distinct modifications of DAF-16/FOXO, which can impact the expression level, subcellular localization, and/or transcriptional activities of DAF-16/FOXO, leading to expression changes of selective DAF-16/FOXO target genes and specific cellular responses (Huang and Tindall, 2007; van der Horst and Burgering, 2007). DAF-16 is thought to promote survival and longevity by mounting a robust response to various stresses, infection, and toxic compounds. Therefore, the precise control of DAF-16 transcriptional activities is a key regulatory step for longevity determination.

Similar to other DNA binding transcription factors, one way for DAF-16/FOXO to achieve specificity in gene regulation depends on its functional interactions with transcriptional co-regulators. Recent exciting findings have revealed several nuclear factors that cooperate with DAF-16/FOXO to regulate gene expression, e.g., SIR-2.1, SMK-1 and BAR-1 (see Chapter 1). Whereas they represent putative positive regulators of DAF-16 in *C. elegans*, nuclear factors that negatively regulate DAF-16 are largely unknown. Since DNA binding transcription factors are often regulated by the interplay between positive and negative regulators, the characterization of DAF-16 negative regulators will be essential for the further elucidation of DAF-16 regulation. In this paper, we report that the *C. elegans* homolog of host cell factor 1 (HCF-1) represents a new longevity determinant and functions as a negative regulator of DAF-16. HCF-1 belongs to a family of highly conserved proteins (Wysocka and Herr, 2003). Loss of *hcf-1* in *C. elegans* induces substantial lifespan extension of up to 40% and robust resistance to specific stress stimuli. For *hcf-1* to modulate lifespan and stress response, it requires the activity of *daf-16*. In

delineating the mechanism by which HCF-1 regulates DAF-16, we found HCF-1 to be a ubiquitously expressed nuclear protein that physically associates with DAF-16. Moreover, loss of *hcf-1* led to increased recruitment of some DAF-16 to its target gene promoters and altered expression of a subset of DAF-16-regulated genes. Given the genetic and biochemical data, we propose that HCF-1 modulates lifespan and stress responses by forming a complex with DAF-16 and restricting the recruitment of a fraction of DAF-16 to its target gene promoters, thereby regulating DAF-16-mediated transcription of specific target genes. Considering that HCF-1 and DAF-16 are both highly conserved through evolution, our findings suggest that HCF-1 likely also regulates FOXO activities and is important for aging in diverse organisms.

3.2 Materials and Methods

3.2.1 *C. elegans* strains

The strains used in this paper were as follow: wild-type N2, *daf-16* (*mgDf47*), *daf-2* (*e1370*), *age-1* (*hx546*), *sqt-1* (*sc13*) *age-1* (*mg44*)/*mnC1* (a kind gift from Dr. Catherine A. Wolkow, National Institute of Aging), *glp-1* (*e2141*), *hcf-1* (*ok559*) (generated by the *C. elegans* Gene Knockout Consortium), *hcf-1* (*pk924*) (a kind gift from Dr. Winship Herr, University of Lausanne, Switzerland), *daf-16* (*mgDf47*);*xrls87*[*daf-16α::gfp::daf-16b*, *rol-6* (*su1006*)] (DAF-16::GFP) (Lee et al., 2001), *daf-16* (*mu86*);*muls71*[*daf-16a::gfp/bKO*, *rol-6* (*su1006*)] (DAF-16::GFP) (Lin et al., 2001) and *muls84*[*Psod-3::gfp*] (Libina et al., 2003). The *hcf-1* (*ok559*) allele was outcrossed 5 times and the *hcf-1* (*pk924*) allele was outcrossed 3 times with the N2 strain in our lab prior to phenotype analyses.

The following double mutant strains were constructed using standard genetic methods: *daf-16(mgDf47);hcf-1(ok559)*, *daf-16(mgDf47);hcf-1(pk924)*, *daf-2(e1370);hcf-1(ok559)*, *daf-2(e1370);hcf-1(pk924)*, *sqt-1(sc13) age-1(mg44)/mnC1;hcf-1(ok559)*, *glp-1(e2141);hcf-1(pk924)*, *daf-16(mu86);muls71[daf-16a::gfp/bKO, rol-6(su1006)];hcf-1(ok559)*, *daf-16(mu86);muls71[daf-16a::gfp/bKO and hcf-1(pk924);sur-5::gfp, muls84[Psod-3::gfp];hcf-1(pk924)*.

All strains were cultured using standard methods (Brenner, 1974). Unless otherwise stated, NGM plates were seeded with *Escherichia coli* OP50 as the food source.

3.2.2 Lifespan assays

For RNAi lifespan assays, RNAi bacteria were grown in Luria broth with 50µg/ml ampicillin at 37°C for 10-16 hours, seeded onto NGM plates containing 2 or 4mM IPTG, and induced at room temperature for about 6 hrs (Lee et al., 2003b). Worms were allowed to lay eggs over-night on RNAi plates at 16°C and the progeny were grown on RNAi plates at 25°C until they developed into young adult stage. The young adult worms were then transferred onto RNAi plates seeded with 3-fold concentrated RNAi bacteria that contained 50µg/ml FUDR to prevent the growth of progeny. For lifespan assays using NGM plates seeded with OP50 bacteria, worms were allowed to lay eggs over-night at 16°C and the progeny were grown on NGM plates at 25°C till young adult stage. The young adult worms were then transferred onto NGM plates that contained 50µg/ml FUDR and seeded with 3-fold concentrated *E. coli* OP50. For lifespan assays involving *daf-2(e1370)* and *daf-2(e1370);hcf-1(pk924)* or *daf-2(e1370);hcf-1(ok559)* worms, progeny were

allowed to grow at 16°C and shifted to 25°C after the L3 larval stage to avoid the constitutive dauer arrest phenotype associated with the *daf-2(e1370)* mutant (Riddle et al., 1981).

For all lifespan assays, worms were aged at 25°C. Worms were scored every day or every other day and those that failed to respond to a gentle prodding with a platinum wire were scored as dead. Animals that bagged, exploded or crawled off the plate were considered as censored. We defined the day when we transferred the young adult worms as day 0 of adult lifespan. Statistical analysis was done using the SPSS software and p values were calculated using the log-rank test. All the lifespan experiments were repeated at least two independent times.

3.2.3 Transgenic animals

A GFP-fused *hcf-1* plasmid (*Phcf-1::hcf-1::gfp*) was created by inserting a genomic fragment that contains ~500bp upstream of the predicted ATG of *hcf-1* and the entire predicted coding region of *hcf-1* into the pPD95_77 plasmid. Transgenic worms were created by microparticle bombardment as previously described (Praitis et al., 2001). The *Phcf-1::hcf-1::gfp* plasmid was co-bombarded with the pJKL702 [*unc-119(+)*] plasmid into *unc-119(ed4)* mutant worms to obtain the strain *unc-119(ed4);rwls3[Phcf-1::hcf-1::gfp, unc-119]*. Multiple independent integrated transgenic lines were examined.

3.2.4 Embryonic and brood size assays

Each single L4 worm was allowed to lay eggs and transferred to a fresh NGM plate every 24 hours until it completed egglay. The number of eggs laid and the number of hatched worms were counted. A total of five worms were used for each strain.

3.2.5 *Nile Red staining*

Nile Red staining was performed as previously described (Ashrafi et al., 2003). Unseeded NGM plates were coated with 0.025µg/ml final concentration Nile Red which had been resuspended in acetone and diluted in H₂O. The Nile red was allowed to diffuse through NGM overnight. The plates were then seeded with OP50 bacteria and left at room temperature overnight. Gravid adult worms were allowed to egglay onto the plates overnight, and progeny allowed to develop to young adult stage. Worms were then monitored using a fluorescent microscope (Leica DM 5000B) and images were captured using a Hamamatsu ORCA-ER camera and the OpenLab Software.

3.2.6 *Stress and dauer assays*

All stress and dauer assays were performed as previously described (Barsyte et al., 2001; Lee et al., 2003a; Lithgow et al., 1995; Yanase et al., 2002).

For the paraquat assay, gravid adult worms of each strain tested were allowed to lay egg on NGM plates seeded with OP50 for 2-3 hrs to produce relatively synchronous populations of progeny. The progeny were allowed to develop at 25°C and when they reached young-adulthood, FUDR was added to the plates at a final concentration of 50µg/ml to prevent the growth of progeny. At day 2-3 of adulthood, worms were washed off the NGM plates and rinsed with M9 buffer three times to remove the OP50 bacteria. Approximately 30 adults were dispensed into each well of a 24-well culture plate containing 300µl of 200mM paraquat (Sigma) in M9 buffer. Triplicate wells were used for each strain and the experiment was repeated at least two independent times.

Worms in the paraquat buffer were scored every 2-3 hrs for survival. Worms that failed to respond to gentle prodding were scored as dead.

For the CdCl₂ assay, synchronized day 2 adult worms were collected as described above and washed by K-medium. Worms were then put into each well of a 24-well culture plate containing 600µl K-medium with 18mM CdCl₂ at 20°C. Triplicate plates for each strain were scored for each time point indicated. Worms that failed to respond to gentle prodding were scored as dead.

For the heat shock assay, synchronous populations of worms were grown as described above. Day 2 adult worms grown on OP50-NGM plates were shifted to 35°C. Duplicate or triplicate plates for each strain were scored for each time point. Because the scoring was done at room temperature, once the worms were pulled from 35°C and scored for survival, they were discarded to avoid the complication of recovery from heat shock during the time of scoring.

For dauer assays, worms at the L4 stage were allowed to lay egg at 16°C over night. The resulting progeny were allowed to develop at the indicated temperature. At ~96 hrs (25°C or 27°C) or ~120 hrs (22°C) after egg lay, the number of dauers and adult worms on each plate were scored. Replica plates were scored for each strain. The dauer assays were repeated two to three times.

3.2.7 *DAF-16::GFP localization assay*

daf-16(mgDf47);xrls87 transgenic strain was used for DAF-16::GFP localization assay (Lee et al., 2001). Worms at the L4 larval stage were picked onto RNAi plates and allowed to lay egg at 16°C for one day. Progenies were

exposed to the RNAi bacteria at 16°C for 5 days until they became gravid adults. The DAF-16::GFP signal was then monitored using a fluorescent microscope (Leica DM 5000B) and images were captured using a Hamamatsu ORCA-ER camera and the OpenLab program.

3.2.8 *Immunostaining*

Worm fixation and immunostaining were performed as previously described (Hurd and Kemphues, 2003). In brief, worms were immobilized and compressed between two poly-lysine coated slides and snap frozen in liquid nitrogen. The cuticle was removed by quickly separating two frozen slides. Worms were then quickly fixed in pre-chilled methanol at -20°C. Incubation with primary and secondary antibodies and washes were done in TBS buffer at room temperature. Fluorescence signal was monitored using a fluorescent microscope (Leica DM 5000B) and images were captured using a Hamamatsu ORCA-ER camera and the OpenLab program.

3.2.9 *IP and immunoblotting*

IP and immunoblotting were carried out as described (Li et al., 2007a). In brief, for IP experiments, worm extracts were made from mixed staged worms by sonication of worms in lysis buffer and subsequent removal of debris by centrifugation. The appropriate antibody was incubated with worm extract at 4°C overnight followed by incubation with protein A slurry (Pierce) at 4°C for 3~6 hrs. The protein A beads were then washed with lysis buffer for 6 times. The bound proteins were eluted by boiling in 2X sample buffer, separated on a SDS gel, transferred onto a nitrocellulose membrane, and followed by standard ECL detection.

3.2.10 Antibodies

To generate polyclonal antiserum against *C. elegans* HCF-1, bacterial recombinant S-tagged fusion protein containing full-length HCF-1 was purified using the S-Tag™ Thrombin Purification Kit (Novagen) and used as an antigen to immunize guinea pigs. The crude anti-HCF-1 antiserum was subsequently purified using S-tagged HCF-1. In brief, the crude anti-HCF-1 antiserum was incubated with purified S-tagged HCF-1 immobilized on nitrocellulose membrane (BA85 Protran® BioScience). Poorly bound proteins were removed by multiple washes in TBS and PBS buffer and the bound anti-HCF-1 antibody was recovered by subsequent elution.

For immunostaining, affinity purified anti-HCF-1 antibody was used as the primary antibody (1:500) and anti-guinea pig conjugated with Cy3 (Jackson ImmunoResearch Laboratories, 1:200) was used as the secondary antibody. For GFP immunostaining, anti-GFP (goat, Rockland) was used as the primary antibody (1:1000) and anti-goat conjugated with FITC (Jackson ImmunoResearch Laboratories, 1:400) was used as the secondary antibody.

For IP, affinity purified anti-HCF-1 and anti-GFP (rabbit, Clontech) antibodies were used.

Antibodies for immunoblotting include: anti-DAF-16 (cC-20) (goat, Santa Cruz), anti-HCF-1, anti-GFP (rabbit, Clontech), anti-ACTIN (mouse, Chemicon), anti-goat (Rockland), anti-mouse (Santa Cruz), anti-guinea pig (Jackson ImmunoResearch Laboratories), and anti-rabbit (Rockland).

3.2.11 RNA isolation and qRT-PCR

Synchronized late L4 staged worms were used for RNA isolation. All the worms for qRT-PCR were grown at 25°C except that in the experiments

using *daf-2(e1370)* mutants, worms were shifted from 16°C to 25°C for 8 hrs prior to harvest. Total RNA from ~10-15µl of worm pellet was isolated using Tri-reagent (Molecular Research Center, Inc.) (Troemel et al., 2006). cDNAs were synthesized with random hexamers using SuperScript™ III First-Strand Kit (Invitrogen). qRT-PCR reactions were performed using iQ™ SYBR® Green Supermix (BIO-RAD) and the MyiQ™ Single Color Real-time PCR Detection System (BIO-RAD). The qRT-PCR conditions were: 95°C for 3 minutes, followed by a 40-cycles of 10 sec at 95°C and 30 sec at 60°C. Melting curve analysis was performed for each primer set at the end to ensure the specificity of the amplified product. *act-1* was used as the internal control and the RNA level of each gene of interest was normalized to the level of *act-1* for comparison. The qRT-PCR experiment was repeated at least three times using independent RNA/cDNA preparations.

Primers for qRT-PCR are listed in Table 3.1.

3.2.12 ChIP

ChIP was performed as previously described with slight modifications (Oh et al., 2006)(IL & JA, personal communication). In brief, ground frozen worm powder was crosslinked using 1% formaldehyde in PBS buffer and subjected to sonication. Immunoprecipitation was performed as described above. The protein-DNA complexes were then eluted from protein A beads and treated with RNase A and proteinase K. Precipitated DNA fragments were purified using QIAquick® PCR purification kit (Qiagen) and subjected to qPCR analysis. qPCR primers for ChIP are listed in Table 3.2.

Table 3.1 Primers for qRT-PCR.

Gene	Sequence		Product
<i>act-1</i>	Forward	5'- CCAGGAATTGCTGATCGTATGCAGAA -3'	133 bp
	Reverse	5'- TGGAGAGGGAAGCGAGGATAGA -3'	
<i>sod-3</i>	Forward	5'- CCAACCAGCGCTGAAATTCAATGG -3'	127 bp
	Reverse	5'- GGAACCGAAGTCGCGCTTAATAGT -3'	
<i>mtl-1</i>	Forward	5'- ATGGCTTGCAAGTGTGACTG -3'	56 bp
	Reverse	5'- CACATTTGTCTCCGCACTTG -3'	
<i>fat-5</i>	Forward	5'- TGGTGAAGAAGCACGATCAG -3'	125 bp
	Reverse	5'- AAGCAGAAGATTCCGACCAA -3'	
M02D8.4	Forward	5'- ATTTGCCAACAAACATGCAA -3'	87 bp
	Reverse	5'- GGTCCACGATGGTGTGTCT -3'	
<i>ges-1</i>	Forward	5'- AGCAACAAGGAAGGGTCGTA -3'	120 bp
	Reverse	5'- CCGATGATCTCCGAAATGAA -3'	
<i>lys-7</i>	Forward	5'-GCGGGTTATTGTGCAGTTTT -3'	114 bp
	Reverse	5'- TCAATTCCGAGTCCAGCTTT -3'	
K09C4.5	Forward	5'- TGGAATTGAACCGACTATTGC -3'	106 bp
	Reverse	5'- GCAAATGGCACAAGAACAAA -3'	
<i>dod-3</i>	Forward	5'- AAAAAGCCATGTTCCCGAAT -3'	137 bp
	Reverse	5'- GCTGCGAAAAGCAAGAAAAT -3'	
F21F3.3	Forward	5'- CCGATTCGTTCTTTTGAAG -3'	138 bp
	Reverse	5'- ACAACCGAATGTTCCAATCC -3'	
<i>hsp-16.1</i>	Forward	5'- GCAGAGGCTCTCCATCTGAA -3'	85 bp
	Reverse	5'- GCTTGAAGTGCAGACATTG -3'	

<i>hsp-12.3</i>	Forward	5'- GCCATTCCAGAAAGGAGATG -3'	93 bp
	Reverse	5'- CGTTTGGCAAGAAGTTGTGA -3'	
C32H11.4	Forward	5'- TTACTTCCCATCGCCAAAGT -3'	117 bp
	Reverse	5'- CAATTCCGGCGATGTATGAT -3'	
F35E12.5	Forward	5'- TCTCGAAGCCAACAAGTTCA -3'	78 bp
	Reverse	5'- TTTCACGGGATCCGTATTTC -3'	
T16G12.1	Forward	5'- CAATGGGAGCTCACTTCGAT -3'	138 bp
	Reverse	5'- TCATCGGCAAGAAGAGTCAA -3'	
<i>dod-24</i>	Forward	5'- TGTCCAACACAACCTGCATT -3'	138 bp
	Reverse	5'- TGTGTCCCGAGTAACAACCA -3'	
F08G5.6	Forward	5'- TGGACAACCCAGATATGCAA -3'	111 bp
	Reverse	5'- GTATGCGATGGAAATGGACA -3'	
<i>dod-22</i>	Forward	5'- TTGTTGGTCCCAAGTTCACA -3'	132 bp
	Reverse	5'- AAGAACTTCGGCTGCTTCAG -3'	
<i>daf-16</i>	Forward	5'- CCAGACGGAAGGCTTAAACT -3'	149 bp
	Reverse	5'- ATTCGCATGAAACGAGAATG -3'	
<i>daf-2</i>	Forward	5'- CGGTGCGAAGAGAGGATATT -3'	97 bp
	Reverse	5'- TACAGAGGTCGCCGTTACTG -3'	
<i>age-1</i>	Forward	5'- AGTGGATTTCGGAACAATGC -3'	135 bp
	Reverse	5'- GGAATCGATCGACACTTTCA -3'	
<i>akt-1</i>	Forward	5'- TCACCGATGCGATATTGTCT -3'	82 bp
	Reverse	5'- AACTCCCCACCAATCAACAC -3'	

Table 3.2 qPCR Primers for ChIP.

Gene	Sequence	
<i>sod-3</i>	Forward	5'- TTTTCAAACCGAAAATTGACC -3'
	Reverse	5'- CAAAGACCTCATCAACAGCAA -3'
<i>mtl-1</i>	Forward	5'- GGCCACCCTCTTTTATCACA -3'
	Reverse	5'- TCAAATTGAGCTGCCTTCTTC -3'
<i>efl-1</i>	Forward	5'- TTTTATCTTCTCATTCAAGCGAAA -3'
	Reverse	5'- GAGACAATGGGAAAGGTGGA -3'
<i>Chr IV non coding</i>	Forward	5'- CTCTTCATTTTGTTTCCTGTGTTTTCC -3'
	Reverse	5'- GAAGGCGGCGGTAATTGTTG -3'

3.3 Results

3.3.1 *hcf-1* is a novel longevity gene.

In a recent genome-wide RNAi screen for new longevity genes (Hamilton et al., 2005), we found that RNAi knock down of the *hcf-1* gene (WB gene ID: WBGene00001827) consistently caused *C. elegans* to live ~20-30% longer than control RNAi treated worms (Figure 3.1A, Table 3.3). *C. elegans hcf-1* encodes a protein that is highly conserved through evolution, but its biological function is just beginning to be elucidated. Mammalian HCF-1 was first identified to be the host cell factor essential for stabilizing the transcriptional complex involving the herpes simplex virus (HSV) VP-16 transcription factor (Wysocka and Herr, 2003). Mammalian HCF-1 has subsequently been shown to play key roles in cell cycle progression, both at the G1/S transition, and at M phase and cytokinesis (Julien and Herr, 2003; Julien and Herr, 2004; Tyagi et al., 2007). In eliciting its diverse biological roles, mammalian HCF-1 acts by binding to and regulating many different transcription and chromatin factors and assembling appropriate protein complexes for context-dependent gene expression regulation (Wysocka and Herr, 2003). *C. elegans* HCF-1 has been shown to complement some of the transcriptional role of mammalian HCF-1 (Lee and Herr, 2001) and to also be required for proper cell cycle progression in worms (Lee et al., 2007) (Figure 3.2). Our data are the first to ascribe a longevity function for HCF-1. To further investigate a role of *hcf-1* in *C. elegans* longevity, we examined the lifespan of two existing *hcf-1* mutant alleles (*ok559* and *pk924*) (Lee et al., 2007). The *hcf-1(ok559)* mutant has an in-frame deletion that should truncate the N-terminal half of the protein, and the *hcf-1(pk924)* mutant has a large deletion

Figure 3.1 *hcf-1* modulates lifespan by acting upstream of *daf-16*, but in parallel to the IIS and germline signaling pathway.

Lifespan of (A) wild-type worms treated with *hcf-1* RNAi, (B) the *hcf-1(ok559)* and *hcf-1(pk924)* deletion mutants, (C) the *daf-16(mgDf47);hcf-1(pk924)* double mutant, (D) the *daf-2(e1370);hcf-1(pk924)* double mutant, (E) the *age-1(mg44);hcf-1(ok559)* double mutant, (F) the *glp-1(e2141);hcf-1(pk924)* double mutant worms. Each of the lifespan experiments was repeated at least two independent times with similar results. Data from representative experiments are shown. Quantitative data and statistical analyses for the experiments shown here are included in Table 3.3.

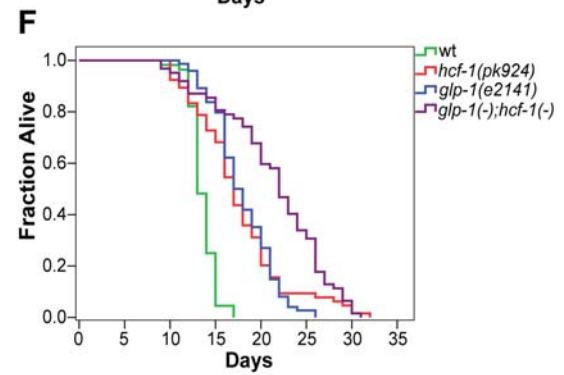
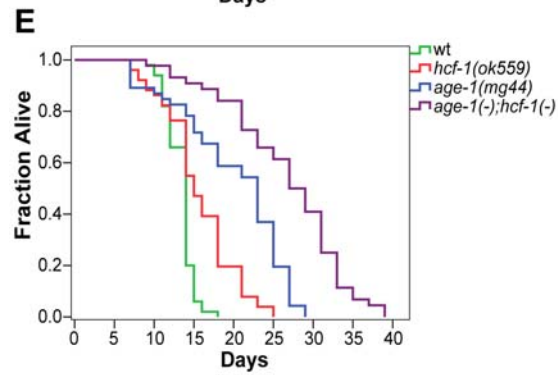
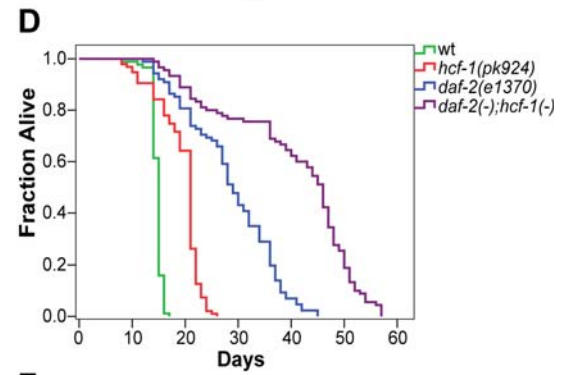
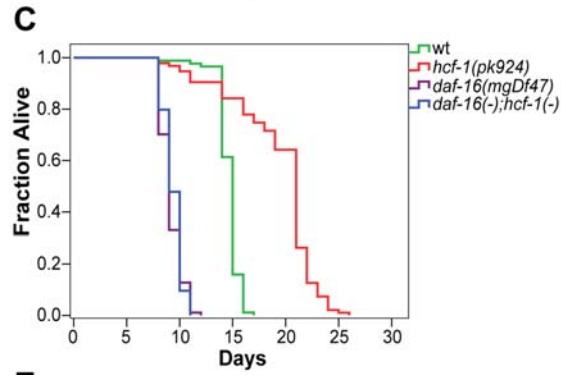
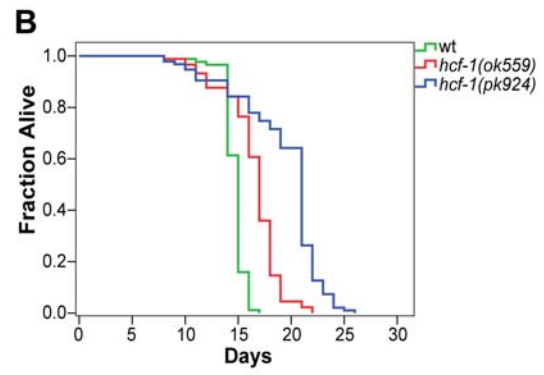
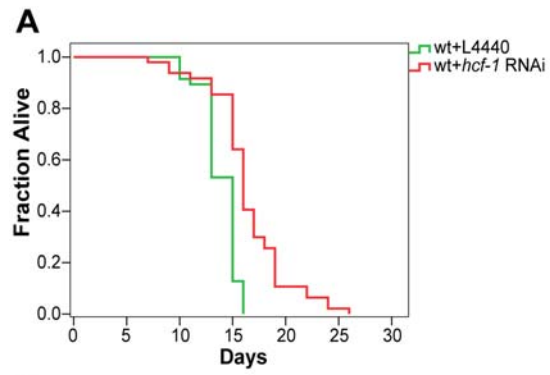


Table 3.3 Inactivation of *hcf-1* results in lifespan increase that is completely dependent on *daf-16*, but likely independent of the IIS and germline pathway.

Strain + RNAi	Mean LS ± SEM (Days)	Total Number of Animals Died/Total	% of wt + L4440	p Value versus wt + L4440
wt + L4440	13.9±0.2	46/47		N.A.
wt + <i>hcf-1</i>	16.5±0.5	47/49	119%	<0.0001

Strain	Mean LS ± SEM (Days)	Total Number of Animals Died/Total	% of wt	p Value versus wt	p Value versus <i>hcf-1(ok559)</i>
wt ^{a,c}	14.7±0.1	88/88		N.A.	<0.0001
<i>hcf-1(ok559)</i> ^{a,c}	16.5±0.3	89/89	112%	<0.0001	N.A.
<i>hcf-1(pk924)</i> ^{a,c}	19.3±0.2	95/95	131%	<0.0001	<0.0001
wt ^b	15.5±0.2	85/90		N.A.	N.A.
<i>hcf-1(pk924)</i> ^b	22.2±0.4	87/90	143%	<0.0001	N.A.

Strain	Mean LS ± SEM (Days)	Total Number of Animals Died/Total	% of wt	p Value versus wt	p Value versus <i>daf-16(mgDf47);hcf-1(pk924)</i>
wt	14.7±0.1	88/88		N.A.	<0.0001
<i>daf-16(mgDf47)</i>	9.2±0.1	94/94	63%	<0.0001	0.2622
<i>hcf-1(pk924)</i>	19.3±0.2	95/95	131%	<0.0001	<0.0001
<i>daf-16(mgDf47);hcf-1(pk924)</i>	9.4±0.1	97/97	64%	<0.0001	N.A.

Strain	Mean LS ± SEM (Days)	Total Number of Animals Died/Total	% of wt	p Value versus wt	p Value versus <i>daf-2(e1370);hcf-1(pk924)</i>
wt	14.7±0.1	88/88		N.A.	<0.0001
<i>daf-2(e1370)</i>	28.7±0.9	87/88	195%	<0.0001	<0.0001
<i>hcf-1(pk924)</i>	19.3±0.2	95/95	131%	<0.0001	<0.0001
<i>daf-2(e1370);hcf-1(pk924)</i>	40.4±1.3	90/90	275%	<0.0001	N.A.

Table 3.3 (continued) Inactivation of *hcf-1* results in lifespan increase that is completely dependent on *daf-16*, but likely independent of the IIS and germline pathway.

Strain	Mean LS ± SEM (Days)	Total Number of Animals Died/Total	% of wt	p Value versus wt	p Value versus <i>age-1(mg44);hcf-1(pk924)</i>
wt	13.4±0.3	50/50		N.A.	<0.0001
<i>age-1(mg44)</i>	20.0±1.0	46/46	149%	<0.0001	<0.0001
<i>hcf-1(ok559)</i>	15.6±0.6	51/51	116%	<0.0001	<0.0001
<i>age-1(mg44);hcf-1(ok559)</i>	26.7±1.1	44/44	196%	<0.0001	N.A.

Strain	Mean LS ± SEM (Days)	Total Number of Animals Died/Total	% of wt	p Value versus wt	p Value versus <i>age-1(mg44);hcf-1(pk924)</i>
wt	13.6±0.2	53/56		N.A.	<0.0001
<i>glp-1(e2141)</i>	18.0±0.4	74/75	132%	<0.0001	<0.0001
<i>hcf-1(pk924)</i>	17.5±0.6	65/66	129%	<0.0001	<0.0001
<i>glp-1(e2141);hcf-1(pk924)</i>	21.4±0.7	62/62	157%	<0.0001	N.A.

The lifespan experiments were repeated at least two independent times with similar results and the data for representative experiments are shown.

The lifespan data were analyzed using the Log-rank test and p values for each individual experiment is shown.

N.A.: not applicable.

^a Representative experiment 1.

^b Representative experiment 2.

^c Results presented in Figure 3.1.

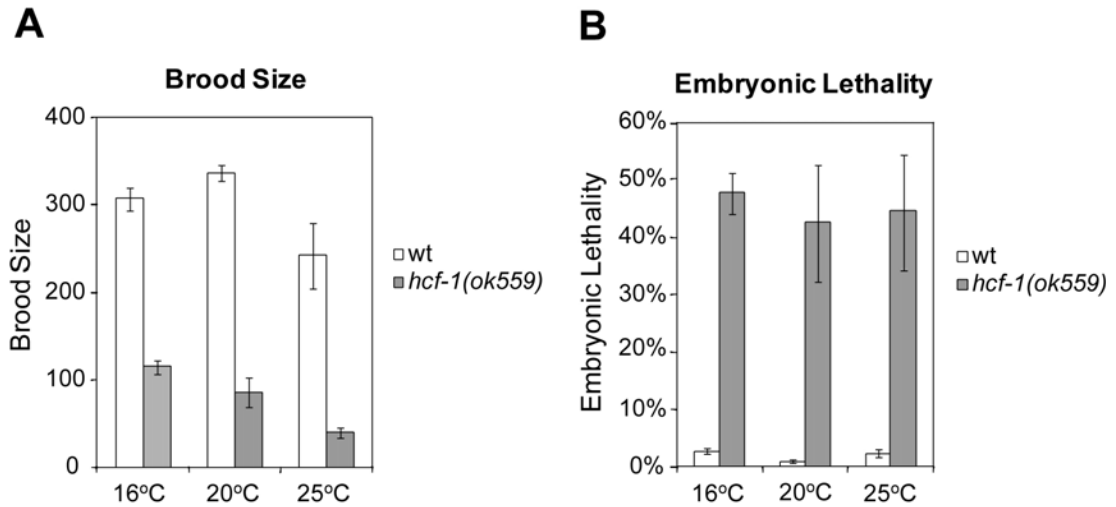


Figure 3.2 The *hcf-1(ok559)* mutant shows reduced brood size and increased embryonic lethality.

The brood size and embryonic lethality were obtained from average of five animals for each group under 16°C, 20°C and 25°C. Error bars indicate standard error of the means.

that should result in a frame shift leading to an early stop codon, and likely represents a null mutant (Figure 3.3) (Lee et al., 2007). As expected based on our observation with the *hcf-1* RNAi worms, we detected up to 40% lifespan extension in the *hcf-1* mutants compared to wild-type worms (Figure 3.1B, Table 3.3). In general, the *hcf-1(pk924)* mutant lives slightly longer than the *hcf-1(ok559)* mutant (Table 3.3), consistent with the possibility that the *pk924* allele is a more severe mutation. We confirmed that the prolonged lifespan associated with the *hcf-1* mutants is due to *hcf-1* deficiency by demonstrating that expression of a C-terminal gfp-tagged *hcf-1* transgene (*hcf-1::gfp*) was able to partially restore normal lifespan in the *hcf-1(pk924)* mutant (Table 3.4).

3.3.2 *HCF-1 is ubiquitously expressed and localizes to the nucleus.*

To further characterize HCF-1 in *C. elegans*, we examined the expression pattern of HCF-1 in worms. Using an affinity-purified polyclonal HCF-1 antibody in immunostaining assays, we observed prominent HCF-1 staining in the nuclei of most, if not all, somatic and germline cells in wild-type worms (Figure 3.4). The HCF-1 expression pattern detected in wild-type worms is highly specific because the *hcf-1(pk924)* and *hcf-1(ok559)* mutants only showed background fluorescence when they were examined using identical immunostaining conditions (Figure 3.4 & data not shown). The nuclear localization of HCF-1 was consistently observed from embryo through larval and adult stages (Figure 3.4 & data not shown) (Lee et al., 2007). Moreover, we observed similar ubiquitous nuclear expression in worms expressing a low-copy number of a functional *hcf-1::gfp* transgene (Figure 3.5). Our results indicate that HCF-1 is ubiquitously expressed and localizes to the nucleus of *C. elegans* under normal culture condition. Interestingly,

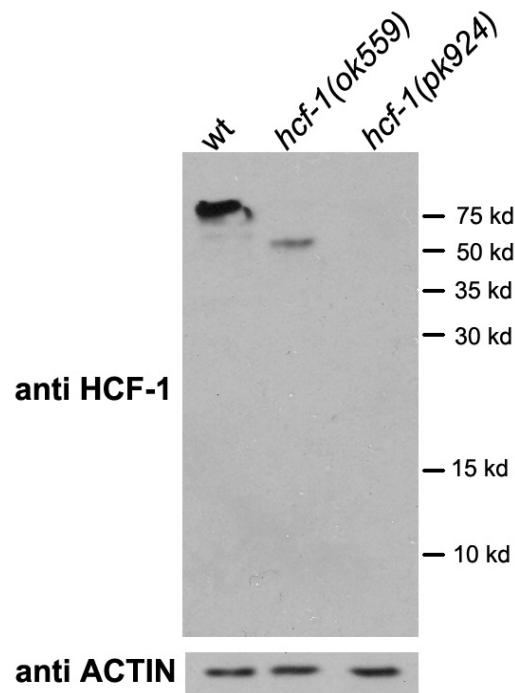


Figure 3.3 The *hcf-1(ok559)* mutant shows weak expression of a truncated HCF-1 protein and the *hcf-1(pk924)* mutant shows no detectable expression of any HCF-1 peptide.

Low levels of a truncated HCF-1 protein in the *hcf-1(ok559)* mutant was detected in immunoblotting assays using an affinity-purified polyclonal HCF-1 antibody generated against a full-length HCF-1 fusion protein. No partial HCF-1 protein was detected in the immunoblotting assays, suggesting that *hcf-1(pk924)* may represent a null mutant. Total protein from mixed populations of worms was separated on 15% SDS gel and followed by immunoblotting with an affinity-purified HCF-1 antibody. Actin level was used as a loading control.

Table 3.4 Expression of a *hcf-1::gfp* transgene partially rescues the lifespan phenotype of *hcf-1(pk924)*.

Strain + RNAi	Mean LS ± SEM (Days)	Total Number of Animals Died/Total	% of wt + L4440	p Value versus <i>hcf-1(pk924)</i> + L4440	p Value versus <i>hcf-1(pk924);hcf-1::gfp</i> + <i>hcf-1</i>
wt + L4440	18.0±0.2	120/120		<0.0001	<0.0001
<i>hcf-1(pk924)</i> + L4440	23.6±0.3	115/120	131%	N.A.	0.0396
<i>hcf-1(pk924)</i> + <i>hcf-1</i>	24.2±0.3	115/120	134%	0.3808	0.0020
<i>hcf-1(pk924);hcf-1::gfp</i> + L4440	20.3±0.3	119/120	113%	<0.0001	<0.0001
<i>hcf-1(pk924);hcf-1::gfp</i> + <i>hcf-1</i>	22.7±0.3	117/120	126%	0.0396	N.A.

Expression of *hcf-1::gfp* in *hcf-1(pk924)* mutant resulted in partial suppression of the long lifespan phenotype. The lifespan suppression caused by *hcf-1::gfp* expression could be reverted by treating the *hcf-1(pk924);hcf-1::gfp* transgenic worms with *hcf-1* RNAi, whereas *hcf-1* RNAi had no effect on the long lifespan of *hcf-1(pk924)* mutant worms, indicating that the reduced lifespan observed in the *hcf-1(pk924);hcf-1::gfp* worms was due to expression of wild-type HCF-1 and that the *hcf-1::gfp* transgene is functional. *hcf-1(pk924);hcf-1::gfp* referred to *hcf-1(pk924);rwls3[Phcf-1::hcf-1::gfp, unc-119]*.

Figure 3.4 HCF-1 is a ubiquitously expressed nuclear protein.

(A) Gravid adults of wild-type and *hcf-1(pk924);sur-5::gfp* mutant worms were immunostained using an affinity-purified HCF-1 antibody. To ensure identical staining conditions, worms from both strains were processed on the same slide. The *hcf-1(pk924)* mutants were marked by SUR-5::GFP to distinguish them from wild-type worms. Endogenous HCF-1 was found to localize in the nucleus of most, if not all, somatic and germline cells in wild-type worms. The *hcf-1(pk924)* mutant worms marked by SUR-5::GFP showed only background signal. DAPI staining was used to indicate the nucleus. Photos were taken at 200X magnification. (B) A magnified image of the head region of the wild-type worm shown in (A).

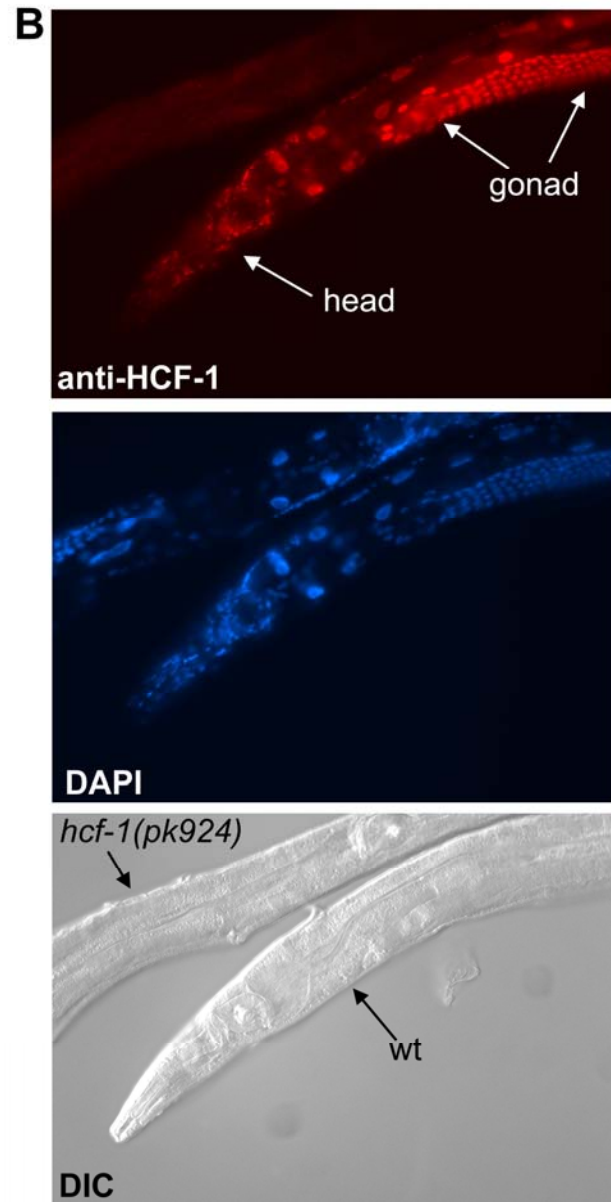
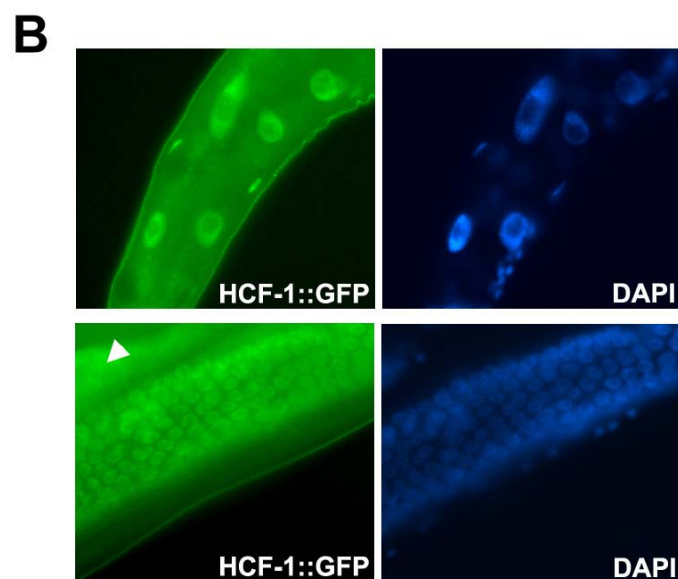
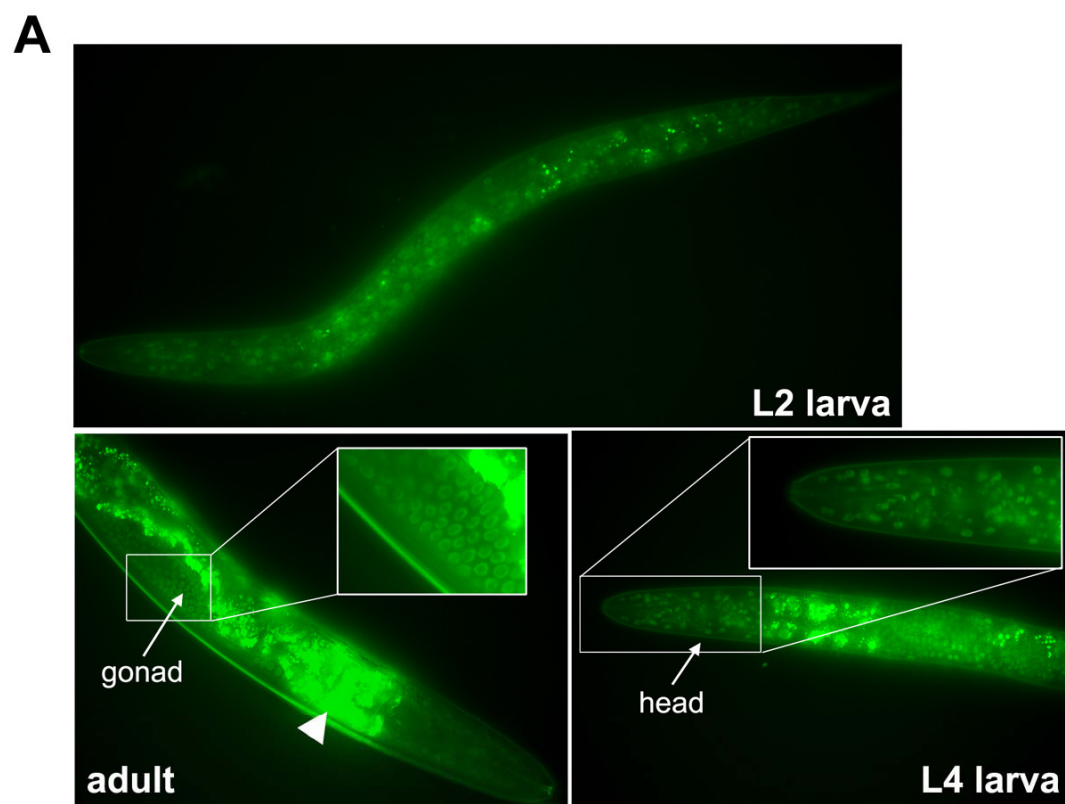


Figure 3.5 GFP-fused HCF-1 is expressed in the nucleus of somatic and germline cells.

(A) The images show the GFP expression of live transgenic worms carrying low-copy number of the *hcf-1::gfp* transgene (*rwls3[Phcf-1::hcf-1::gfp, unc-119]*) at different developmental stages under normal culture condition. HCF-1::GFP is expressed in the nucleus of somatic and germline cells. Arrowhead indicates the high levels of autofluorescence observed in the intestine of the adult worm (bottom left panel).

(B) *hcf-1::gfp* worms were fixed and immunostained using anti-GFP. HCF-1::GFP is detected in the nucleus of somatic (upper panel) and germline cells (bottom panel). DAPI staining was used to indicate the nucleus. Photos were taken at 400X magnification. Arrowhead indicates the autofluorescence observed in the intestine.



mammalian HCF-1 is also predominantly a nuclear protein (Kristie et al., 1995) and its nuclear localization is thought to be important for its role in regulating gene expression.

3.3.3 *hcf-1* modulates lifespan in a *daf-16*-dependent manner.

To characterize how *hcf-1* modulates *C. elegans* lifespan, we asked whether *hcf-1* may genetically interact with any known longevity factors in *C. elegans*. Because DAF-16/FOXO is one of the best characterized longevity determinants, we tested the epistatic relationship between *hcf-1* and *daf-16*. We created double mutants containing the *hcf-1(pk924)* or *hcf-1(ok559)* and the null *daf-16(mgDf47)* mutations. We found that the *daf-16(mgDf47);hcf-1(pk924)* or *daf-16(mgDf47);hcf-1(ok559)* double mutant had a lifespan indistinguishable from that of the *daf-16(mgDf47)* single mutant, which is ~20% shorter than wild-type worms (Lin et al., 2001) (Figure 3.1C, Table 3.3&3.5). We obtained similar results with *hcf-1(ok559)* mutant worms treated with *daf-16* RNAi (Table 3.5). Our results indicate that *hcf-1* requires the activity of *daf-16* to modulate longevity in *C. elegans* and suggest that *hcf-1* may be a novel upstream regulator of *daf-16*.

3.3.4 *hcf-1* likely acts in parallel to the IIS and germline pathway to modulate lifespan.

Given the epistatic relationship between *hcf-1* and *daf-16*, we wondered whether *hcf-1* modulates *C. elegans* lifespan by functioning in the IIS pathway, a well-established upstream regulator of *daf-16*. To test this, we examined the genetic interactions between *hcf-1* and two major components of the IIS pathway: *daf-2*/insulin/IGF receptor and *age-1*/PI3K. We reasoned that if *hcf-1* normally affects *C. elegans* lifespan by acting in the IIS pathway, then loss of

Table 3.5 Inactivation of *hcf-1* results in lifespan increase that is completely dependent on *daf-16*, but likely independent of the IIS pathway.

Strain	Mean LS ± SEM (Days)	Total Number of Animals Died/Total	% of wt	p Value versus wt	p Value versus <i>daf-16(mgDf47);hcf-1(ok559)</i>
wt	13.1±0.5	34/34		N.A.	<0.0001
<i>daf-16(mgDf47)</i>	10.8±0.3	38/38	82%	<0.0001	0.8135
<i>hcf-1(ok559)</i>	18.0±0.8	38/38	137%	<0.0001	<0.0001
<i>daf-16(mgDf47);hcf-1(ok559)</i>	11.0±0.3	41/41	84%	<0.0001	N.A.

Strain + RNAi	Mean LS ± SEM (Days)	Total Number of Animals Died/Total	% of wt+L4440	p Value versus wt + L4440	p Value versus <i>hcf-1(ok559) + daf-16</i>
wt + L4440	13.6±0.3	48/48		N.A.	<0.0001
wt + <i>daf-16</i>	9.9±0.2	28/28	73%	<0.0001	0.1278
<i>hcf-1(ok559) + L4440</i>	16.3±0.6	27/27	120%	<0.0001	<0.0001
<i>hcf-1(ok559) + daf-16</i>	10.3±0.2	36/36	76%	<0.0001	N.A.

Strain	Mean LS ± SEM (Days)	Total Number of Animals Died/Total	% of wt	p Value versus wt	p Value versus <i>daf-2(e1370);hcf-1(ok559)</i>
wt	13.9±0.4	46/50		N.A.	<0.0001
<i>daf-2(e1370)</i>	30.3±1.3	50/50	218%	<0.0001	0.0112
<i>hcf-1(ok559)</i>	18.6±0.6	50/50	134%	<0.0001	<0.0001
<i>daf-2(e1370);hcf-1(ok559)</i>	35.9±1.0	51/51	257%	<0.0001	N.A.

Strain + RNAi	Mean LS ± SEM (Days)	Total Number of Animals Died/Total	% of wt + L4440	p Value versus wt + L4440	p Value versus <i>hcf-1(ok559) + daf-2</i>
wt + L4440	14.5±0.2	118/118		N.A.	<0.0001
wt + <i>daf-2</i>	27.4±0.4	38/38	189%	<0.0001	<0.0001
<i>hcf-1(ok559) + L4440</i>	16.0±0.5	37/37	110%	<0.0001	<0.0001
<i>hcf-1(ok559) + daf-2</i>	30.2±0.4	38/38	208%	<0.0001	N.A.

Table 3.5 (continued) Inactivation of *hcf-1* results in lifespan increase that is completely dependent on *daf-16*, but likely independent of the IIS pathway.

Strain + RNAi	Mean LS ± SEM (Days)	Total Number of Animals Died/Total	% of wt + L4440	p Value versus wt + L4440	p Value versus <i>hcf-1(ok559)</i> + <i>age-1</i>
wt + L4440	14.5±0.2	118/118		N.A.	<0.0001
wt + <i>age-1</i>	21.1±0.3	77/78	146%	<0.0001	<0.0001
<i>hcf-1(ok559)</i> + L4440	16.0±0.5	37/37	110%	<0.0001	<0.0001
<i>hcf-1(ok559)</i> + <i>age-1</i>	26.5±0.5	44/44	183%	<0.0001	N.A.

The lifespan experiments were repeated at least two independent times with similar results and the data for representative experiments are shown.

The lifespan data were analyzed using the Log-rank test and p values for each individual experiment are shown. N.A.: not applicable.

hcf-1 would not have a major impact on the longevity of worms already lacking IIS signaling. We created double mutants containing the *hcf-1(pk924)* or *hcf-1(ok559)* and either the *daf-2(e1370)* or the *age-1(mg44)* mutations. Consistent with previous findings (Kenyon et al., 1993), the *daf-2(e1370)* temperature-sensitive mutant showed an approximately 2-fold increase in lifespan compared to wild-type worms at the non-permissive temperature 25°C (Figure 3.1D, Table 3.3&3.5). Interestingly, the *daf-2(e1370);hcf-1(pk924)* or *daf-2(e1370);hcf-1(ok559)* double mutant lived considerably longer than either the *daf-2(e1370)* or *hcf-1(pk924)* or *hcf-1(ok559)* single mutant (Figure 3.1D, Table 3.3&3.5), and exhibited a lifespan increase that is greater than the sum of the effect for the two single mutations.

We obtained similar results with the *age-1(mg44);hcf-1(ok559)* double mutant. *age-1(mg44)* is a null mutant and, when maintained as a homozygous strain, exhibits an unconditional dauer arrest phenotype (Gottlieb and Ruvkun, 1994; Morris et al., 1996). To avoid this, we collected *age-1(mg44)* or *age-1(mg44);hcf-1(ok559)* homozygous mutant adults born from *age-1(mg44)/+* or *age-1(mg44)/+;hcf-1(ok559)* parents for lifespan analysis. These *age-1(mg44)* and *hcf-1(ok559);age-1(mg44)* worms completely lacked zygotic *age-1* expression; however, they inherited sufficient maternal *age-1* message to develop normally (Morris et al., 1996). Similar to previous results (Morris et al., 1996), the *age-1(mg44)* zygotic null mutant worms lived much longer than wild-type worms (Figure 3.1E, Table 3.3). The *age-1(mg44);hcf-1(ok559)* double mutant worms lived considerably longer than either the *age-1(mg44)* or *hcf-1(ok559)* single mutant (Figure 3.1E, Table 3.3), and exhibited a lifespan increase that is even greater than the sum of the effect for the single mutations. RNAi knock down of *daf-2* or *age-1* in the *hcf-1(ok559)* mutant

gave similar results (Table 3.5). The genetic results described here indicate that loss of *hcf-1* and loss of IIS act synergistically to extend lifespan in *C. elegans* and suggest that *hcf-1* likely functions in a pathway in parallel to IIS. Although the *hcf-1(pk924)* mutation is a putative null mutation, the *daf-2(e1370)* mutation is a temperature sensitive mutation, and a small amount of maternal AGE-1 protein may have persisted in the *age-1(mg44);hcf-1(ok559)* double mutant, it remains possible that loss of *hcf-1* increases lifespan by further decreasing *daf-2* signaling.

Since germline proliferation has been implicated in *C. elegans* lifespan modulation, we wondered whether the extended lifespan of the *hcf-1* mutant is related to the brood size defect of this mutant (Lee et al., 2007)(Figure 3.2). In this regard, we tested the lifespan of the double mutant *glp-1(e2141);hcf-1(pk924)*. The *glp-1(e2141)* mutant completely lacks germline cells at the non-permissive temperature 25°C and is long-lived (Arantes-Oliveira et al., 2002). If the *hcf-1* mutant is long-lived due to its partial defect in germline proliferation, then we would expect *hcf-1* deficiency not to affect the lifespan of worms completely lacking germline cells. We found that the *glp-1(e2141);hcf-1(pk924)* double mutant lived much longer than the *glp-1(e2141)* or *hcf-1(pk924)* single mutants at 25°C (Figure 3.1F, Table 3.3). Therefore, loss of *hcf-1* can continue to extend the lifespan of worms that completely lack germline cells and are sterile, suggesting that *hcf-1* has a function in lifespan modulation that is beyond its role in germline and brood size regulation.

3.3.5 Loss of *hcf-1* promotes resistance to specific environmental stress.

Since DAF-16/FOXO is well known to regulate stress responses (Honda and Honda, 1999; Kenyon, 2005; Yanase et al., 2002), we tested

whether the *hcf-1* mutants may exhibit differential response to environmental stress stimuli. To assay for a response to acute oxidative stress, we challenged wild-type or *hcf-1* mutant adult worms with a high-dose of paraquat, a superoxide-inducing agent, and monitored their survival. We found that the *hcf-1(pk924)* mutant worms were considerably more resistant to the paraquat treatment compared to wild-type worms at multiple time points throughout the experiment (Figure 3.6A). Moreover, the paraquat resistance of the *hcf-1(pk924)* mutants was dependent on *daf-16*, as the *daf-16(mgDf47);hcf-1(pk924)* double mutant was sensitive to paraquat, similar to that of the *daf-16(mgDf47)* single mutant (Figure 3.6B). Interestingly, the *hcf-1(ok559)* mutant worms had survival kinetics very similar to that of wild-type worms in the paraquat assay, suggesting that the *hcf-1(ok559)* mutant, while long-lived, was not more resistant to a high dose of paraquat treatment compared to wild-type worms. No HCF-1 protein is detected in the *hcf-1(pk924)* mutant, whereas some truncated protein accumulates in the *hcf-1(ok559)* mutant (Figure 3.3). Therefore, it is possible that resistance to a high level of oxidative stress only becomes apparent when HCF-1 is completely lost.

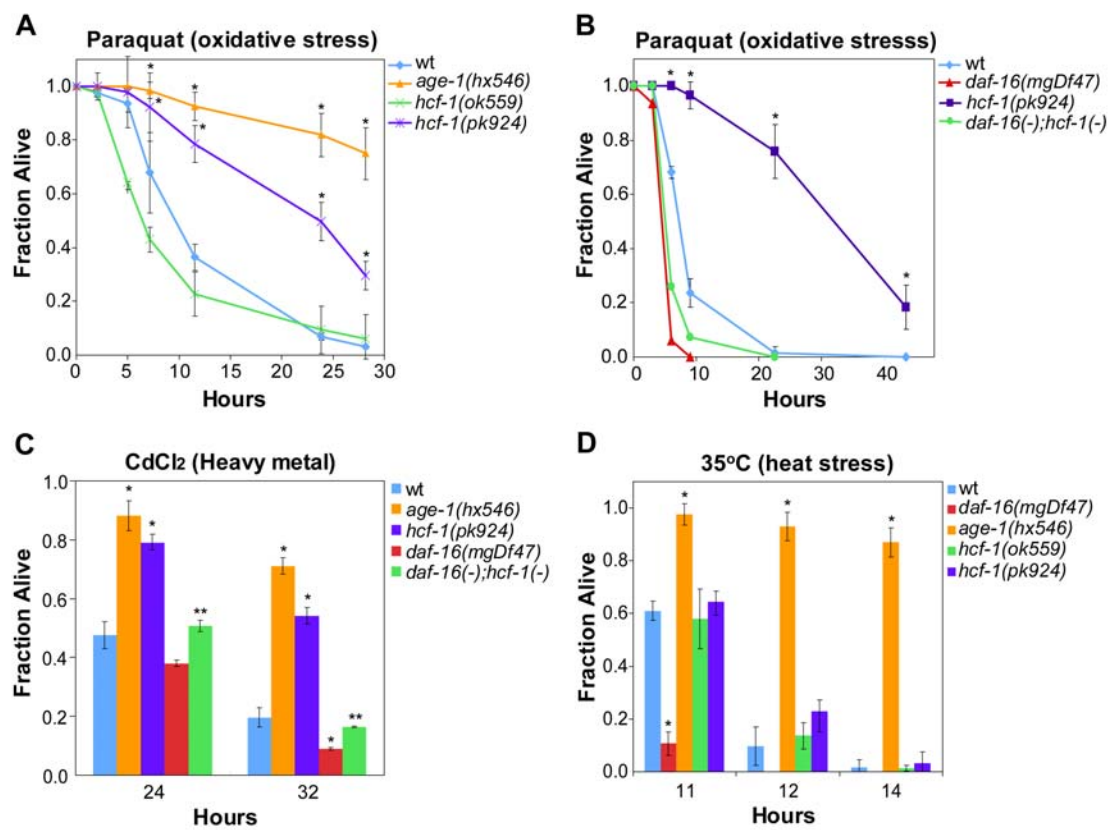
To assay for a response to heavy metal stress, we challenged wild-type or *hcf-1* mutant adult worms with cadmium (Barsyte et al., 2001) and monitored their survival. Similar to what we observed with the paraquat assay, the *hcf-1(pk924)* mutant worms were more resistant to the cadmium exposure compared to wild-type worms at multiple time points (Figure 3.6C). Importantly, the cadmium resistance of the *hcf-1(pk924)* mutant was also *daf-16*-dependent (Figure 3.6C).

Figure 3.6 Loss of *hcf-1* results in heightened resistance to specific environmental stresses.

(A) The *hcf-1(pk924)* mutant worms exhibited increased survival in 200mM paraquat compared to wild-type worms. (B) The enhanced paraquat resistance of *hcf-1(pk924)* was dependent on *daf-16*. (C) The *hcf-1(pk924)* mutant worms showed increased survival in CdCl₂ (18mM) that was *daf-16* dependent. (D) The *hcf-1(pk924)* and *hcf-1(ok559)* mutants and wild-type worms showed similar survival kinetics when cultured at 35°C. The *age-1(hx546)* and *daf-16(mgDf47)* worms were included as controls as they have been previously reported to be either resistant or sensitive to paraquat, heavy metal or heat shock, respectively (Barsyte et al., 2001; Lithgow et al., 1995; Yanase et al., 2002)

For the stress assays, duplicate to quadruplicate samples were examined for each strain. Mean fraction alive indicates the average survival among the multiplicates and error bars represent the standard deviation of the multiplicates. P value was calculated using Student's t-Test. *: P value < 0.05 when compared to wild-type (wt). **: P value < 0.05 when compared to *hcf-1(pk924)*.

Each of the stress assays was repeated at least two independent times with similar results and the data of representative experiments are shown.



To assay for a response to heat stress, we shifted adult wild-type and *hcf-1* mutant worms to 35°C and monitored their survival. We found that the *hcf-1* mutants and wild-type worms behaved very similarly throughout the time course of the heat shock treatment (Figure 3.6D). As previously reported (Lithgow et al., 1995), the *age-1(hx546)* mutant worms survived much longer and the *daf-16(mgDf47)* mutant worms died much faster than wild-type worms at 35°C. We therefore concluded that loss of *hcf-1* did not result in altered response to acute heat shock. Taken together, our results indicate that loss of *hcf-1* results in worms that are resistant to paraquat and cadmium exposure, but not to heat shock, suggesting that *hcf-1* is required for specific stress response.

Considering that DAF-16 also plays a key role in dauer formation and fat metabolism in *C. elegans* (Gottlieb and Ruvkun, 1994; Ogg et al., 1997; Riddle and Albert, 1997), we tested whether the *hcf-1* mutants exhibit any dauer or fat phenotypes. We found that the *hcf-1(ok559)* mutant exhibits no dauer phenotype, whereas the *hcf-1(pk924)* null mutant exhibits a weak dauer exit phenotype. When monitored at 25°C, a typical temperature for testing a strong dauer phenotype, both *hcf-1* mutants developed normally, whereas the *daf-2(e1370)* mutant formed 100% dauer (Table 3.6). When monitored at 27°C, a temperature commonly used to test for a weak dauer formation phenotype, neither *hcf-1* mutant behaved differently from wild-type worms (Table 3.6). Lastly, we tested the *daf-2;hcf-1* double mutants at 22°C, which represents a well-established sensitized condition (Lee et al., 2003a) for assaying a weak dauer recovery phenotype. Single and double mutant worms harboring the *daf-2(e1370)* mutation were incubated at the compromised

temperature of 22°C. Under this condition, the *daf-2(ts)* worms enter dauer for ~3 days and then recover to become reproductive adults. We found that the *hcf-1(pk924)* mutation prevented dauer exit, whereas the *hcf-1(ok559)* mutation had no effect (Table 3.6). These results indicate that loss of *hcf-1* is associated with a weak dauer phenotype. Using the vital dye Nile Red, which stains lipid droplets in worms and represents a sensitive way to monitor fat storage (Ashrafi et al., 2003), we did not detect any substantial differences in fat storage between *hcf-1* mutants and wild-type worms (Figure 3.7).

3.3.6 HCF-1 regulates the expression of a subset of DAF-16 regulated genes.

Our genetic data suggest that *hcf-1* acts upstream of *daf-16* to affect *C. elegans* lifespan and stress responses. Since increased DAF-16 nuclear localization and transcriptional activities have been shown to extend lifespan in *C. elegans*, we tested whether HCF-1 may regulate the localization, expression level, and/or transcriptional activities of DAF-16. Using transgenic worms expressing GFP-fused DAF-16 to monitor the subcellular localization of DAF-16, we did not detect any altered DAF-16 localization in *hcf-1*-deficient worms (Figure 3.8A). Using quantitative reverse transcription PCR (qRT-PCR) and immunoblotting to examine the RNA and protein expression levels of *daf-16* and the major components of the IIS pathway, including *daf-2*, *age-1*, and *akt-1*, we observed no obvious differences in their expression levels in the *hcf-1(ok559)* and *hcf-1(pk924)* mutants compared to wild-type worms (Figure 3.8B and data not shown). Taken together, our results suggest that HCF-1 is not likely to affect the subcellular localization or the expression level of DAF-16.

To test whether HCF-1 may affect the transcriptional activities of DAF-16, we measured the message levels of DAF-16-regulated genes in the *hcf-1*

Table 3.6 Inactivation of *hcf-1* results in a weak dauer exit phenotype.

Temperature	Strain	Total number	% of Dauer
25°C	wt	>100	0%
	<i>daf-2(e1370)</i>	>100	100%
	<i>hcf-1(ok559)</i>	>100	0%
27°C	wt	>100	0%
	<i>hcf-1(ok559)</i>	>100	0%
22°C	wt	159	0%
	<i>daf-2(e1370)</i>	311	21.9%
	<i>hcf-1(ok559)</i>	85	0%
	<i>daf-2(e1370);hcf-1(ok559)</i>	131	22.1%

Temperature	Strain	Total number	% of Dauer
25°C	wt	203	0%
	<i>daf-2(e1370)</i>	113	100%
	<i>hcf-1(pk924)</i>	87	0%
	<i>daf-2(e1370);hcf-1(pk924)</i>	41	100%
27°C	wt	160	1.3%
	<i>hcf-1(pk924)</i>	61	1.6%
22°C	wt	200	0%
	<i>daf-2(e1370)</i>	130	23.1%
	<i>hcf-1(pk924)</i>	124	0%
	<i>daf-2(e1370);hcf-1(pk924)</i>	35	82.9%

Synchronized populations of worms were obtained by egg-lay at 16°C and then shifted to the indicated temperature for development. Dauers were scored three days after temperature shift. *hcf-1(ok559)* allele did not exhibit any dauer phenotypes at 22°C, 25°C and 27°C. *hcf-1(pk924)* allele exhibited enhanced dauer exit phenotype under sensitized condition at 22°C in the *daf-2(e1370)* mutant background (ref) but showed no dauer phenotype at 25°C and 27°C. A representative experiment is shown.

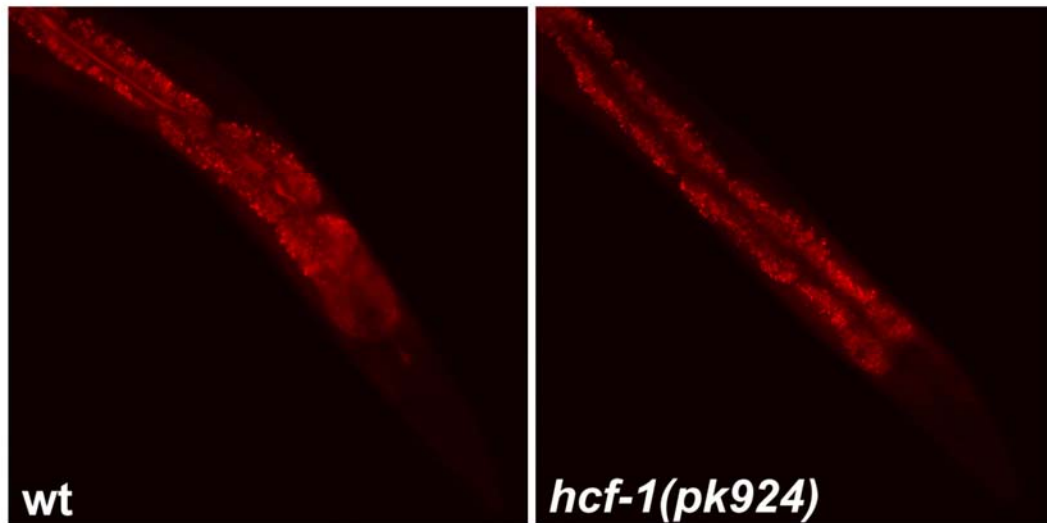
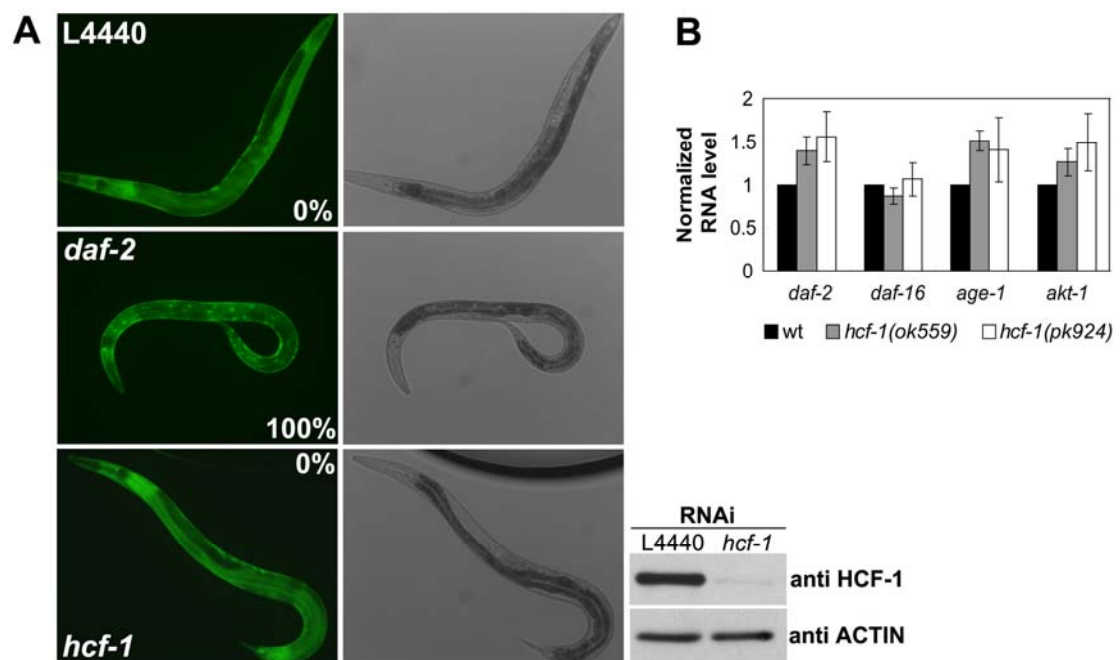


Figure 3.7 Loss of *hcf-1* does not affect fat storage.

Fat storage in *hcf-1(pk924)* and wild-type worms were monitored by staining with the vital dye Nile Red (Ashrafi et al., 2003). Nile Red staining pattern of *hcf-1(pk924)* was similar to that in wild-type worms.

Figure 3.8 Loss of *hcf-1* does not result in altered DAF-16 subcellular localization or a change in DAF-16 expression level.

(A) Transgenic worms over-expressing DAF-16::GFP (*daf-16(mgDf47);xrls87*) were treated with empty vector L4440 control RNAi, *hcf-1* RNAi, or *daf-2* RNAi at 16°C for 5 days. DAF-16::GFP exhibited diffuse expression pattern in both the control RNAi and the *hcf-1* RNAi knock down worms. *hcf-1* RNAi was able to substantially reduce HCF-1 levels (bottom right panel). *daf-2* RNAi was included as a positive control as it is known to stimulate robust nuclear localization of DAF-16::GFP. Photos showed the DAF-16::GFP expression pattern and DIC images of live day 2 gravid adults. Nuclear localization was verified using DIC. A total of ~60-70 worms were scored and the percentage of worms showing DAF-16::GFP nuclear localization was shown in the photo. Worm extracts made from the DAF-16::GFP worms treated with control or *hcf-1* RNAi were immunoblotted using anti-HCF-1 antibody (A, bottom right panels). (B) The RNA levels of *daf-16*, *daf-2*, *age-1* and *akt-1* in wild-type, *hcf-1(ok559)* and *hcf-1(pk924)* worms were quantified using qRT-PCR. The data for three independent experiments were pooled, and the mean normalized RNA level and SEM for each gene in the *hcf-1* mutant and wild-type worms are shown. *act-1* was used as an internal control and the RNA level of each gene was normalized to the *act-1* level. The mean normalized RNA level for each gene in wild-type (wt) worms was set as 1. None of the genes tested showed any significant expression change in the *hcf-1* mutants compared to wild-type worms.



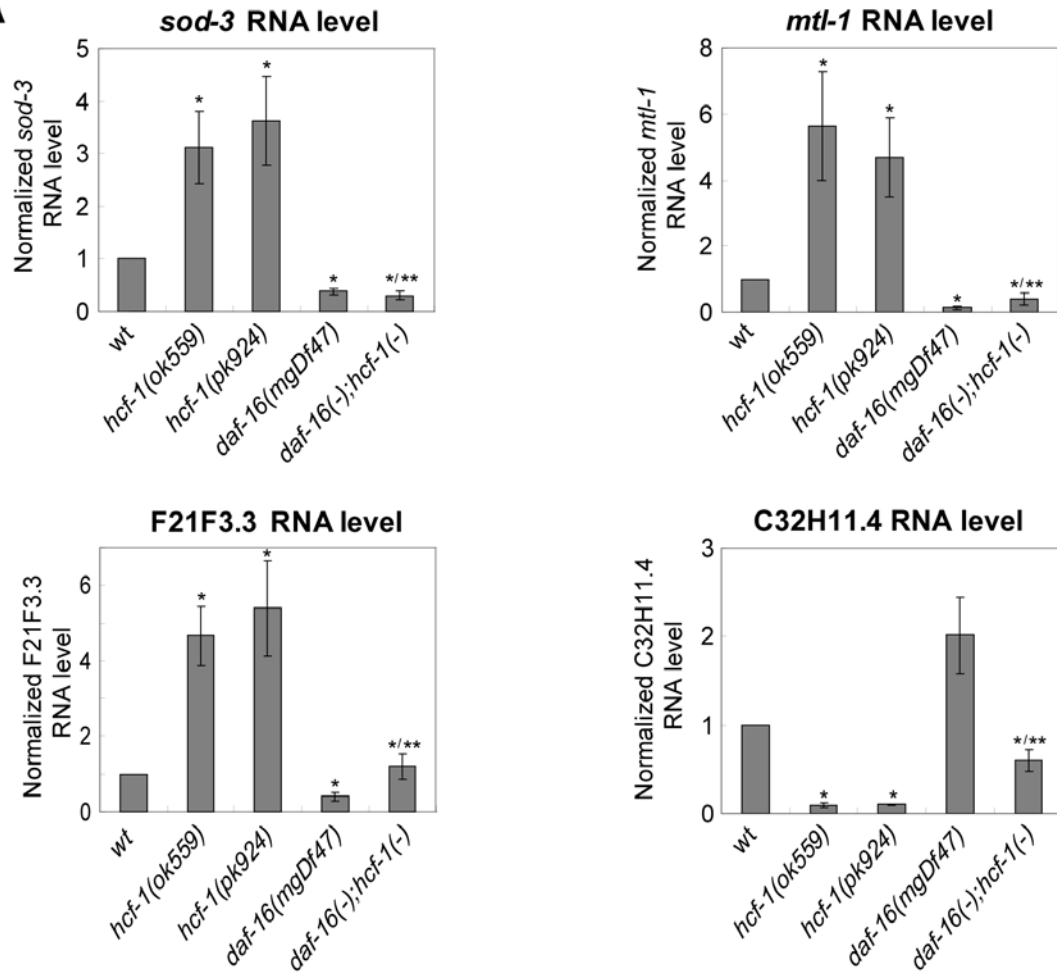
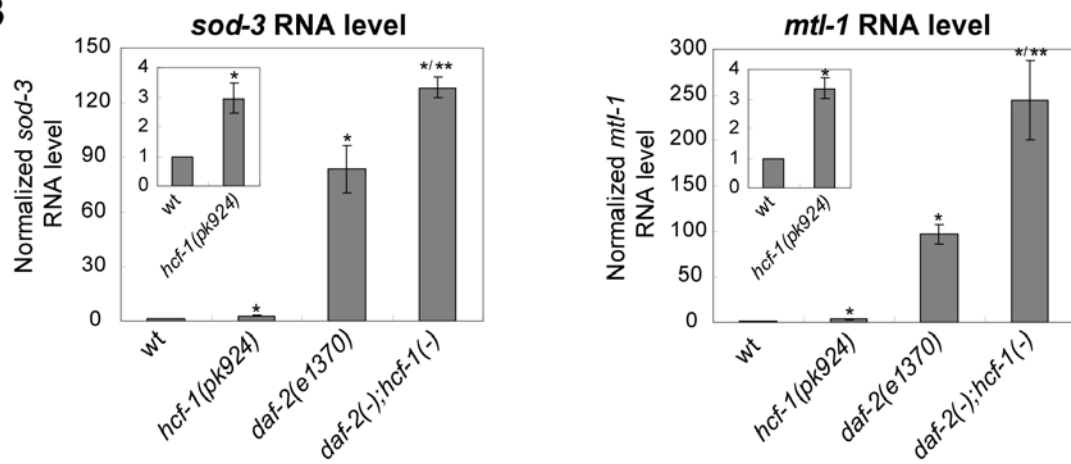
mutant and wild-type worms using qRT-PCR. *sod-3*, which encodes an iron/manganese superoxide dismutase, is one of the best characterized DAF-16 target genes (Honda and Honda, 1999; Murphy et al., 2003) and its transcription is directly up-regulated by DAF-16 (Oh et al., 2006). Interestingly, we found that the RNA level of endogenous *sod-3* was significantly elevated 3-4 fold in both the *hcf-1(ok559)* and *hcf-1(pk924)* mutants as compared to wild-type worms (Figure 3.9A). Importantly, the elevated expression of *sod-3* in the *hcf-1* mutant worms is completely dependent on *daf-16* because in the *daf-16(mgDf47);hcf-1(ok559)* double mutant, the level of *sod-3* expression remained low and was similar to that seen in the *daf-16(mgDf47)* single mutant worms (Figure 3.9A). In corroboration of our qRT-PCR results, we observed elevated levels of GFP expression in *Psod-3::gfp* transgenic worms, which express a GFP reporter driven by the *sod-3* promoter, in *hcf-1(pk924)* mutant background (Figure 3.10).

To investigate whether *hcf-1* may generally affect the transcriptional activities of DAF-16, we surveyed additional DAF-16-regulated genes as reported in previous microarray studies (Murphy et al., 2003). The previous studies have focused on DAF-16 targets that are responsive to IIS and we verified that all the genes we chose to test exhibit *daf-2/daf-16* responsiveness under our assaying conditions (Table 3.7). Among the 11 DAF-16-activated genes examined, we found that in addition to *sod-3*, the expression levels of *mtl-1*, which encodes a metallothionein, and *F21F3.3*, which encodes a farnesyl cysteine-carboxyl methyltransferase, showed a statistically significant, greater than 2-fold up-regulation in the *hcf-1* mutants compared to wild-type worms (Figure 3.9A, Table 3.7). Importantly, the elevated expression of *mtl-1* in *hcf-1* mutant worms is completely dependent on *daf-16* (Figure 3.9A) and

Figure 3.9 Loss of *hcf-1* promotes the DAF-16 transcriptional regulation of several target genes.

(A) The expression of *sod-3*, *mtl-1* and *F21F3.3* was elevated and that of *C32H11.4* was repressed in the *hcf-1* mutants. The elevated expression of *sod-3* and *mtl-1* in the *hcf-1* mutants was completely dependent on *daf-16*; that of *F21F3.3* and *C32H11.4* was partially dependent on *daf-16*. *: P value < 0.05 when compared to wild-type (wt). **: P value < 0.05 when compared to *hcf-1(ok559)*. (B) The expression of *sod-3* and *mtl-1* in the *daf-2(e1370);hcf-1(pk924)* double mutant showed synergistic upregulation when compared to the expression in either *hcf-1(pk924)* or *daf-2(e1370)* single mutant. *: P value < 0.05 when compared to wild-type (wt). **: P value < 0.05 when compared to *daf-2(e1370)*. The quantitative data are summarized in Table 3.7.

The RNA levels of *sod-3*, *mtl-1*, *F21F3.3* and *C32H11.4* were quantified using qRT-PCR and normalized to the internal control *act-1*. The data for at least three independent experiments were pooled, and the mean normalized RNA level and SEM for each gene in the indicated strains are shown. The mean normalized RNA level for each gene in wt worms was set as 1. P value was calculated using Student's t-Test. For *sod-3* or *mtl-1* expression, we analyzed for a synergistic effect in *daf-2(e1370);hcf-1(pk924)* compared to *daf-2(e1370)* or *hcf-1(pk924)* using 2-way ANOVA analysis.

A**B**

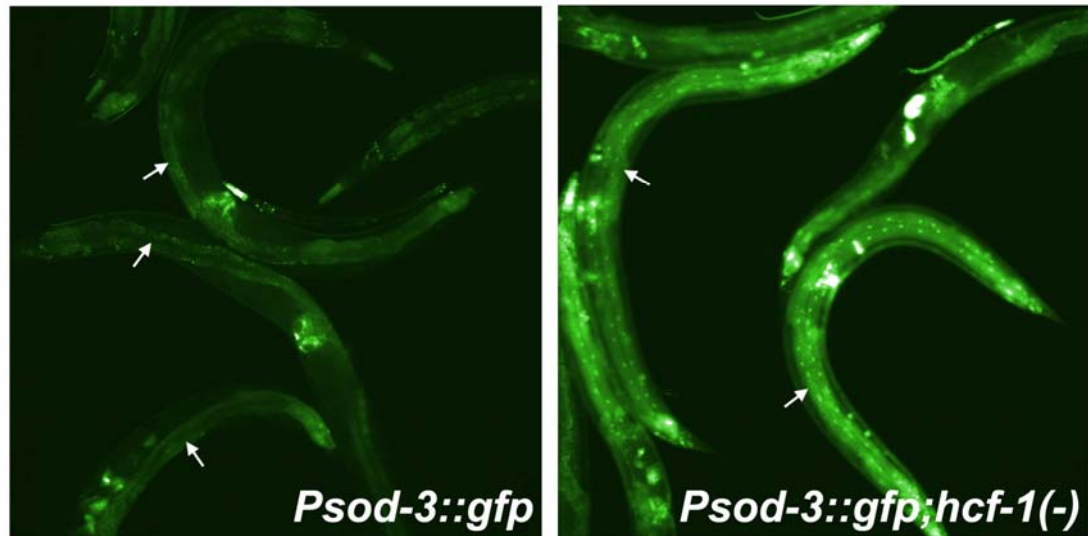


Figure 3.10 *Psod-3::gfp* expression level is elevated in *hcf-1(pk924)* mutants.

The GFP levels of *Psod-3::gfp* (*mul84[Psod-3::gfp]*) in *hcf-1(pk924)* mutant was elevated (right panel) compared to that in wild-type background (left panel). Synchronized day 2 adults were shown in the photos. Arrowhead indicates the intestinal autofluorescence.

that of *F21F3.3* is partially dependent on *daf-16* (Figure 3.9A). Among the 6 DAF-16-repressed genes examined, we found that the expression level of *C32H11.4*, which encodes a protein of unknown function, showed a statistically significant, greater than 2-fold down-regulation in the *hcf-1* mutants compared to wild-type worms (Figure 3.9A, Table 3.7). Similar to that of *F21F3.3*, the repressed expression of *C32H11.4* is partially dependent on *daf-16* (Figure 3.9A). The partial dependency suggests that additional factors might cooperate with DAF-16 to regulate *F21F3.3* and *C32H11.4* expression in the *hcf-1* mutants.

We also noticed that the expression of *hsp-16.1*, which encodes a heat shock protein, and *fat-5*, which encodes a delta-9 fatty acid desaturase, was significantly upregulated and repressed, respectively, in the *hcf-1* mutants (Table 3.7). However, the altered expression of *fat-5* and *hsp-16.1* in the *hcf-1* mutants did not require *daf-16* (data not shown). These results suggest that although *hsp-16.1* and *fat-5* are robust DAF-16 targets in response to *daf-2* signaling (Table 3.7), they do not appear to be significantly regulated by DAF-16 in response to *hcf-1* deficiency. Moreover, whereas *fat-5* is activated by DAF-16 in response to reduced *daf-2* signaling, its expression was repressed in the *hcf-1* mutant in a *daf-16*-independent manner. Many of the DAF-16 downstream genes we surveyed are likely regulated by multiple different transcription factors. For example, *hsp-16.1* is likely also regulated by the heat shock factor HSF-1. It is possible that in the *hcf-1* mutants, different transcription factor(s) play a major role in mediating the expression change of *hsp-16.1* and *fat-5*, and DAF-16 only plays a minor role or is not involved in their gene expression regulation. The expression of the remaining DAF-16

Table 3.7 Inactivation of *hcf-1* results in significant expression changes of a subset of DAF-16 regulated genes.

(A) DAF-16 upregulated genes:

Gene id	Fold change in <i>hcf-1(pk924)/wt</i> ±SEM	Fold change in <i>daf-2(-)/wt</i> ±SEM	P value of t-Test (<i>hcf-1(pk924)</i> compared to wt)	Description
<i>hsp-16.1^a</i>	5.93±3.23	5.49±0.74	0.0301	Heat shock protein
F21F3.3	5.39±1.27	10.90±2.06	0.0260	Farnesyl cysteine-carboxyl methyltransferase
<i>mtl-1</i>	4.69±1.18	96.96±11.07	0.0352	Metallothionein
<i>sod-3</i>	3.63±0.84	83.45±12.98	0.0355	Iron/manganese superoxide dismutase
<i>dod-3</i>	2.04±1.08	192.60±15.49	0.3879	Uncharacterized protein
<i>ges-1</i>	1.56±0.66	2.06±0.12	0.4438	Carboxylesterase expressed in gut cells
M02D8.4	1.44±0.45	2.99±0.49	0.3815	Protein similar to asparagine synthase
K09C4.5	1.19±0.21	2.18±0.06	0.4181	Permease of the major facilitator superfamily
<i>hsp-12.3</i>	1.07±0.07	5.90±0.18	0.3909	Heat shock protein
<i>lys-7</i>	0.85±0.05	2.15±0.16	0.0408	Antimicrobial lysozyme
<i>fat-5^a</i>	0.32±0.08	3.34±0.14	0.0009	Delta-9 fatty acid desaturase

(B) DAF-16 downregulated genes:

Gene id	Fold change in <i>hcf-1(pk924)/wt</i> ±SEM	Fold change in <i>daf-2(-)/wt</i> ±SEM	P value of t-Test (<i>hcf-1(pk924)</i> compared to wt)	Description
C32H11.4	0.11±0.01	0.04±0.01	0.0000	Uncharacterized protein
F08G5.6	0.61±0.03	0.46±0.03	0.0003	Uncharacterized protein
F35E12.5	0.61±0.13	0.08±0.01	0.0387	Uncharacterized protein
T16G12.1	1.11±0.18	0.47±0.01	0.5616	Puromycin-sensitive aminopeptidase and related aminopeptidases
<i>dod-24</i>	1.49±0.30	0.01±0.00	0.1750	Uncharacterized protein
<i>dod-22</i>	1.49±0.44	0.16±0.07	0.1243	Uncharacterized protein

Table 3.7 (continued) Inactivation of *hcf-1* results in significant expression changes of a subset of DAF-16 regulated genes.

(C) *daf-16*-dependent gene regulation:

Gene id	Fold change in <i>hcf-1(ok559)/wt</i> ±SEM	Fold change in <i>daf-16(mgDf47)/wt</i> ±SEM	Fold change in <i>daf-16(mgDf47);hcf-1(ok559)/wt</i> ±SEM	P value of t-Test (<i>daf-16(mgDf47);hcf-1(ok559)</i> compared to <i>daf-16(mgDf47)</i>)
<i>sod-3</i>	3.12±0.70	0.38±0.06	0.30±0.08	0.4740
<i>mtl-1</i>	5.64±1.62	0.15±0.04	0.39±0.17	0.5451
F21F3.3	4.66±0.78	0.40±0.10	1.20±0.34	0.0665
C32H11.4	0.09±0.02	2.01±0.43	0.60±0.12	0.0333

(D) Synergistic gene regulation by *hcf-1* and *daf-2*:

Gene id	Fold change in <i>hcf-1(pk924)/wt</i> ±SEM	Fold change in <i>daf-2(e1370)/wt</i> ±SEM	Fold change in <i>daf-2(e1370);hcf-1(pk924)/wt</i> ±SEM	P value of 2-way ANOVA test
<i>sod-3</i>	2.95±0.50	83.45±12.98	128.2±5.59	0.0164
<i>mtl-1</i>	3.37±0.36	96.96±11.07	244.40±43.59	0.0121

The RNA levels of multiple DAF-16 regulated genes were quantified using qRT-PCR. The data for three to six independent experiments were pooled, and the mean fold-change in expression and SEM for each gene in *hcf-1* mutant compared to the wild-type worms is shown. *act-1* was used as an internal control and the RNA level of each gene was normalized to the *act-1* level. P value was calculated using Student's t-Test (A-C). For analysis of synergistic effects, 2-way ANOVA test was used (D).

The gene list was selected from the Class 1 or Class 2 genes reported in the DAF-16 microarray study (Murphy et al., 2003). Upregulation or downregulation by DAF-16 was verified under our experimental conditions. Genes shaded in grey showed significant expression changes ≥ 2 fold in the *hcf-1(pk924)* mutant (p value < 0.05) and the expression change was *daf-16* dependent (A-B). ^a: The expression changes in *hcf-1(-)* in those genes are not *daf-16* dependent.

target genes either did not show a significant change in the *hcf-1* mutants, or their expression change was less than 2-fold.

Consistent with our genetic data in which *hcf-1* appears to act in parallel to *daf-2* signaling to affect lifespan, the expression of *sod-3* and *mtl-1* was synergistically up-regulated in the *daf-2(e1370);hcf-1(pk924)* double mutant compared to either *daf-2(e1370)* or *hcf-1(pk924)* single mutant (Figure 3.9B, Table 3.7). Taken together, our results suggest that *hcf-1* is only able to affect the expression of selective DAF-16 target genes. Moreover, our data indicate that *hcf-1* inactivation leads to *daf-16*-dependent up-regulation of three different DAF-16 activated genes and *daf-16*-dependent down-regulation of a DAF-16 repressed gene, suggesting that *hcf-1* normally participates in the inhibition of DAF-16 transcriptional activity. Importantly, the dependence of *hcf-1* on *daf-16* to elicit gene expression changes correlates with the requirement of *daf-16* in *hcf-1*-mediated lifespan modulation, suggesting that the ability of HCF-1 to regulate DAF-16 transcriptional activity is likely linked to its role in longevity. Considering that *C. elegans* HCF-1 is normally localized to the nucleus, and that its mammalian homolog has a known role in gene expression regulation, we hypothesize that HCF-1 modulates *C. elegans* lifespan by regulating the transcriptional activity of DAF-16 at a subset of target genes that are particularly important for stress response and longevity assurance.

3.3.7 HCF-1 forms a protein complex with DAF-16.

We next examined how HCF-1 might affect the transcriptional activity of DAF-16. In mammalian cells, HCF-1 is thought to regulate gene expression by binding to various transcription and chromatin factors (Piluso et al., 2002;

Tyagi et al., 2007; Vogel and Kristie, 2000; Wysocka et al., 2003). In *C. elegans*, DAF-16 localizes to both cytoplasm and nucleus under normal culture condition, and HCF-1 appears predominantly nuclear in most cells (Lee et al., 2001; Lee et al., 2007; Lin et al., 2001)(Figure 3.4&3.5), suggesting that DAF-16 and HCF-1 co-localize in the nucleus (Figure 3.11). We therefore tested whether *C. elegans* HCF-1 may physically associate with DAF-16. Since we did not have an antibody that could detect endogenous DAF-16 robustly, we performed co-immunoprecipitation (co-IP) experiments using worm strains that lack endogenous DAF-16, but carry in low-copy number a functional gfp-fused *daf-16* transgene (*daf-16(mu86);muls71*) (Lin et al., 2001). We found that when an affinity-purified HCF-1 antibody was used to immunoprecipitate HCF-1 from extracts of the *daf-16::gfp* transgenic worms, DAF-16::GFP was co-immunoprecipitated (Figure 3.12B). This interaction appeared specific because when co-IP experiments were done using extracts of *daf-16::gfp* worms that also harbor the *hcf-1(ok559)* deletion (*daf-16(mu86);hcf-1(ok559);muls71*), we were not able to immunoprecipitate HCF-1 or to co-immunoprecipitate DAF-16::GFP (Figure 3.12B). Furthermore, using identical co-IP conditions, we did not recover the irrelevant Psod-3::GFP (a GFP reporter driven by the *sod-3* promoter) upon HCF-1 immunoprecipitation, indicating that the protein-protein interaction detected between DAF-16::GFP and HCF-1 is not likely mediated by the GFP tag. We obtained similar results using reciprocal co-IP experiments (Figure 3.12A). Our results suggest that HCF-1 is able to form a specific protein complex with DAF-16 in *C. elegans*.

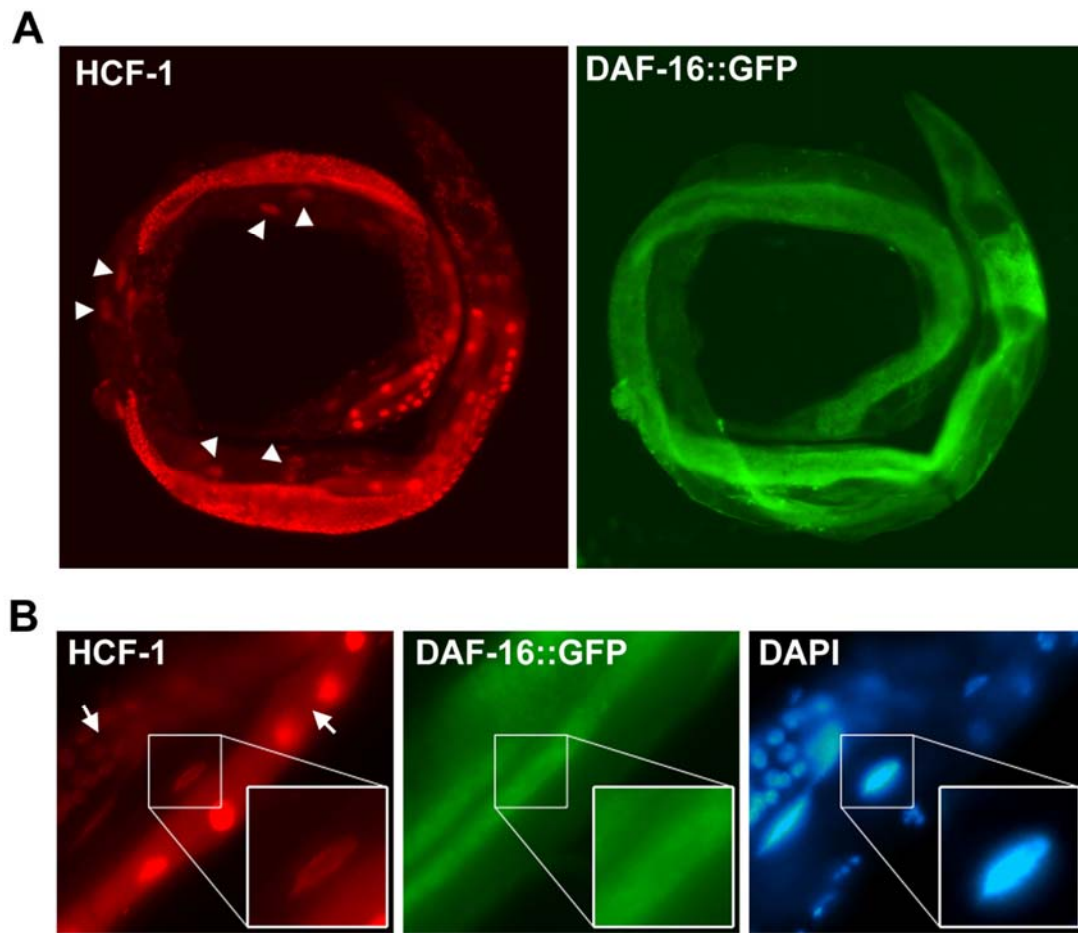


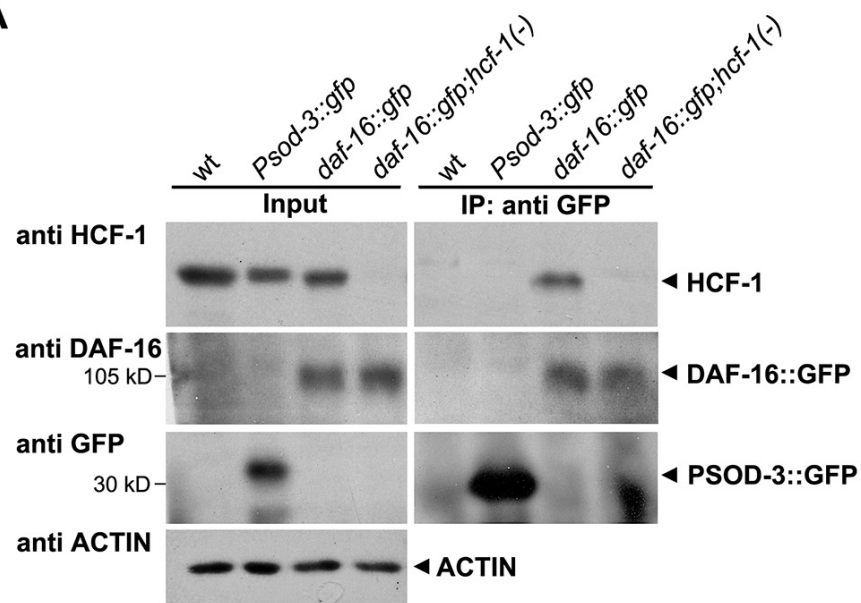
Figure 3.11 HCF-1 co-localizes with DAF-16::GFP in the nucleus.

Transgenic worms over-expressing DAF-16::GFP (*daf-16(mgDf47);xrls87*) were immunostained with anti-HCF-1. Photos were taken at 100X (A) or 400X (B) magnification and representative images are shown. Under normal culturing condition, DAF-16::GFP was diffusely localized in the cytoplasm and nucleus as previously reported (Lee et al., 2001; Lin et al., 2001). HCF-1 co-localized with DAF-16::GFP in the nucleus of non-germline cells. DAPI staining was used to indicate the nucleus. Arrowheads indicate the nucleus of intestinal cells. Arrows indicate the gonad of the worms where DAF-16::GFP expression is absent due to transgene silencing (Kelly and Fire, 1998).

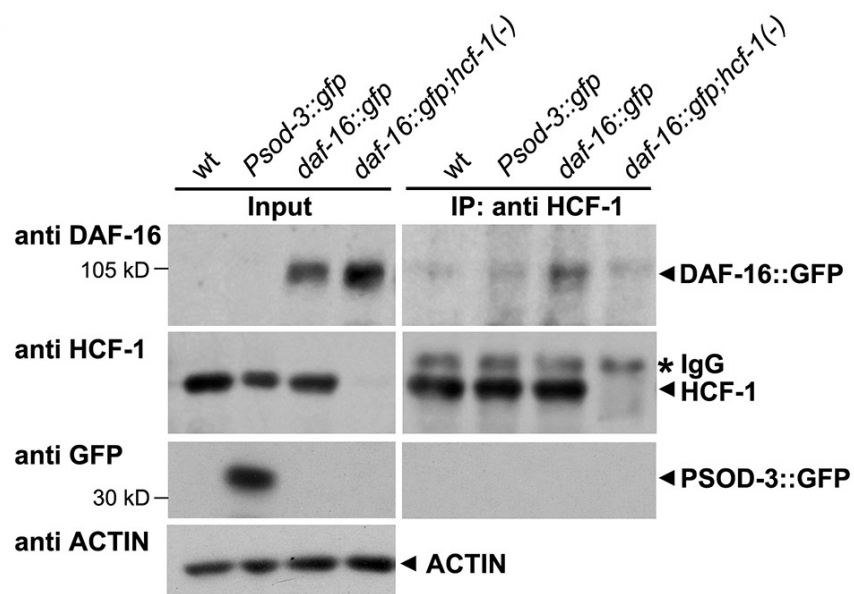
Figure 3.12 HCF-1 forms a protein complex with DAF-16 in *C. elegans*.

Worm extracts were made from mixed stage worms and subjected to immunoprecipitation. Extracts from wild-type (wt), *Psod-3::gfp*, *daf-16::gfp* (*daf-16(mu86);muls71*), and *daf-16::gfp;hcf-1(-)* (*daf-16(mu86);hcf-1(ok559);muls71*) worms were either immunoprecipitated using anti-GFP antibody (A) or anti-HCF-1 antibody (B). The immunoprecipitated protein complexes were subsequently immunoblotted using anti-HCF-1, anti-DAF-16, or anti-GFP antibodies. *Psod-3::gfp* worms were used as a negative control to indicate that there was no interaction between the GFP tag and HCF-1. For Input, 50µg of total protein was loaded per lane. For immunoprecipitation, 2mg of total protein was used.

A



B



3.3.8 Loss of *hcf-1* leads to enhanced enrichment of DAF-16 on its target gene promoters.

To further elucidate the molecular mechanism by which HCF-1 regulates DAF-16-mediated transcription, we performed chromatin immunoprecipitation (ChIP) experiments to test how HCF-1 might affect DAF-16 enrichment on target gene promoters. For the ChIP experiments, we employed *daf-16::gfp* worms (*daf-2(e1370);daf-16(mgDf47);daf-16::gfp*) and anti-GFP immunoprecipitation to capture DAF-16. As previously reported (Oh et al., 2006), DAF-16 was enriched at the promoter of *sod-3* when the IIS pathway was inactivated (Figure 3.13A). We also examined the DAF-16 target gene *mtl-1* and found that DAF-16 was enriched on its promoter (Figure 3.13A). Under the same ChIP conditions, we did not detect HCF-1 enrichment at the *sod-3* or *mtl-1* promoters, but detected great enrichment of HCF-1 at the promoter of *efl-1* (Figure 3.13B). *efl-1* is the *C. elegans* *E2f1* gene; in mammalian cells, HCF-1 is highly enriched at the promoter region of *E2f1* (Takahashi et al., 2000). Thus, our results demonstrate a conserved role of HCF-1 at the *efl-1/E2f1* promoter in worms, and suggest that HCF-1 is not likely to present at *sod-3* or *mtl-1* promoters. Considering our co-IP results showing that HCF-1 and DAF-16 physically associate in worms (Figure 3.12), our ChIP results suggest that the HCF-1/DAF-16 complex is probably not present at the promoters of DAF-16 target genes. However, it remains possible that HCF-1 is a component of a large protein complex that associates with DAF-16 at target gene promoters, and our cross-linking conditions cannot capture the presence of HCF-1 at those promoters. For the other *hcf-1*-regulated, *daf-16*-dependent genes (Table 3.7; *F21F3.3* & *C32H11.4*), we

Figure 3.13 Loss of *hcf-1* enhances the enrichment of DAF-16 on the promoters of its target genes.

Chromatin immunoprecipitation (ChIP) was performed using *daf-2(e1370);daf-16(mgDf47);daf-16::gfp* worms treated with control RNAi (L4440) or *hcf-1* RNAi. Synchronized adult worms of the different strains were incubated at 25°C for ~6 hours to inactivate *daf-2* and to induce robust DAF-16::GFP nuclear localization. Worm extracts were subjected to immunoprecipitation using anti-GFP, anti-HCF-1, or anti-rabbit IgG (Rb). The recovered DNA was quantitated using qPCR. Regions around the DAF-16 binding element (DBE) at the *sod-3* or *mtl-1* promoters, as well as a putative non-coding region of chromosome IV not containing any DBE were monitored. The figure shows one representative experiment. Error bars represent the SEM of the duplicated reactions in qPCR. Similar results were obtained for three independent experiments.

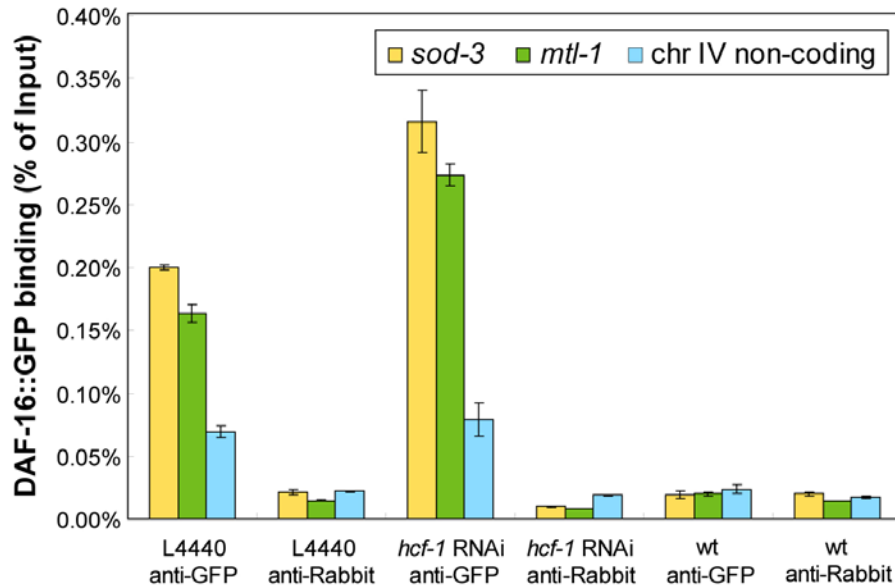
A

Figure 3.13 (continued) (A): DAF-16 enrichment at the promoters of *sod-3* or *mtl-1* is enhanced upon *hcf-1* RNAi. DAF-16 was robustly enriched at the *sod-3* or *mtl-1* promoters after anti-GFP ChIP compared to that of anti-Rb (anti-GFP/anti-Rb at *sod-3* promoter: ~9 fold; anti-GFP/anti-Rb at *mtl-1* promoter: ~11 fold). The fold enrichment of DAF-16 at *sod-3* or *mtl-1* is consistently greater than that at the non-specific chr IV region: *sod-3*/chr IV: ~2.9 fold; *mtl-1*/chr IV: ~2.4 fold. As a control, anti-GFP ChIP in wild-type (wt) worms (not expressing *daf-16::gfp*) showed background signal that was very similar to that of anti-Rb. Upon *hcf-1* RNAi knockdown, DAF-16 enrichment at the *sod-3* or *mtl-1* promoters was greatly increased. anti-GFP/anti-Rb at *sod-3* promoter: ~33 fold (vs. ~9 fold for L4440 RNAi); anti-GFP/anti-Rb at *mtl-1* promoter: ~33 fold (vs. ~11 fold for L4440 RNAi). In contrast, for the non-specific chr IV region, anti-GFP/anti-Rb: ~4 fold (vs. ~3 fold for L4440 RNAi). These data indicate that in the absence of HCF-1, a greater amount of DAF-16 becomes recruited to the *sod-3* or *mtl-1* promoters, but the non-specific binding of DAF-16 to the chr IV region is not substantially changed.

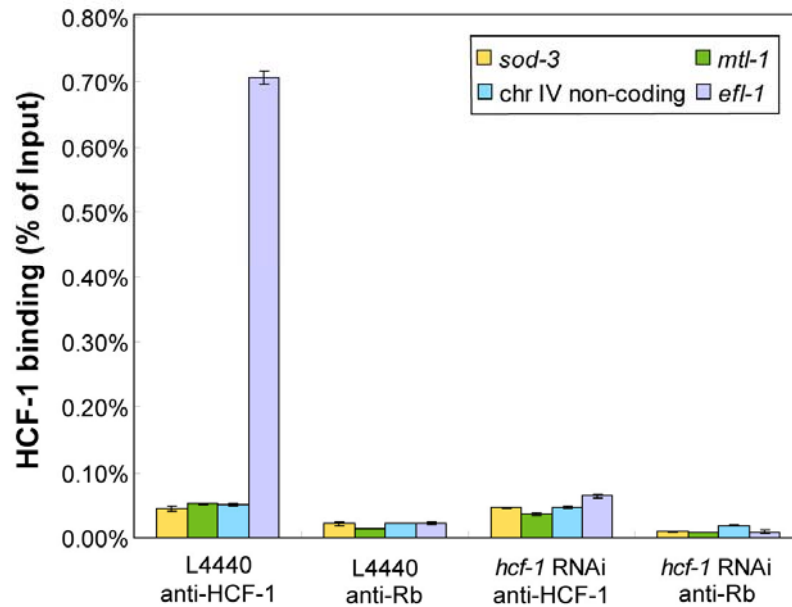
B

Figure 3.13 (continued) (B) HCF-1 is greatly enriched at the *efl-1* promoter, but not at *sod-3* or *mtl-1* promoters. *efl-1* is the *C. elegans* homolog of *E2f1*, which has been shown to be a direct target of HCF-1 in mammalian cells (Takahashi et al., 2000). The region of the *efl-1* promoter containing conserved E2F1 binding element was included as a positive control for anti-HCF-1 ChIP. Whereas HCF-1 was found to be greatly enriched at the *efl-1* promoter, it was not substantially enriched at the promoters of *sod-3* or *mtl-1*, or the chr IV non-coding region. As a control, when *hcf-1* was knocked down by RNAi, the enrichment of HCF-1 on the promoter of *efl-1* was greatly reduced.

either did not identify a putative DAF-16 binding element or did not detect DAF-16 enrichment at the promoter regions we surveyed, suggesting that they might not be DAF-16 direct targets. We next tested whether the enrichment of DAF-16 on *sod-3* or *mtl-1* promoters would be affected when *hcf-1* was RNAi depleted. As a control, we showed that the enrichment of HCF-1 on the *efl-1* promoter was substantially reduced when *hcf-1* was knocked down by RNAi. Interestingly, under the same RNAi conditions, we consistently observed an enhanced enrichment of DAF-16 to the *sod-3* and *mtl-1* promoters in multiple independent trials (Figure 3.13A). These results suggest that in the absence of HCF-1, more DAF-16 is able to localize to the promoters of its target genes.

3.4 Discussion

Our study has revealed the *C. elegans* homolog of host cell factor 1 to be an important longevity determinant and transcriptional regulator of DAF-16. Our data indicate that HCF-1 is necessary for maintaining normal lifespan and stress response in *C. elegans*, as loss of *hcf-1* results in mutant worms with substantially extended longevity and heightened resistance to specific stress stimuli. In modulating *C. elegans* lifespan and stress response, *hcf-1* completely depends on the activity of *daf-16*, but likely acts independently of the IIS pathway. In elucidating the mechanism by which HCF-1 regulates DAF-16, we showed that HCF-1 is a ubiquitously expressed nuclear protein and forms a protein complex with DAF-16 in *C. elegans*. Interestingly, in the absence of *hcf-1*, greater enrichment of DAF-16 at its target gene promoters is observed and more robust DAF-16-mediated regulation of selective transcriptional targets is detected. Based on our results, we propose that HCF-1 modulates *C. elegans* lifespan and stress response by acting as a novel

negative regulator of DAF-16. Normally, HCF-1 associates with DAF-16 and limits a fraction of DAF-16 from accessing its target gene promoters. In the absence of HCF-1, more DAF-16 is released to localize to target gene promoters to confer greater transcriptional regulation of selective target genes (Figure 3.14). Altered expression of this subset of target genes likely contributes to the stress resistance and prolonged longevity phenotypes observed in the *hcf-1* mutant worms.

Our results are the first to ascribe a longevity and stress response function to the highly conserved transcriptional regulator HCF-1. Mammalian HCF-1 was first identified as a major host cell factor required for HSV VP16-induced immediate early gene transcription (Wysocka and Herr, 2003). In addition to its role in HSV infection, HCF-1 is also essential for cell cycle progression. Elegant studies have revealed that mammalian HCF-1 is required for appropriate transition from G1 to S phase, and also proper progression of M phase and cytokinesis (Julien and Herr, 2003; Julien and Herr, 2004; Tyagi et al., 2007). Importantly, mammalian and *C. elegans* HCF-1 share conserved functions. *C. elegans* HCF-1 is able to stabilize the VP16-induced complex; Moreover, *C. elegans hcf-1* mutants produce small broods and exhibit low penetrance of embryonic lethality (Lee et al., 2007) (Figure 3.2), both phenotypes consistent with a role of HCF-1 in cell proliferation. Furthermore, *C. elegans hcf-1* mutant embryos show low penetrance of mitotic and cytokinetic defects (Lee et al., 2007). As HSV is a human specific virus, it is thought that VP16 likely mimicks a cellular interaction with HCF-1 and co-opts human HCF-1 for productive HSV lytic infection. Given the well-established and conserved role of HCF-1 in cell cycle control, it is interesting to consider whether the cell proliferation function of HCF-1 is linked to its role in longevity

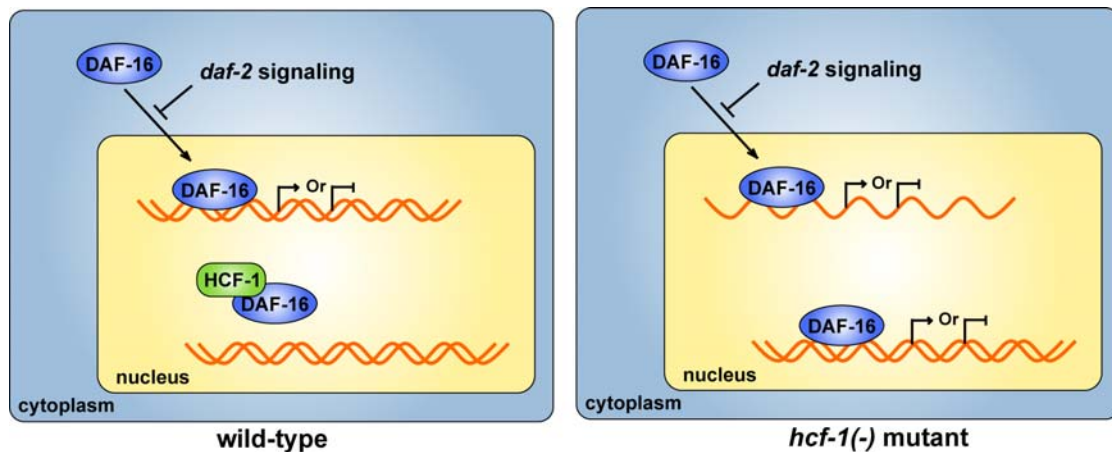


Figure 3.14 The model.

We propose that in wild-type *C. elegans*, HCF-1 associates with a fraction of DAF-16 in the nucleus and limits the recruitment of some DAF-16 to its target gene promoters. Inactivation of *hcf-1* allows more DAF-16 to access its target gene promoters and enforces DAF-16-mediated regulation of selective target genes, which likely contributes to the prolonged lifespan and enhanced stress resistance phenotypes of the *hcf-1* mutants.

and stress response. In adult *C. elegans*, the only proliferative tissue is the germline. Whereas a defect in germline stem cell proliferation is known to cause lifespan increase, our genetic studies showed that *hcf-1* deficiency can continue to extend the lifespan of worms completely lacking germline (Figure 3.1F, Table 3.3), suggesting that the longevity function of *hcf-1* is likely not linked to its role in cell proliferation. The high degree of functional conservation between *C. elegans* and mammalian HCF-1 suggests that mammalian HCF-1 likely also participates in stress response and longevity determination. Therefore, HCF-1 may very well represent a new universal longevity determinant.

Our model proposes that HCF-1 affects lifespan and stress response by forming a protein complex with DAF-16 and regulating DAF-16 recruitment to target gene promoters and DAF-16-mediated gene transcription. This model is consistent with the known roles of mammalian HCF-1. For VP16-induced immediate early (IE) gene expression, binding of HCF-1 to VP16 is thought to help recruit the activating Set1/Ash2 histone methyltransferase complex to IE-gene promoters (Wysocka and Herr, 2003). For its role in G1/S transition, mammalian HCF-1 has been found to recruit the Set1/Ash2 histone methyltransferase activating complex to E2F1 and the Sin3 histone deacetylase repressive complex to E2F4 at the appropriate times of the cell cycle, which likely helps to reinforce the activating or repressive functions of the respective E2F family members (Tyagi et al., 2007). The role of HCF-1 in regulating the transcription factor Miz-1 is particularly relevant to this study. HCF-1 has been shown to physically associate with Miz-1 and antagonize Miz-1-mediated transactivation by interfering with the association of Miz-1 and the histone deacetylase P300 (Piluso et al., 2002). Furthermore, HCF-1, via its

various functional motifs, has been shown to mediate protein-protein interactions with a large number of polypeptides, including transcription factors LZIP/Luman, Zhangfei, HPIP, Sp1, & GABP β , protein phosphatase PP1, and cell-death protein PDCD2 (Wysocka and Herr, 2003). HCF-1 is emerging as an extremely versatile scaffolding protein, capable of binding to many different transcription and chromatin factors via its different conserved motifs, and assembling appropriate protein complexes for proper context-dependent gene expression regulation (Piluso et al., 2002; Tyagi et al., 2007; Vogel and Kristie, 2000; Wysocka et al., 2003).

Our qRT-PCR results suggest that HCF-1 is only able to regulate the DAF-16-mediated transcription of a select group of previously identified DAF-16 target genes. Considering that the DAF-16 target genes we surveyed were previously determined to be responsive to *daf-2*//S, and since our genetic studies suggest that *hcf-1* and *daf-2* might act in parallel pathways and converge onto *daf-16* (Figure 3.1), it is not surprising that some of the gene expression changes caused by *hcf-1* deficiency would be distinct from that caused by reduced *daf-2* signaling. It can be argued that HCF-1 might represent a weaker regulator of DAF-16 compared to DAF-2, and its effect on some of the DAF-16-regulated genes might simply be missed in our analysis as it is likely to be much weaker than that in the *daf-2* mutant (Table 3.7). Whereas a weaker effect model is possible, we favor the model that HCF-1 represents a gene-specific regulator of DAF-16. In our analysis, we noticed that the impact of *hcf-1* deficiency on DAF-16 target gene regulation is not always much weaker than reduced *daf-2* signaling. For instance, the expression fold change of *F21F3.3* in *hcf-1*(-) was comparable with that in *daf-2*(-) (~5 fold vs ~11 fold). On the other hand, there are genes, e.g., *dod-3* &

dod-24, whose expression change in *daf-2(-)* is as great as that of *sod-3* or *mtl-1* (~100 fold), however, unlike *sod-3* and *mtl-1*, their gene expression did not show a significant change in *hcf-1(-)*. Future whole genome expression profiling experiments will provide a global view of whether HCF-1 acts as a gene-specific negative regulator of DAF-16. Considering that HCF-1 and DAF-16/FOXO are highly conserved across species, it is very likely that mammalian HCF-1 also conserves the function of FOXO regulation. Whereas *C. elegans* only has one *daf-16* gene, mammals have four FOXO genes. Context specific regulators of FOXOs are critical in ensuring specificity on gene expression regulation and subsequent biological responses (Huang and Tindall, 2007). Our findings in *C. elegans* raise the intriguing possibility that mammalian HCF-1 represents a new regulator of one or more of the FOXO proteins.

An important next question is how HCF-1 might achieve its specificity in influencing DAF-16 transcriptional targets. A simple hypothesis is that the association between HCF-1 and DAF-16 may be regulated based upon upstream stimulus. For example, signals that induce altered subcellular localization of HCF-1 or DAF-16 may disrupt the HCF-1/DAF-16 interaction. Both HCF-1 and DAF-16 has been shown to shuttle between the nucleus and cytoplasm under specific conditions (Hsin and Kenyon, 1999; Huang and Tindall, 2007; Lin et al., 2001; Mahajan et al., 2002; Oh et al., 2005). In addition, DAF-16/FOXO and HCF-1 proteins have been shown to be extensively modified post-translationally (Huang and Tindall, 2007; Lee et al., 2001; Li et al., 2007b; Lin et al., 2001; Wang et al., 2007; Wysocka et al., 2001). It is possible that different modifications on HCF-1 and/or DAF-16 will substantially affect their association. Lastly, the specificity toward target genes

can also be conferred at the level of the transcriptional complex assembly. Under this scenario, additional co-regulators of DAF-16 will likely come into play. Whereas HCF-1 represents the only nuclear negative regulator of DAF-16 known in *C. elegans*, several DAF-16 nuclear positive regulators have been reported, including SIR-2.1 (Berdichevsky et al., 2006), SMK-1 (Wolff et al., 2006), and BAR-1 (Essers et al., 2005). Future research to elucidate the interplay among the various DAF-16 co-activators and HCF-1 will greatly advance our understanding of the mechanistic details of how DAF-16 transcriptional activities can be appropriately regulated.

Our data indicate that an important function of HCF-1 may be to modulate responses to specific environmental stress stimuli. Interestingly, only the *hcf-1(pk924)* allele showed resistance to paraquat and cadmium treatment, and neither of the *hcf-1* mutant alleles demonstrated altered response to heat shock. These results suggest that a general heightened response to a wide-range of environmental stresses is not likely to account for the lifespan increase observed in the *hcf-1* mutant worms. However, it is important to also consider that in the stress assays, worms were challenged with a high dose of an acute stress, which is very different from the low level of chronic stress worms experience as they grow old in longitudinal assays. The involvement of *hcf-1* in stress response nicely fits with the overall theme that HCF-1 is a gene-specific transcriptional regulator of DAF-16. It is well established that distinct stress stimuli are able to induce DAF-16/FOXO to regulate different target genes (Huang and Tindall, 2007; van der Horst and Burgering, 2007). We propose that the main role of HCF-1 is to help fine-tune the regulation of a subset of DAF-16-regulated genes to modulate survival under specific conditions. Taken together, we showed that HCF-1 is essential

for longevity maintenance and that it functions as a negative regulator of DAF-16 in *C. elegans*. As HCF-1 and DAF-16/FOXO are highly conserved from *C. elegans* to mammals, our findings have important implications for FOXO regulation and longevity determination in diverse organisms.

3.5 Acknowledgements

We are grateful to Drs. K. Kemphues, R. Weiss, D. Kim and members of the Lee lab for critical reading of the manuscript. We thank members of the Lee, Liu, Kemphues, and Vatamaniuk labs for insightful discussions. We especially thank Nirav Amin and Yuang Jiang for assistance with immunostaining and Bingsi Li for help with bombardment experiments. We are grateful to Drs. Jun Liu, Soyoung Lee, Winship Herr, Gary Ruvkun, Catherine Wolkow, the CGC, and the *C. elegans* Gene Knockout Consortium for providing the strains required for this work.

Funding

This work was supported by a New Scholar Award in Aging from the Ellison Medical Foundation and a R01 grant AG024425-01 from the NIA awarded to SSL.

CHAPTER 4

CONCLUSIONS AND FUTURE PERSPECTIVES

The evolutionarily conserved forkhead transcription factor DAF-16/FOXO has important roles in diverse biological processes (Antebi, 2007; van der Horst and Burgering, 2007). In the last decade, many studies have been done to understand how it is finely tuned to execute its diverse functions. Studies from different organisms consistently point out that the regulation of DAF-16/FOXO requires a complex network that can act at different levels, e.g., cytoplasm/nucleus translocation, protein stability and transcriptional activity inside of the nucleus. Despite the progress made so far, our understanding in this field is still very limited. My work summarized in this dissertation has uncovered two novel factors that negatively regulate DAF-16 in different ways in *C. elegans*.

In chapter 2, I described the role of the 14-3-3 protein FTT-2 in binding DAF-16 and regulating DAF-16 by sequestering it in the cytoplasm. FTT-2 was identified in an RNAi screen for factors involved in dauer formation. RNAi knock down of *ftt-2* specifically enhances IIS-mediated dauer formation. FTT-2 binds DAF-16 *in vivo* and depletion of FTT-2 causes the nuclear accumulation of DAF-16 and eventually enhances its transcriptional activities. In mammalian cells, 14-3-3 ζ isoform binds to phosphorylated FOXO3a and sequesters FOXO3a in the cytoplasm (Brunet et al., 1999). Thus my work also indicates the conserved function of 14-3-3 proteins in regulating DAF-16/FOXO.

Interestingly, RNAi knock down of *par-5/ftt-1*, the only other 14-3-3 gene in *C. elegans*, did not show any notable effect on DAF-16 regulation, indicating that the closely related members of the 14-3-3 family have been assigned different tasks despite their high sequence homology. Numerous

studies from plants and mammalian cells have found that 14-3-3 proteins have isoform-specific functions (Roberts and de Bruxelles, 2002). My work further provides the evidence from *C. elegans* in support of this idea.

It is not clear how the isoform-specific functions are achieved. Although FTT-2 and PAR-5 are highly conserved in the coding region (~85.9% sequence identity at the amino acid level (Wang and Shakes, 1997)), it is possible that the remaining divergent residues determine the specificity of their substrate. Alternatively, the different expression patterns of FTT-2 and PAR-5 may be responsible for their specific functions as they are expressed in different developmental stages and different tissues (Wang and Shakes, 1997; Wang et al., 2006a). Future functional study by swapping the promoter and coding regions between *ftt-2* and *par-5* may be helpful to answer this question.

Another interesting and important question is what are the other factors involved in FTT-2-regulated DAF-16 cytoplasm-nucleus translocation. In mammalian cells, 14-3-3 can be phosphorylated by JNK and the phosphorylation disrupts the interaction between 14-3-3 and FOXOs and release FOXOs from the retention by 14-3-3 (Sunayama et al., 2005). It would be interesting to know whether JNK-1, the *C. elegans* ortholog of JNK, has a conserved role in regulating the interaction between FTT-2 and DAF-16. In addition, an unbiased genome-wide RNAi screen for suppressors of DAF-16 nuclear localization upon *ftt-2* depletion will be informative to identify the factors involved in DAF-16 nuclear translocation downstream of *ftt-2*.

Unlike FTT-2, the other DAF-16 regulator, the host cell factor HCF-1 negatively regulates DAF-16 transcriptional activity inside of the nucleus. *hcf-1(-)* mutant shows lifespan extension and stress resistance phenotype which is *daf-16* dependent. It is a ubiquitous nuclear protein and physically associates

with DAF-16 in the nucleus. Interestingly, there is more DAF-16 recruited to the promoters of its target genes which leads to altered expression of a subset of DAF-16-regulated genes upon loss of *hcf-1*. Therefore HCF-1 negatively regulates DAF-16 activity by limiting it from accessing its target DNA.

The major cellular role of HCF-1 has been shown previously to be in cell proliferation (Julien and Herr, 2003; Julien and Herr, 2004; Tyagi et al., 2007). In this thesis I described the first evidence that HCF-1 has a role in the aging process by regulating the activity of DAF-16 in *C. elegans*. Many questions remain to be answered. For example, although co-IP experiments suggested that HCF-1 forms a protein complex with DAF-16, it is not clear whether this occurs through direct binding. Further investigation using *in vitro* pull down assay is required to answer this question. If HCF-1 can directly bind DAF-16, then what domain is responsible for the direct interaction? Members of HCF protein family have two highly conserved domains: the N-terminus Kelch domain and C-terminus Fn3 repeats. Both domains can directly interact with a number of transcription or chromatin modification factors involved in cell proliferation in mammalian systems (Wysocka and Herr, 2003). Mapping the interacting domain would provide useful information in understanding how DAF-16 is regulated. A similar yeast two hybrid or *in vitro* pull down assay using a series of truncated proteins would shed light on this question.

If the interaction between HCF-1 and DAF-16 is indirect, then what mediate(s) the interaction? An even more general question is what else might be involved in the protein complex. Several DAF-16 co-factors have been previously reported and they are candidate components of the DAF-16/HCF-1 complex. For example, the protein deacetylase SIR-2.1 has been shown to interact with DAF-16 and my work suggests that HCF-1 also binds SIR-2.1 *in*

vivo (see Appendix II). Thus a possible model is that the three proteins DAF-16, HCF-1 and SIR-2.1 form a protein complex. Though my preliminary gel filtration results favor this model (see Appendix III), more studies are needed to further test it. Besides SIR-2.1, another candidate is FTT-2. The 14-3-3 proteins have been proposed to mediate the interaction between SIR-2.1 and DAF-16 in the nucleus upon stress stimuli (Berdichevsky et al., 2006). 14-3-3 proteins are naturally scaffolding proteins. Thus it would be interesting to test if FTT-2 also mediates the interaction between HCF-1 and DAF-16. The candidate-based approach is straightforward but may miss important proteins that have not been reported. As an alternative and better way, a systematic study is required for a comprehensive view of the HCF-1/DAF-16 protein complex. One approach is to use mass spectrometry to identify all the components in the purified HCF-1/DAF-16 protein complex.

Another interesting direction is to understand how HCF-1 is regulated to regulate DAF-16. Though dominantly nuclear localized, studies from mammalian systems showed that HCF-1 is able to shuttle between the cytoplasm and the nucleus (Mahajan et al., 2002), which provides a possible way to regulate its function. Besides, *C. elegans* HCF-1 has four potential phosphorylation sites (Wysocka et al., 2001). The responsible kinase hasn't been identified and the biological consequence of HCF-1 phosphorylation is not clear. It would be very interesting to test if the phosphorylation status of HCF-1 can have impacts on DAF-16 regulation

In this study, we propose that HCF-1 is a co-factor of DAF-16 to regulate the expression of a subset of DAF-16 target genes. However, we were not able to survey all the DAF-16 target genes at this stage. Thus a genome-wide gene profiling will be very helpful to test this model in the future.

Both HCF-1 and DAF-16/FOXO are structurally and functionally conserved across species. It will be exciting to test if the HCF-1-mediated DAF-16/FOXO regulation is also conserved in mammals.

APPENDIX I

GENETIC INTERACTIONS BETWEEN *HCF-1* AND OTHER KNOWN LONGEVITY FACTORS IN *C. ELEGANS*

In chapter 3, I discussed the epistasis relationship between *hcf-1* and *daf-16*, the germline and IIS pathway. Although IIS is the best characterized signaling cascade in aging process, multiple other pathways have been proposed to regulate lifespan in *C. elegans* as well, including genes involved in mitochondrial respiration, SIR2 signaling and the dietary restriction pathway (Antebi, 2007; Kenyon, 2005). In order to fully understand the role of HCF-1 in lifespan regulation, we also tested the genetic interactions between *hcf-1* and some of the other longevity genes.

As described in chapter 1, SMK-1 is identified as a DAF-16 co-factor in stress resistance and lifespan regulation (Wolff et al., 2006). We wondered whether SMK-1 also mediates the lifespan regulation by HCF-1. We knocked down *smk-1* by RNAi in *hcf-1(pk924)* and found that two different RNAi constructs (one targets the full length *smk-1* gene and the other targets part of *smk-1*) consistently suppressed the lifespan extension in *hcf-1(-)* mutant (Table I.1). However, in contrast to *daf-16*, the suppression by loss of *smk-1* was only partial.

SIR-2.1 is another important longevity factor that activates DAF-16 upon stress stimuli. Thus we also asked if SIR-2.1 is involved in HCF-1-mediated lifespan regulation. We first treated the *sir-2.1(ok434)* null mutant (Wang and Tissenbaum, 2006) with *hcf-1* RNAi. In multiple independent trials, we found that the lifespan increase induced by *hcf-1* RNAi was partially blunted in the *sir-2.1(ok434)* deletion mutant (Table I.1). Furthermore, two

different isolates of the *sir-2.1(ok434) hcf-1(ok559)* double mutant exhibited a lifespan that was either as short as the *sir-2.1(ok434)* single mutant, or in between that of the *hcf-1(ok559)* or the *sir-2.1(ok434)* single mutant (Table I.1). The double mutant results corroborate with the RNAi results and indicate that *sir-2.1* is at least partially required for the lifespan increase associated with *hcf-1* deficiency.

Both SIR-2.1 and SMK-1 are co-factors of DAF-16. Whereas depleting *daf-16* can fully suppress the lifespan extension caused by loss of *hcf-1*, knocking down either of the co-factors has only moderate effects. Therefore, it is possible that both *sir-2.1* and *smk-1* act downstream of *hcf-1* and converge on *daf-16* in lifespan regulation (Figure I.1). It would be important to test whether simultaneous loss of *sir-2.1* and *smk-1* might have synergistic effects in suppressing *hcf-1* mediated lifespan extension. Further studies are needed to test this model.

Materials and Methods

Strains

The strains used were as follow: wt, *hcf-1(ok559)* (generated by the *C. elegans* Gene Knockout Consortium), *hcf-1(pk924)* (a kind gift from Dr. Winship Herr, University of Lausanne, Switzerland), *sir-2.1(ok434)*. The *hcf-1(ok559)* allele was outcrossed 5 times and the *hcf-1(pk924)* allele was outcrossed 3 times with the wt strain in our lab prior to phenotype analyses.

The *sir-2.1(ok434) hcf-1(ok559)* double mutant strain was constructed using multiple rounds of recombination because *sir-2.1* and *hcf-1* are located close to each other on chromosome IV. In brief, the *sir-2.1(ok434)* mutant was

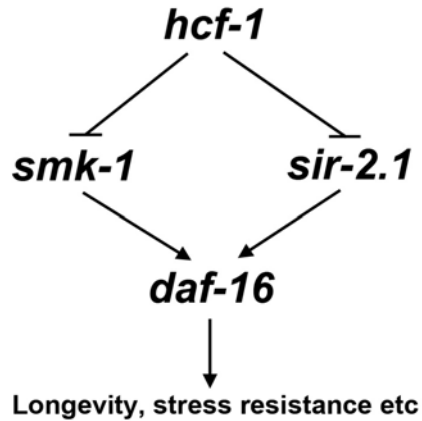


Figure I.1 A possible epistasis relationship between *hcf-1* and *sir-2.1* and *smk-1* in regulating *daf-16*.

crossed into the *unc-5(e53) dpy-20(e1282)* strain (a kind gift from Dr. Jun Liu, Cornell University) to obtain the *sir-2.1(ok434) unc-5(e53)* double mutant strain. Similarly, the *hcf-1(ok559)* mutant was crossed into the *unc-5(e53) dpy-20(e1282)* strain to obtain the *hcf-1(ok559) dpy-20(e1282)* double mutant strain. The *sir-2.1(ok434) unc-5(e53)* strain was then crossed into the *hcf-1(ok559) dpy-20(e1282)* strain to obtain the *sir-2.1(ok434) hcf-1(ok559)* double mutant strain. The *sir-2.1(ok434) hcf-1(ok559)* double mutant was outcrossed 2 times prior to lifespan analyses.

Lifespan assay

The lifespan assay was performed as described in chapter 3.

Acknowledgements

I thank Atsushi Ebata, Terri Iwata and Gizem Rizki for helping repeat the lifespan assays.

Table I.1 *hcf-1* acts upstream of *smk-1* and *sir-2.1* in lifespan regulation.

Strain + RNAi	Mean LS ± SEM (Days)	Total Number of Animals Died/Total	% of wt + L4440	p Value versus wt + L4440	p Value versus wt + <i>corresponding RNAi</i>
wt + L4440	13.9±0.4	78/78		N.A.	N.A.
wt + <i>smk-1</i> (1) ^b	8.2±0.1	90/90	59%	<0.0001	N.A.
wt + <i>smk-1</i> (2) ^b	10.3±0.2	86/89	74%	<0.0001	N.A.
<i>hcf-1</i> (pk924) + L4440	22.5±0.5	91/91	162%	<0.0001	<0.0001
<i>hcf-1</i> (pk924) + <i>smk-1</i> (1) ^b	9.8±0.1	92/92	71%	<0.0001	<0.0001
<i>hcf-1</i> (pk924) + <i>smk-1</i> (2) ^b	12.1±0.3	88/90	87%	<0.0001	<0.0001

Strain + RNAi	Mean LS ± SEM (Days)	Total Number of Animals Died/Total	% of wt + L4440	p Value versus wt + L4440	p Value versus <i>sir-2.1(ok434)</i> + <i>hcf-1</i>
wt + L4440	14.0±0.3	60/62		N.A.	<0.0001
wt + <i>hcf-1</i>	17.4±0.3	83/85	124%	<0.0001	<0.0001
<i>sir-2.1(ok434)</i> + L4440	14.0±0.2	80/88	100%	0.9834	<0.0001
<i>sir-2.1(ok434)</i> + <i>hcf-1</i>	15.5±0.3	100/101	111%	<0.0001	N.A.

Strain	Mean LS ± SEM (Days)	Total Number of Animals Died/Total	% of wt	p Value versus wt	p Value versus <i>sir-2.1(ok434) hcf-1(ok559)</i> (isolate 1/isolate 2)
wt	14.7±0.1	88/88		N.A.	0.1142/0.0072
<i>sir-2.1(ok434)</i>	14.2±0.1	90/90	97%	0.0653	0.6957/0.0002
<i>hcf-1(ok559)</i>	16.5±0.3	89/89	112%	<0.0001	<0.0001/0.0035
<i>sir-2.1(ok434) hcf-1(ok559)-1^a</i>	13.4±0.3	86/88	91%	0.1142	N.A./0.0001
<i>sir-2.1(ok434) hcf-1(ok559)-2^a</i>	15.0±0.3	97/97	102%	0.0072	0.0001/N.A.

The lifespan extension in *hcf-1(-)* mutant can be partially suppressed by loss of *smk-1* or *sir-2.1*.

The lifespan experiments were repeated at least two independent times with similar results and the data for representative experiments are shown. The lifespan data were analyzed using the Log-rank test and p values for each individual experiment are shown. N.A.: not applicable.

^a: Two different isolates.

^b: Two different RNAi constructs. (1) targets full length of *smk-1*. (2) targets partial length of *smk-1*.

APPENDIX II

HCF-1 INTERACTS WITH THE PROTEIN DEACETYLASE SIR-2.1

The genetic data presented in Appendix I suggested that *hcf-1* acts upstream of *sir-2.1* to affect *C. elegans* lifespan. I further asked if HCF-1 can interact with SIR-2.1 since both proteins are nuclear localized.

In the co-IP experiment, I found that when HCF-1 was immunoprecipitated from extracts of the worms over-expressing SIR-2.1, SIR-2.1 was co-immunoprecipitated (Figure II.1A, right panels). This interaction appeared specific because when co-IP experiments was done using extracts from *hcf-1(ok559)* mutant background, I was not able to immunoprecipitate HCF-1 or to co-immunoprecipitate SIR-2.1 (Figure II.1A, right panels). In reciprocal co-IP experiments I obtained similar results (Figure II.1A, left panels). My results suggest that HCF-1 is able to form a specific protein complex with SIR-2.1 in *C. elegans*.

Because DAF-16 and SIR-2.1 are known to form a complex in *C. elegans* (Berdichevsky et al., 2006; Wang et al., 2006a), I next tested whether the presence of SIR-2.1 or DAF-16 is required for HCF-1 to form a complex with DAF-16 or SIR-2.1, respectively. I performed co-IP experiments using DAF-16::GFP over-expression worms lacking SIR-2.1 or SIR-2.1 over-expression worms lacking DAF-16 (Figure II.1B). The results showed that HCF-1 co-immunoprecipitated with DAF-16 or SIR-2.1 in the absence of SIR-2.1 or DAF-16, respectively (Figure II.1B), indicating that HCF-1 is able to independently form a complex with DAF-16 or SIR-2.1 in worms.

The physical interaction between HCF-1 and SIR-2.1 may have biological consequence in regulating SIR-2.1 activity. Thus I tested whether

the expression of SIR-2.1 target genes can be regulated by loss of *hcf-1*. *sod-3*, one of the best characterized DAF-16 target genes, is also induced by SIR-2.1 (Viswanathan et al., 2005). In chapter 3, I showed that *sod-3* expression increased in *hcf-1(-)* mutants. I found that the elevated expression of *sod-3* in the *hcf-1* mutant worms is completely dependent *sir-2.1* because in the *hcf-1(ok559) sir-2.1(ok434)* double mutant, the level of *sod-3* expression remained low and was similar to that seen in the *sir-2.1(ok434)* single mutant worms (Figure II.2). When I expanded the test with more SIR-2.1 target genes, I found that the elevated expression of *mtl-1* in *hcf-1(-)* mutants is also partially dependent on *sir-2.1* (Figure II.2). However, it is worth mentioning that the altered expression of some genes in *hcf-1(-)* mutants is not dependent on *sir-2.1* (data not shown). Therefore, by binding to SIR-2.1, HCF-1 can regulate its activity in gene expression for selective targets.

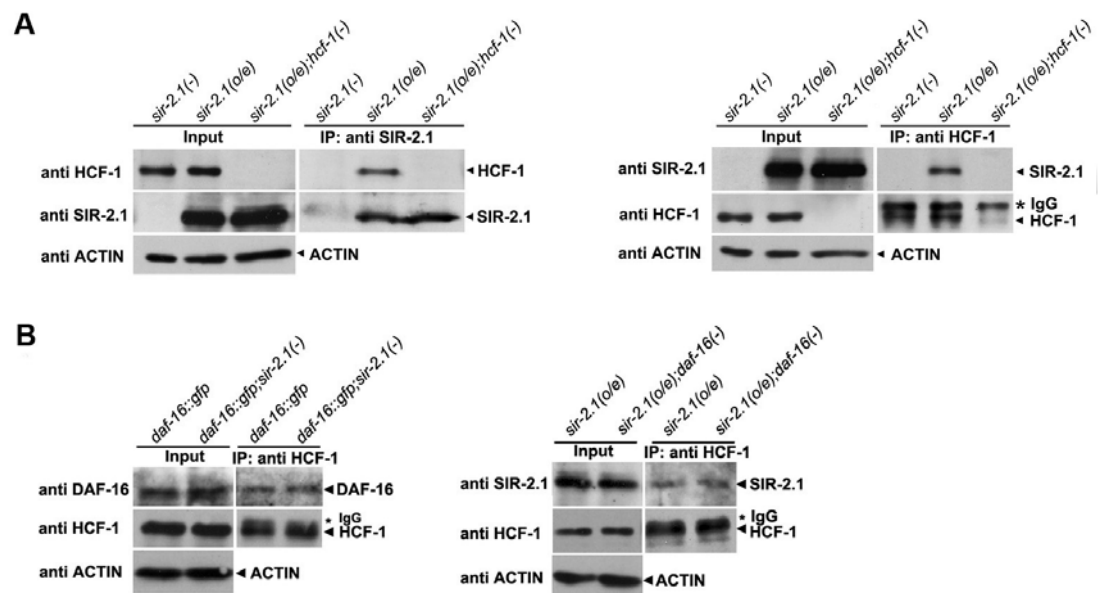
Materials and Methods

Strains

The strains used were as follow: wt, *hcf-1(ok559)* (generated by the *C. elegans* Gene Knockout Consortium), *sir-2.1(ok434)*, *sir-2.1(ok434) hcf-1(ok559)*(see Appendix I), *gel-3[sir-2.1 rol-6(su1006)]* (*sir-2.1* high copy over-expression) (Tissenbaum and Guarente, 2001) and *daf-16(mu86);muls71[daf-16a::gfp/bKO, rol-6(su1006)]* (low copy over-expression of DAF-16::GFP) (Lin et al., 2001). The *hcf-1(ok559)* allele was outcrossed 5 times with the wt strain in our lab prior to phenotype analyses.

Figure II.1 HCF-1 forms protein complexes with SIR-2.1 in *C. elegans*.

Worm extracts were made from mixed stage worms and subjected to immunoprecipitation. (A) Extracts from *sir-2.1(-)* (*sir-2.1(ok434)*), *sir-2.1(o/e)* (*geln3[sir-2.1 rol-6(su1006)]*), and *sir-2.1(o/e);hcf-1(-)* (*hcf-1(ok559);geln3[sir-2.1 rol-6(su1006)]*) worms were either immunoprecipitated using anti-SIR-2.1 antibody (left panel) or anti-HCF-1 antibody (right panel). The immunoprecipitated protein complexes were subsequently immunoblotted using anti-HCF-1, or anti-SIR-2.1 antibody. For Input, 10µg of total protein was loaded per lane. For immunoprecipitation, 400µg of total protein was used. (B) Extracts from *daf-16::gfp* (*daf-16(mu86);muls71*) and *daf-16::gfp;sir-2.1(-)* (*daf-16(mu86);muls71;sir-2.1(ok434)*) (left panel), *sir-2.1(o/e)* (*geln3[sir-2.1 rol-6(su1006)]*) and *sir-2.1(o/e);daf-16(-)* (*geln3[sir-2.1 rol-6(su1006)];daf-16(mgDf47)*) (right panel) were immunoprecipitated using anti-HCF-1 antibody followed by immunoblotting using anti DAF-16 (left) or anti-SIR-2.1 (right). Either 2mg total protein was used for immunoprecipitation and 50µg was used as input (left) or 400µg total protein was used for immunoprecipitation and 10µg was used as input (right). Immunoblotting with anti-Actin antibody was included to ensure similar loading of each input lane.



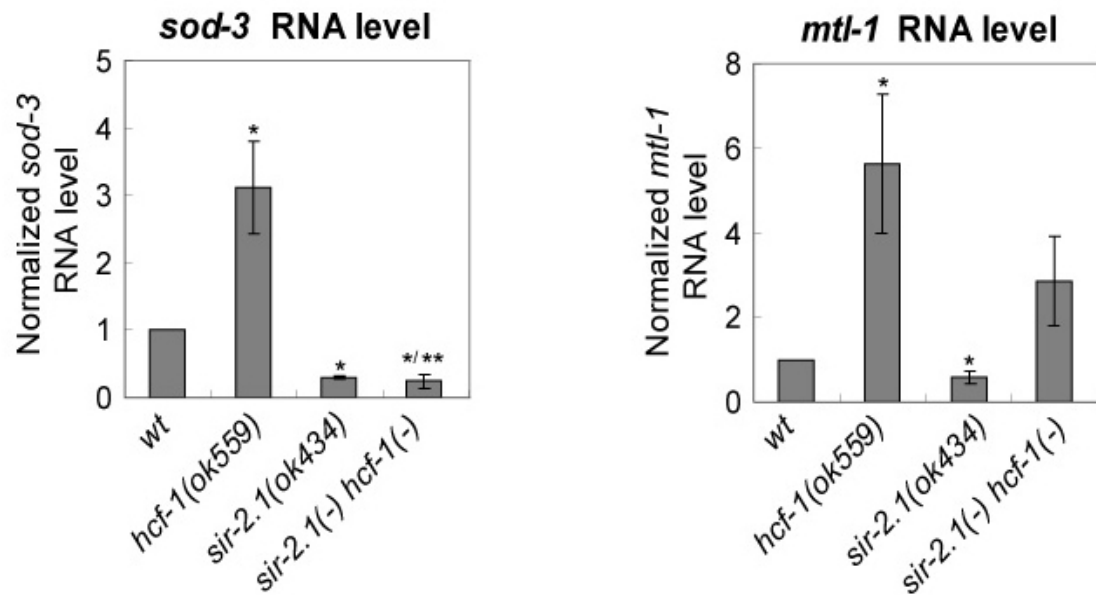


Figure II.2 Loss of *hcf-1* promotes the SIR-2.1-mediated transcriptional regulation of several target genes.

The elevated expression of *sod-3* in the *hcf-1* mutants was completely dependent on *sir-2.1*; that of *mtl-1* was partially dependent on *sir-2.1*. *: P value < 0.05 (student t-test) when compared to wild-type (wt). **: P value < 0.05 (student t-test) when compared to *hcf-1(ok559)*.

The following double mutant strains were constructed using standard genetic methods: *geln3[sir-2.1 rol-6(su1006)];hcf-1(ok559)*, *geln3[sir-2.1 rol-6(su1006)];daf-16(mgDf47)* and *daf-16(mu86);muls71[daf-16a::gfp/bKO, rol-6(su1006)];sir-2.1(ok434)*.

qRT-PCR and immunoprecipitation

qRT-PCR and immunoprecipitation was performed as described in chapter 3.

Antibodies

Antibodies for immunoprecipitation include: affinity purified anti-HCF-1 and anti-SIR-2.1 (rabbit, a kind gift from Dr. David Sinclair, Harvard Medical School).

Antibodies for immunoblotting include: anti-DAF-16 (cC-20) (goat, Santa Cruz), anti-HCF-1, anti-SIR-2.1 (rabbit, Novus), anti-ACTIN (mouse, Chemicon), anti-goat (Rockland), anti-mouse (Santa Cruz), anti-guinea pig (Jackson ImmunoResearch Laboratories), and anti-rabbit (Rockland). The One-Step Complete IP-Western kit (GenScript Corporation) was used to reduce the rabbit IgG background after immunoprecipitation.

APPENDIX III

ATTEMPTS TO DISSECT THE HCF-1/DAF-16 COMPLEX BY GEL FILTRATION

Mammalian HCF-1 functions as a scaffolding protein in many cases. It is able to bind to many different transcription and chromatin factors via its different conserved motifs, and assembling appropriate protein complexes (Piluso et al., 2002; Tyagi et al., 2007; Vogel and Kristie, 2000; Wysocka et al., 2003). Thus it is possible that the HCF-1/DAF-16 protein complex consists of other component(s). Identification of the other factors in the complex would be very helpful to understand the regulation of DAF-16. In order to dissect the HCF-1/DAF-16 complex, I used gel filtration followed by immunoblotting to check if any other candidate proteins are in the same complex. Gel filtration has been widely used to separate proteins or protein complexes based on the molecular size (Hagel, 2001). Proteins or protein complexes in a mixture can be fractionated and each fraction collected represents a group of similar molecular size.

When the total proteins from the DAF-16::GFP worms were fractionated and immunoblotted, DAF-16 and HCF-1 were found to both enriched in fraction 9 (Figure III.1, top panel), suggesting that they are found in protein complexes of similar molecular size. If there are any other factors involved in the HCF-1/DAF-16 complex, they should be enriched in the same fraction as HCF-1 and DAF-16. An interesting candidate is SIR-2.1. SIR-2.1 has been found to bind to DAF-16 (Berdichevsky et al., 2006; Wang et al., 2006a) and my work suggested that SIR-2.1 also interacts with HCF-1 (see Appendix II). Thus it is possible that SIR-2.1 is in the same protein complex with DAF-16

and HCF-1. Indeed, the immunoblotting results showed that SIR-2.1 was also enriched in fraction 9 (Figure III.1, top panel). The co-fractionation of DAF-16, HCF-1 and SIR-2.1 indicates that the three proteins are in protein complexes of similar sizes. In order to further test if they are in the same complex, I also fractionated the total proteins from *daf-16(mgDf47);sir-2.1(ok434)*. If the three proteins are in irrelevant protein complexes of similar sizes, then loss of DAF-16 and SIR-2.1 will not affect the distribution pattern of HCF-1. However I found that in the absence of DAF-16 and SIR-2.1, the enrichment of HCF-1 shifted to fraction 10 or 11 representing a smaller complex (Figure III.1, middle panel). Therefore, DAF-16 and SIR-2.1 are also involved in the complex containing HCF-1. When *daf-16(mgDf47);hcf-1(pk924)* double mutants were used in the gel filtration experiment, although the “peak shift” for SIR-2.1 was not clear (Figure III.1, bottom panel), the distribution pattern of SIR-2.1 obviously changed in the absence of DAF-16 and HCF-1: it became more broadly distributed (Figure III.1, bottom panel). Thus, DAF-16 and HCF-1 are likely also present in the complex with SIR-2.1. It is still not clear why the distribution pattern change of HCF-1 and SIR-2.1 is different in corresponding double mutant background.

The preliminary gel filtration data suggest that DAF-16, HCF-1 and SIR-2.1 are likely in the same protein complex. However, one limitation of this study came from the resolution of the column. The protein complex was found to be larger than 669kD (Figure III.1, top panel) and the column used in this study does not have a good resolution for large proteins. Thus a better column is required to repeat this experiment in the future. Despite the limitation of this study, the technique of gel filtration itself has been proven to be a powerful tool to study protein complexes. It can be easily adapted and applied to any other

candidates that might be involved in the HCF-1/DAF-16 complex suggested by the other studies.

Materials and Methods

Strains

The strains used were as follow: *xrls87[daf-16 α ::gfp::daf-16b, rol-6(su1006)]* (DAF-16::GFP) (Lee et al., 2001).

The following double mutant strains were constructed using standard genetic methods: *daf-16(mgDf47);hcf-1(pk924)* and *daf-16(mgDf47);sir-2.1(ok434)*.

Gel filtration

The Superdex 120 column (GE Healthcare) was used in the gel filtration and it was calibrated by Gel Filtration Calibration Kit HMW (GE Healthcare). Total worm lysates were made as described in chapter 3 and filtered and ~ 1.5mg of total protein in 100 μ l was loaded into the column. Gel filtration was performed according to the manual. Each fraction was collected in a 70 μ l volume after V_0 . Total proteins collected in each fraction were subjected to SDS-PAGE gel followed by immunoblotting analysis.

Antibodies

Antibodies for immunoblotting are described in Appendix II.

Acknowledgements

I thank Man-Hee Suh for sharing his knowledge and helping me with the gel filtration experiment. I am also grateful for MacCHESS in Cornell University for providing the facilities for gel filtration.

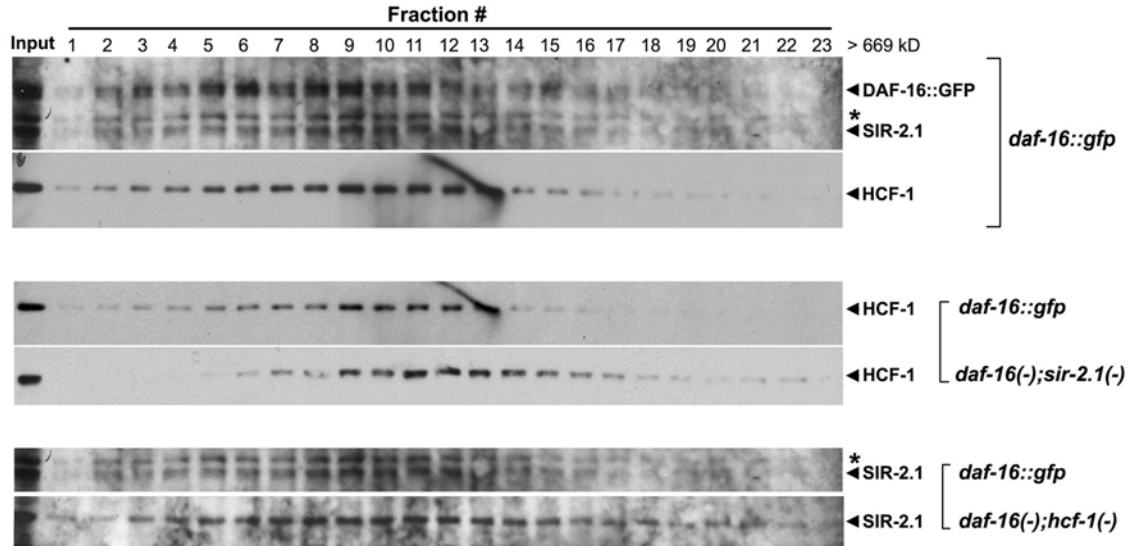


Figure III.1 DAF-16, HCF-1 and SIR-2.1 are likely in the same protein complex.

DAF-16, HCF-1 and SIR-2.1 were co-enriched in fraction 9 when gel filtration was performed using total lysates from DAF-16::GFP worms followed by immunoblotting as indicated (top panel). In the *daf-16(mgDf47);sir-2.1(ok434)* double mutants, the enrichment of HCF-1 shifted to fraction 10 or 11, indicating that the protein complex containing HCF-1 also involves DAF-16 and SIR-2.1 (middle panel). In the *daf-16(mgDf47);hcf-1(pk924)* double mutants, it is not clear whether there was a peak shift for SIR-2.1, but the distribution of SIR-2.1 substantially changed to a broader way in the absence of DAF-16 and HCF-1 (bottom panel). *: non-specific band recognized by anti-DAF-16 antibody.

REFERENCES

- Agarwal-Mawal, A., Qureshi, H. Y., Cafferty, P. W., Yuan, Z., Han, D., Lin, R., and Paudel, H. K. (2003). 14-3-3 connects glycogen synthase kinase-3 beta to tau within a brain microtubule-associated tau phosphorylation complex. *J Biol Chem* **278**, 12722-8.
- Albert, P. S., Brown, S. J., and Riddle, D. L. (1981). Sensory control of dauer larva formation in *Caenorhabditis elegans*. *J Comp Neurol* **198**, 435-51.
- Antebi, A. (2007). Genetics of aging in *Caenorhabditis elegans*. *PLoS Genet* **3**, 1565-71.
- Aoki, M., Jiang, H., and Vogt, P. K. (2004). Proteasomal degradation of the FoxO1 transcriptional regulator in cells transformed by the P3k and Akt oncoproteins. *Proc Natl Acad Sci U S A* **101**, 13613-7.
- Apfeld, J., and Kenyon, C. (1998). Cell nonautonomy of *C. elegans* daf-2 function in the regulation of diapause and life span. *Cell* **95**, 199-210.
- Arantes-Oliveira, N., Apfeld, J., Dillin, A., and Kenyon, C. (2002). Regulation of life-span by germ-line stem cells in *Caenorhabditis elegans*. *Science* **295**, 502-5.
- Ashrafi, K., Chang, F. Y., Watts, J. L., Fraser, A. G., Kamath, R. S., Ahringer, J., and Ruvkun, G. (2003). Genome-wide RNAi analysis of *Caenorhabditis elegans* fat regulatory genes. *Nature* **421**, 268-72.
- Barsyte, D., Lovejoy, D. A., and Lithgow, G. J. (2001). Longevity and heavy metal resistance in daf-2 and age-1 long-lived mutants of *Caenorhabditis elegans*. *Faseb J* **15**, 627-34.
- Berdichevsky, A., Viswanathan, M., Horvitz, H. R., and Guarente, L. (2006). *C. elegans* SIR-2.1 interacts with 14-3-3 proteins to activate DAF-16 and extend life span. *Cell* **125**, 1165-77.
- Berman, J. R., and Kenyon, C. (2006). Germ-cell loss extends *C. elegans* life span through regulation of DAF-16 by kri-1 and lipophilic-hormone signaling. *Cell* **124**, 1055-68.
- Birkenkamp, K. U., and Coffey, P. J. (2003). Regulation of cell survival and proliferation by the FOXO (Forkhead box, class O) subfamily of Forkhead transcription factors. *Biochem Soc Trans* **31**, 292-7.
- Bishop, N. A., and Guarente, L. (2007). Genetic links between diet and lifespan: shared mechanisms from yeast to humans. *Nat Rev Genet* **8**, 835-44.
- Brenner, S. (1974). The genetics of *Caenorhabditis elegans*. *Genetics* **77**, 71-94.

- Brunet, A., Bonni, A., Zigmond, M. J., Lin, M. Z., Juo, P., Hu, L. S., Anderson, M. J., Arden, K. C., Blenis, J., and Greenberg, M. E. (1999). Akt promotes cell survival by phosphorylating and inhibiting a Forkhead transcription factor. *Cell* **96**, 857-68.
- Brunet, A., Sweeney, L. B., Sturgill, J. F., Chua, K. F., Greer, P. L., Lin, Y., Tran, H., Ross, S. E., Mostoslavsky, R., Cohen, H. Y., Hu, L. S., Cheng, H. L., Jedrychowski, M. P., Gygi, S. P., Sinclair, D. A., Alt, F. W., and Greenberg, M. E. (2004). Stress-dependent regulation of FOXO transcription factors by the SIRT1 deacetylase. *Science* **303**, 2011-5.
- Cahill, C. M., Tzivion, G., Nasrin, N., Ogg, S., Dore, J., Ruvkun, G., and Alexander-Bridges, M. (2001). Phosphatidylinositol 3-kinase signaling inhibits DAF-16 DNA binding and function via 14-3-3-dependent and 14-3-3-independent pathways. *J Biol Chem* **276**, 13402-10.
- Calnan, D. R., and Brunet, A. (2008). The FoxO code. *Oncogene* **27**, 2276-88.
- Chen, M. S., Ryan, C. E., and Piwnicka-Worms, H. (2003). Chk1 kinase negatively regulates mitotic function of Cdc25A phosphatase through 14-3-3 binding. *Mol Cell Biol* **23**, 7488-97.
- Clancy, D. J., Gems, D., Harshman, L. G., Oldham, S., Stocker, H., Hafen, E., Leivers, S. J., and Partridge, L. (2001). Extension of life-span by loss of CHICO, a Drosophila insulin receptor substrate protein. *Science* **292**, 104-6.
- Curtis, R., Geesaman, B. J., and DiStefano, P. S. (2005). Ageing and metabolism: drug discovery opportunities. *Nat Rev Drug Discov* **4**, 569-80.
- Daitoku, H., Hatta, M., Matsuzaki, H., Aratani, S., Ohshima, T., Miyagishi, M., Nakajima, T., and Fukamizu, A. (2004). Silent information regulator 2 potentiates Foxo1-mediated transcription through its deacetylase activity. *Proc Natl Acad Sci U S A* **101**, 10042-7.
- Datta, S. R., Katsov, A., Hu, L., Petros, A., Fesik, S. W., Yaffe, M. B., and Greenberg, M. E. (2000). 14-3-3 proteins and survival kinases cooperate to inactivate BAD by BH3 domain phosphorylation. *Mol Cell* **6**, 41-51.
- Davis, R. J. (2000). Signal transduction by the JNK group of MAP kinases. *Cell* **103**, 239-52.
- DeLille, J. M., Sehnke, P. C., and Ferl, R. J. (2001). The arabidopsis 14-3-3 family of signaling regulators. *Plant Physiol* **126**, 35-8.
- Dillin, A., Crawford, D. K., and Kenyon, C. (2002). Timing requirements for insulin/IGF-1 signaling in *C. elegans*. *Science* **298**, 830-4.
- Dong, M. Q., Venable, J. D., Au, N., Xu, T., Park, S. K., Cociorva, D., Johnson, J. R., Dillin, A., and Yates, J. R., 3rd. (2007). Quantitative mass

- spectrometry identifies insulin signaling targets in *C. elegans*. *Science* **317**, 660-3.
- Essers, M. A., de Vries-Smits, L. M., Barker, N., Polderman, P. E., Burgering, B. M., and Korswagen, H. C. (2005). Functional interaction between beta-catenin and FOXO in oxidative stress signaling. *Science* **308**, 1181-4.
- Essers, M. A., Weijzen, S., de Vries-Smits, A. M., Saarloos, I., de Ruiter, N. D., Bos, J. L., and Burgering, B. M. (2004). FOXO transcription factor activation by oxidative stress mediated by the small GTPase Ral and JNK. *Embo J* **23**, 4802-12.
- Flatt, T., Min, K. J., D'Alterio, C., Villa-Cuesta, E., Cumbers, J., Lehmann, R., Jones, D. L., and Tatar, M. (2008). *Drosophila* germ-line modulation of insulin signaling and lifespan. *Proc Natl Acad Sci U S A* **105**, 6368-73.
- Forrest, A., and Gabrielli, B. (2001). Cdc25B activity is regulated by 14-3-3. *Oncogene* **20**, 4393-401.
- Friedman, D. B., and Johnson, T. E. (1988). A mutation in the age-1 gene in *Caenorhabditis elegans* lengthens life and reduces hermaphrodite fertility. *Genetics* **118**, 75-86.
- Fu, H., Subramanian, R. R., and Masters, S. C. (2000). 14-3-3 proteins: structure, function, and regulation. *Annu Rev Pharmacol Toxicol* **40**, 617-47.
- Fu, H., Xia, K., Pallas, D. C., Cui, C., Conroy, K., Narsimhan, R. P., Mamon, H., Collier, R. J., and Roberts, T. M. (1994). Interaction of the protein kinase Raf-1 with 14-3-3 proteins. *Science* **266**, 126-9.
- Furuyama, T., Nakazawa, T., Nakano, I., and Mori, N. (2000). Identification of the differential distribution patterns of mRNAs and consensus binding sequences for mouse DAF-16 homologues. *Biochem J* **349**, 629-34.
- Gems, D., Sutton, A. J., Sundermeyer, M. L., Albert, P. S., King, K. V., Edgley, M. L., Larsen, P. L., and Riddle, D. L. (1998). Two pleiotropic classes of daf-2 mutation affect larval arrest, adult behavior, reproduction and longevity in *Caenorhabditis elegans*. *Genetics* **150**, 129-55.
- Giannakou, M. E., and Partridge, L. (2007). Role of insulin-like signalling in *Drosophila* lifespan. *Trends Biochem Sci* **32**, 180-8.
- Gottlieb, S., and Ruvkun, G. (1994). daf-2, daf-16 and daf-23: genetically interacting genes controlling Dauer formation in *Caenorhabditis elegans*. *Genetics* **137**, 107-20.
- Grozinger, C. M., and Schreiber, S. L. (2000). Regulation of histone deacetylase 4 and 5 and transcriptional activity by 14-3-3-dependent cellular localization. *Proc Natl Acad Sci U S A* **97**, 7835-40.

- Hagel, L. (2001). Gel-filtration chromatography. *Curr Protoc Mol Biol* **Chapter 10**, Unit 10 9.
- Halaschek-Wiener, J., Khattra, J. S., McKay, S., Pouzyrev, A., Stott, J. M., Yang, G. S., Holt, R. A., Jones, S. J., Marra, M. A., Brooks-Wilson, A. R., and Riddle, D. L. (2005). Analysis of long-lived *C. elegans* daf-2 mutants using serial analysis of gene expression. *Genome Res* **15**, 603-15.
- Hamilton, B., Dong, Y., Shindo, M., Liu, W., Odell, I., Ruvkun, G., and Lee, S. S. (2005). A systematic RNAi screen for longevity genes in *C. elegans*. *Genes Dev* **19**, 1544-55.
- Hertweck, M., Gobel, C., and Baumeister, R. (2004). *C. elegans* SGK-1 is the critical component in the Akt/PKB kinase complex to control stress response and life span. *Dev Cell* **6**, 577-88.
- Holzenberger, M., Dupont, J., Ducos, B., Leneuve, P., Geloën, A., Even, P. C., Cervera, P., and Le Bouc, Y. (2003). IGF-1 receptor regulates lifespan and resistance to oxidative stress in mice. *Nature* **421**, 182-7.
- Honda, Y., and Honda, S. (1999). The daf-2 gene network for longevity regulates oxidative stress resistance and Mn-superoxide dismutase gene expression in *Caenorhabditis elegans*. *Faseb J* **13**, 1385-93.
- Hsin, H., and Kenyon, C. (1999). Signals from the reproductive system regulate the lifespan of *C. elegans*. *Nature* **399**, 362-6.
- Hsu, A. L., Murphy, C. T., and Kenyon, C. (2003). Regulation of aging and age-related disease by DAF-16 and heat-shock factor. *Science* **300**, 1142-5.
- Hu, M. C., Lee, D. F., Xia, W., Golfman, L. S., Ou-Yang, F., Yang, J. Y., Zou, Y., Bao, S., Hanada, N., Saso, H., Kobayashi, R., and Hung, M. C. (2004). IκappaB kinase promotes tumorigenesis through inhibition of forkhead FOXO3a. *Cell* **117**, 225-37.
- Hu, P. J., Xu, J., and Ruvkun, G. (2006). Two membrane-associated tyrosine phosphatase homologs potentiate *C. elegans* AKT-1/PKB signaling. *PLoS Genet* **2**, e99.
- Hua, Q. X., Nakagawa, S. H., Wilken, J., Ramos, R. R., Jia, W., Bass, J., and Weiss, M. A. (2003). A divergent INS protein in *Caenorhabditis elegans* structurally resembles human insulin and activates the human insulin receptor. *Genes Dev* **17**, 826-31.
- Huang, H., Regan, K. M., Wang, F., Wang, D., Smith, D. I., van Deursen, J. M., and Tindall, D. J. (2005). Skp2 inhibits FOXO1 in tumor suppression through ubiquitin-mediated degradation. *Proc Natl Acad Sci U S A* **102**, 1649-54.

- Huang, H., and Tindall, D. J. (2007). Dynamic FoxO transcription factors. *J Cell Sci* **120**, 2479-87.
- Hurd, D. D., and Kemphues, K. J. (2003). PAR-1 is required for morphogenesis of the *Caenorhabditis elegans* vulva. *Dev Biol* **253**, 54-65.
- Ichimura, T., Isobe, T., Okuyama, T., Takahashi, N., Araki, K., Kuwano, R., and Takahashi, Y. (1988). Molecular cloning of cDNA coding for brain-specific 14-3-3 protein, a protein kinase-dependent activator of tyrosine and tryptophan hydroxylases. *Proc Natl Acad Sci U S A* **85**, 7084-8.
- Irie, K., Gotoh, Y., Yashar, B. M., Errede, B., Nishida, E., and Matsumoto, K. (1994). Stimulatory effects of yeast and mammalian 14-3-3 proteins on the Raf protein kinase. *Science* **265**, 1716-9.
- Jones, D. H., Ley, S., and Aitken, A. (1995). Isoforms of 14-3-3 protein can form homo- and heterodimers in vivo and in vitro: implications for function as adapter proteins. *FEBS Lett* **368**, 55-8.
- Julien, E., and Herr, W. (2003). Proteolytic processing is necessary to separate and ensure proper cell growth and cytokinesis functions of HCF-1. *Embo J* **22**, 2360-9.
- Julien, E., and Herr, W. (2004). A switch in mitotic histone H4 lysine 20 methylation status is linked to M phase defects upon loss of HCF-1. *Mol Cell* **14**, 713-25.
- Kaeberlein, M., Burtner, C. R., and Kennedy, B. K. (2007). Recent developments in yeast aging. *PLoS Genet* **3**, e84.
- Kaeberlein, M., McVey, M., and Guarente, L. (1999). The SIR2/3/4 complex and SIR2 alone promote longevity in *Saccharomyces cerevisiae* by two different mechanisms. *Genes Dev* **13**, 2570-80.
- Kawano, T., Ito, Y., Ishiguro, M., Takuwa, K., Nakajima, T., and Kimura, Y. (2000). Molecular cloning and characterization of a new insulin/IGF-like peptide of the nematode *Caenorhabditis elegans*. *Biochem Biophys Res Commun* **273**, 431-6.
- Kelly, W. G., and Fire, A. (1998). Chromatin silencing and the maintenance of a functional germline in *Caenorhabditis elegans*. *Development* **125**, 2451-6.
- Kenyon, C. (2005). The plasticity of aging: insights from long-lived mutants. *Cell* **120**, 449-60.
- Kenyon, C., Chang, J., Gensch, E., Rudner, A., and Tabtiang, R. (1993). A *C. elegans* mutant that lives twice as long as wild type. *Nature* **366**, 461-4.
- Kimura, K. D., Tissenbaum, H. A., Liu, Y., and Ruvkun, G. (1997). *daf-2*, an insulin receptor-like gene that regulates longevity and diapause in *Caenorhabditis elegans*. *Science* **277**, 942-6.

- Kobayashi, Y., Furukawa-Hibi, Y., Chen, C., Horio, Y., Isobe, K., Ikeda, K., and Motoyama, N. (2005). SIRT1 is critical regulator of FOXO-mediated transcription in response to oxidative stress. *Int J Mol Med* **16**, 237-43.
- Kristie, T. M., Pomerantz, J. L., Twomey, T. C., Parent, S. A., and Sharp, P. A. (1995). The cellular C1 factor of the herpes simplex virus enhancer complex is a family of polypeptides. *J Biol Chem* **270**, 4387-94.
- Lambert, A. J., and Brand, M. D. (2007). Research on mitochondria and aging, 2006-2007. *Aging Cell* **6**, 417-20.
- Larsen, P. L., Albert, P. S., and Riddle, D. L. (1995). Genes that regulate both development and longevity in *Caenorhabditis elegans*. *Genetics* **139**, 1567-83.
- Lee, R. Y., Hench, J., and Ruvkun, G. (2001). Regulation of *C. elegans* DAF-16 and its human ortholog FKHRL1 by the daf-2 insulin-like signaling pathway. *Curr Biol* **11**, 1950-7.
- Lee, S., and Herr, W. (2001). Stabilization but not the transcriptional activity of herpes simplex virus VP16-induced complexes is evolutionarily conserved among HCF family members. *J Virol* **75**, 12402-11.
- Lee, S., Horn, V., Julien, E., Liu, Y., Wysocka, J., Bowerman, B., Hengartner, M. O., and Herr, W. (2007). Epigenetic Regulation of Histone H3 Serine 10 Phosphorylation Status by HCF-1 Proteins in *C. elegans* and Mammalian Cells. *PLoS ONE* **2**, e1213.
- Lee, S. S., Kennedy, S., Tolonen, A. C., and Ruvkun, G. (2003a). DAF-16 target genes that control *C. elegans* life-span and metabolism. *Science* **300**, 644-7.
- Lee, S. S., Lee, R. Y., Fraser, A. G., Kamath, R. S., Ahringer, J., and Ruvkun, G. (2003b). A systematic RNAi screen identifies a critical role for mitochondria in *C. elegans* longevity. *Nat Genet* **33**, 40-8.
- Li, J., Tewari, M., Vidal, M., and Lee, S. S. (2007a). The 14-3-3 protein FTT-2 regulates DAF-16 in *Caenorhabditis elegans*. *Dev Biol* **301**, 82-91.
- Li, W., Gao, B., Lee, S. M., Bennett, K., and Fang, D. (2007b). RLE-1, an E3 ubiquitin ligase, regulates *C. elegans* aging by catalyzing DAF-16 polyubiquitination. *Dev Cell* **12**, 235-46.
- Li, W., Kennedy, S. G., and Ruvkun, G. (2003). daf-28 encodes a *C. elegans* insulin superfamily member that is regulated by environmental cues and acts in the DAF-2 signaling pathway. *Genes Dev* **17**, 844-58.
- Libina, N., Berman, J. R., and Kenyon, C. (2003). Tissue-specific activities of *C. elegans* DAF-16 in the regulation of lifespan. *Cell* **115**, 489-502.
- Lin, K., Dorman, J. B., Rodan, A., and Kenyon, C. (1997). daf-16: An HNF-3/forkhead family member that can function to double the life-span of *Caenorhabditis elegans*. *Science* **278**, 1319-22.

- Lin, K., Hsin, H., Libina, N., and Kenyon, C. (2001). Regulation of the *Caenorhabditis elegans* longevity protein DAF-16 by insulin/IGF-1 and germline signaling. *Nat Genet* **28**, 139-45.
- Lithgow, G. J., White, T. M., Melov, S., and Johnson, T. E. (1995). Thermotolerance and extended life-span conferred by single-gene mutations and induced by thermal stress. *Proc Natl Acad Sci U S A* **92**, 7540-4.
- Longo, V. D., and Kennedy, B. K. (2006). Sirtuins in aging and age-related disease. *Cell* **126**, 257-68.
- Mahajan, S. S., Little, M. M., Vazquez, R., and Wilson, A. C. (2002). Interaction of HCF-1 with a cellular nuclear export factor. *J Biol Chem* **277**, 44292-9.
- Martin, H., Patel, Y., Jones, D., Howell, S., Robinson, K., and Aitken, A. (1993). Antibodies against the major brain isoforms of 14-3-3 protein. An antibody specific for the N-acetylated amino-terminus of a protein. *FEBS Lett* **331**, 296-303.
- Masters, S. C., Pederson, K. J., Zhang, L., Barbieri, J. T., and Fu, H. (1999). Interaction of 14-3-3 with a nonphosphorylated protein ligand, exoenzyme S of *Pseudomonas aeruginosa*. *Biochemistry* **38**, 5216-21.
- Matsuzaki, H., Daitoku, H., Hatta, M., Tanaka, K., and Fukamizu, A. (2003). Insulin-induced phosphorylation of FKHR (Foxo1) targets to proteasomal degradation. *Proc Natl Acad Sci U S A* **100**, 11285-90.
- McElwee, J., Bubb, K., and Thomas, J. H. (2003). Transcriptional outputs of the *Caenorhabditis elegans* forkhead protein DAF-16. *Aging Cell* **2**, 111-21.
- Morris, J. Z., Tissenbaum, H. A., and Ruvkun, G. (1996). A phosphatidylinositol-3-OH kinase family member regulating longevity and diapause in *Caenorhabditis elegans*. *Nature* **382**, 536-9.
- Morton, D. G., Shakes, D. C., Nugent, S., Dichoso, D., Wang, W., Golden, A., and Kemphues, K. J. (2002). The *Caenorhabditis elegans* par-5 gene encodes a 14-3-3 protein required for cellular asymmetry in the early embryo. *Dev Biol* **241**, 47-58.
- Motta, M. C., Divecha, N., Lemieux, M., Kamel, C., Chen, D., Gu, W., Bultsma, Y., McBurney, M., and Guarente, L. (2004). Mammalian SIRT1 represses forkhead transcription factors. *Cell* **116**, 551-63.
- Murakami, S., and Johnson, T. E. (1996). A genetic pathway conferring life extension and resistance to UV stress in *Caenorhabditis elegans*. *Genetics* **143**, 1207-18.
- Murphy, C. T., McCarroll, S. A., Bargmann, C. I., Fraser, A., Kamath, R. S., Ahringer, J., Li, H., and Kenyon, C. (2003). Genes that act downstream

- of DAF-16 to influence the lifespan of *Caenorhabditis elegans*. *Nature* **424**, 277-83.
- Myers, M. G., Jr., and White, M. F. (1996). Insulin signal transduction and the IRS proteins. *Annu Rev Pharmacol Toxicol* **36**, 615-58.
- Obsil, T., Ghirlando, R., Klein, D. C., Ganguly, S., and Dyda, F. (2001). Crystal structure of the 14-3-3zeta:serotonin N-acetyltransferase complex. a role for scaffolding in enzyme regulation. *Cell* **105**, 257-67.
- Ogg, S., Paradis, S., Gottlieb, S., Patterson, G. I., Lee, L., Tissenbaum, H. A., and Ruvkun, G. (1997). The Fork head transcription factor DAF-16 transduces insulin-like metabolic and longevity signals in *C. elegans*. *Nature* **389**, 994-9.
- Ogg, S., and Ruvkun, G. (1998). The *C. elegans* PTEN homolog, DAF-18, acts in the insulin receptor-like metabolic signaling pathway. *Mol Cell* **2**, 887-93.
- Oh, S. W., Mukhopadhyay, A., Dixit, B. L., Raha, T., Green, M. R., and Tissenbaum, H. A. (2006). Identification of direct DAF-16 targets controlling longevity, metabolism and diapause by chromatin immunoprecipitation. *Nat Genet* **38**, 251-7.
- Oh, S. W., Mukhopadhyay, A., Svazikapa, N., Jiang, F., Davis, R. J., and Tissenbaum, H. A. (2005). JNK regulates lifespan in *Caenorhabditis elegans* by modulating nuclear translocation of forkhead transcription factor/DAF-16. *Proc Natl Acad Sci U S A* **102**, 4494-9.
- Paradis, S., Ailion, M., Toker, A., Thomas, J. H., and Ruvkun, G. (1999). A PDK1 homolog is necessary and sufficient to transduce AGE-1 PI3 kinase signals that regulate diapause in *Caenorhabditis elegans*. *Genes Dev* **13**, 1438-52.
- Paradis, S., and Ruvkun, G. (1998). *Caenorhabditis elegans* Akt/PKB transduces insulin receptor-like signals from AGE-1 PI3 kinase to the DAF-16 transcription factor. *Genes Dev* **12**, 2488-98.
- Peng, C. Y., Graves, P. R., Thoma, R. S., Wu, Z., Shaw, A. S., and Piwnicka-Worms, H. (1997). Mitotic and G2 checkpoint control: regulation of 14-3-3 protein binding by phosphorylation of Cdc25C on serine-216. *Science* **277**, 1501-5.
- Pierce, S. B., Costa, M., Wisotzkey, R., Devadhar, S., Homburger, S. A., Buchman, A. R., Ferguson, K. C., Heller, J., Platt, D. M., Pasquinelli, A. A., Liu, L. X., Doberstein, S. K., and Ruvkun, G. (2001). Regulation of DAF-2 receptor signaling by human insulin and ins-1, a member of the unusually large and diverse *C. elegans* insulin gene family. *Genes Dev* **15**, 672-86.

- Piluso, D., Bilan, P., and Capone, J. P. (2002). Host cell factor-1 interacts with and antagonizes transactivation by the cell cycle regulatory factor Miz-1. *J Biol Chem* **277**, 46799-808.
- Plas, D. R., and Thompson, C. B. (2003). Akt activation promotes degradation of tuberlin and FOXO3a via the proteasome. *J Biol Chem* **278**, 12361-6.
- Pozuelo Rubio, M., Geraghty, K. M., Wong, B. H., Wood, N. T., Campbell, D. G., Morrice, N., and Mackintosh, C. (2004). 14-3-3-affinity purification of over 200 human phosphoproteins reveals new links to regulation of cellular metabolism, proliferation and trafficking. *Biochem J* **379**, 395-408.
- Praitis, V., Casey, E., Collar, D., and Austin, J. (2001). Creation of low-copy integrated transgenic lines in *Caenorhabditis elegans*. *Genetics* **157**, 1217-26.
- Riddle, D.-L., and Albert, P.-S. (1997). Genetic and environmental regulation of Dauer larva development. In "Cold Spring Harbor Monograph Series; *C. elegans* II. 1997; 33: 739 768" (D. L. Riddle, T. Blumenthal, B. J. Meyer, and J. R. Priess, Eds.). Cold Spring Harbor Laboratory Press {a}, 10 Skyline Drive, Plainview, New York 11803, USA.
- Riddle, D. L., Swanson, M. M., and Albert, P. S. (1981). Interacting genes in nematode dauer larva formation. *Nature* **290**, 668-71.
- Rine, J., and Herskowitz, I. (1987). Four genes responsible for a position effect on expression from HML and HMR in *Saccharomyces cerevisiae*. *Genetics* **116**, 9-22.
- Roberts, M. R., and de Bruxelles, G. L. (2002). Plant 14-3-3 protein families: evidence for isoform-specific functions? *Biochem Soc Trans* **30**, 373-8.
- Rogina, B., and Helfand, S. L. (2004). Sir2 mediates longevity in the fly through a pathway related to calorie restriction. *Proc Natl Acad Sci U S A* **101**, 15998-6003.
- Rual, J. F., Ceron, J., Koreth, J., Hao, T., Nicot, A. S., Hirozane-Kishikawa, T., Vandenhaute, J., Orkin, S. H., Hill, D. E., van den Heuvel, S., and Vidal, M. (2004). Toward improving *Caenorhabditis elegans* phenome mapping with an ORFeome-based RNAi library. *Genome Res* **14**, 2162-8.
- Russell, S. J., and Kahn, C. R. (2007). Endocrine regulation of ageing. *Nat Rev Mol Cell Biol* **8**, 681-91.
- Samuelson, A. V., Carr, C. E., and Ruvkun, G. (2007). Gene activities that mediate increased life span of *C. elegans* insulin-like signaling mutants. *Genes Dev* **21**, 2976-94.
- Simmer, F., Tijsterman, M., Parrish, S., Koushika, S. P., Nonet, M. L., Fire, A., Ahringer, J., and Plasterk, R. H. (2002). Loss of the putative RNA-

- directed RNA polymerase RRF-3 makes *C. elegans* hypersensitive to RNAi. *Curr Biol* **12**, 1317-9.
- Sunayama, J., Tsuruta, F., Masuyama, N., and Gotoh, Y. (2005). JNK antagonizes Akt-mediated survival signals by phosphorylating 14-3-3. *J Cell Biol* **170**, 295-304.
- Takahashi, Y., Rayman, J. B., and Dynlacht, B. D. (2000). Analysis of promoter binding by the E2F and pRB families in vivo: distinct E2F proteins mediate activation and repression. *Genes Dev* **14**, 804-16.
- Tatar, M., Kopelman, A., Epstein, D., Tu, M. P., Yin, C. M., and Garofalo, R. S. (2001). A mutant *Drosophila* insulin receptor homolog that extends lifespan and impairs neuroendocrine function. *Science* **292**, 107-10.
- Tavernarakis, N., Wang, S. L., Dorovkov, M., Ryazanov, A., and Driscoll, M. (2000). Heritable and inducible genetic interference by double-stranded RNA encoded by transgenes. *Nat Genet* **24**, 180-3.
- Timmons, L., Court, D. L., and Fire, A. (2001). Ingestion of bacterially expressed dsRNAs can produce specific and potent genetic interference in *Caenorhabditis elegans*. *Gene* **263**, 103-12.
- Tissenbaum, H. A., and Guarente, L. (2001). Increased dosage of a sir-2 gene extends lifespan in *Caenorhabditis elegans*. *Nature* **410**, 227-30.
- Troemel, E. R., Chu, S. W., Reinke, V., Lee, S. S., Ausubel, F. M., and Kim, D. H. (2006). p38 MAPK regulates expression of immune response genes and contributes to longevity in *C. elegans*. *PLoS Genet* **2**, e183.
- Tullet, J. M., Hertweck, M., An, J. H., Baker, J., Hwang, J. Y., Liu, S., Oliveira, R. P., Baumeister, R., and Blackwell, T. K. (2008). Direct inhibition of the longevity-promoting factor SKN-1 by insulin-like signaling in *C. elegans*. *Cell* **132**, 1025-38.
- Tyagi, S., Chabes, A. L., Wysocka, J., and Herr, W. (2007). E2F activation of S phase promoters via association with HCF-1 and the MLL family of histone H3K4 methyltransferases. *Mol Cell* **27**, 107-19.
- van der Heide, L. P., and Smidt, M. P. (2005). Regulation of FoxO activity by CBP/p300-mediated acetylation. *Trends Biochem Sci* **30**, 81-6.
- van der Horst, A., and Burgering, B. M. (2007). Stressing the role of FoxO proteins in lifespan and disease. *Nat Rev Mol Cell Biol* **8**, 440-50.
- van der Horst, A., de Vries-Smits, A. M., Brenkman, A. B., van Triest, M. H., van den Broek, N., Colland, F., Maurice, M. M., and Burgering, B. M. (2006). FOXO4 transcriptional activity is regulated by monoubiquitination and USP7/HAUSP. *Nat Cell Biol* **8**, 1064-73.
- van der Horst, A., Tertoolen, L. G., de Vries-Smits, L. M., Frye, R. A., Medema, R. H., and Burgering, B. M. (2004). FOXO4 is acetylated

- upon peroxide stress and deacetylated by the longevity protein hSir2(SIRT1). *J Biol Chem* **279**, 28873-9.
- Viswanathan, M., Kim, S. K., Berdichevsky, A., and Guarente, L. (2005). A role for SIR-2.1 regulation of ER stress response genes in determining *C. elegans* life span. *Dev Cell* **9**, 605-15.
- Vogel, J. L., and Kristie, T. M. (2000). The novel coactivator C1 (HCF) coordinates multiprotein enhancer formation and mediates transcription activation by GABP. *Embo J* **19**, 683-90.
- Wang, M. C., Bohmann, D., and Jasper, H. (2003). JNK signaling confers tolerance to oxidative stress and extends lifespan in *Drosophila*. *Dev Cell* **5**, 811-6.
- Wang, M. C., Bohmann, D., and Jasper, H. (2005). JNK extends life span and limits growth by antagonizing cellular and organism-wide responses to insulin signaling. *Cell* **121**, 115-25.
- Wang, W., and Shakes, D. C. (1996). Molecular evolution of the 14-3-3 protein family. *J Mol Evol* **43**, 384-98.
- Wang, W., and Shakes, D. C. (1997). Expression patterns and transcript processing of *ftt-1* and *ftt-2*, two *C. elegans* 14-3-3 homologues. *J Mol Biol* **268**, 619-30.
- Wang, Y., Oh, S. W., Deplancke, B., Luo, J., Walhout, A. J., and Tissenbaum, H. A. (2006a). *C. elegans* 14-3-3 proteins regulate life span and interact with SIR-2.1 and DAF-16/FOXO. *Mech Ageing Dev* **127**, 741-7.
- Wang, Y., Oh, S. W., Deplancke, B., Luo, J., Walhout, A. J., and Tissenbaum, H. A. (2006b). *C. elegans* 14-3-3 proteins regulate life span and interact with SIR-2.1 and DAF-16/FOXO. *Mech Ageing Dev*.
- Wang, Y., and Tissenbaum, H. A. (2006). Overlapping and distinct functions for a *Caenorhabditis elegans* SIR2 and DAF-16/FOXO. *Mech Ageing Dev* **127**, 48-56.
- Wang, Z., Pandey, A., and Hart, G. W. (2007). Dynamic interplay between O-GlcNAcylation and GSK-3-dependent phosphorylation. *Mol Cell Proteomics*.
- Wolff, S., and Dillin, A. (2006). The trifecta of aging in *Caenorhabditis elegans*. *Exp Gerontol* **41**, 894-903.
- Wolff, S., Ma, H., Burch, D., Maciel, G. A., Hunter, T., and Dillin, A. (2006). SMK-1, an essential regulator of DAF-16-mediated longevity. *Cell* **124**, 1039-53.
- Wolkow, C. A., Munoz, M. J., Riddle, D. L., and Ruvkun, G. (2002). Insulin receptor substrate and p55 orthologous adaptor proteins function in the *Caenorhabditis elegans* *daf-2*/insulin-like signaling pathway. *J Biol Chem* **277**, 49591-7.

- Wook Oh, S., Mukhopadhyay, A., Dixit, B. L., Raha, T., Green, M. R., and Tissenbaum, H. A. (2006). Identification of direct DAF-16 targets controlling longevity, metabolism and diapause by chromatin immunoprecipitation. *Nat Genet* **38**, 251-7.
- Wysocka, J., and Herr, W. (2003). The herpes simplex virus VP16-induced complex: the makings of a regulatory switch. *Trends Biochem Sci* **28**, 294-304.
- Wysocka, J., Liu, Y., Kobayashi, R., and Herr, W. (2001). Developmental and cell-cycle regulation of *Caenorhabditis elegans* HCF phosphorylation. *Biochemistry* **40**, 5786-94.
- Wysocka, J., Myers, M. P., Laherty, C. D., Eisenman, R. N., and Herr, W. (2003). Human Sin3 deacetylase and trithorax-related Set1/Ash2 histone H3-K4 methyltransferase are tethered together selectively by the cell-proliferation factor HCF-1. *Genes Dev* **17**, 896-911.
- Yaffe, M. B. (2002). How do 14-3-3 proteins work?-- Gatekeeper phosphorylation and the molecular anvil hypothesis. *FEBS Lett* **513**, 53-7.
- Yaffe, M. B., Rittinger, K., Volinia, S., Caron, P. R., Aitken, A., Leffers, H., Gamblin, S. J., Smerdon, S. J., and Cantley, L. C. (1997). The structural basis for 14-3-3:phosphopeptide binding specificity. *Cell* **91**, 961-71.
- Yanase, S., Yasuda, K., and Ishii, N. (2002). Adaptive responses to oxidative damage in three mutants of *Caenorhabditis elegans* (age-1, mev-1 and daf-16) that affect life span. *Mech Ageing Dev* **123**, 1579-87.